



Sílvia Andreia da Silva Fernandes Rebocho

Mestre em Biotecnologia

**Biotransformation/separation
routes to obtain pure enantiomers**

Dissertação para obtenção do Grau de Doutor em

Química Sustentável

Orientadora: Susana Barreiros,

Professora Associada com Agregação,
LAQV/REQUIMTE, FCT-UNL

Co-orientadores:

Alexandre Paiva, Investigador

Doutorado, LAQV/REQUIMTE, FCT-UNL

Carlos Afonso, Professor Catedrático, FFUL



Outubro de 2015

Universidade Nova de Lisboa

Sílvia Andreia da Silva Fernandes Rebocho

Mestre em Biotecnologia

**Biotransformation/separation
routes to obtain pure enantiomers**

Dissertação para obtenção do Grau de Doutor em

Química Sustentável

Orientadora: Susana Barreiros,

Professora Associada com Agregação,
LAQV/REQUIMTE, FCT-UNL

Co-orientadores: Alexandre Paiva, Investigador

Doutorado, LAQV/REQUIMTE, FCT-UNL

Carlos Afonso, Professor Catedrático, FFUL



FACULDADE DE
CIÊNCIAS E TECNOLOGIA
UNIVERSIDADE NOVA DE LISBOA

Outubro de 2015

Copyright

Sílvia Andreia da Silva Fernandes Rebocho

Universidade Nova de Lisboa, Faculdade de Ciências e Tecnologia

A Faculdade de Ciências e Tecnologia e Universidade Nova de Lisboa têm o direito, perpétuo e sem limites geográficos, de arquivar e publicar esta dissertação através de exemplares impressos reproduzidos em papel ou de forma digital, ou por qualquer outro meio conhecido ou que venha a ser inventado, e de a divulgar através de repositórios científicos e de admitir a sua cópia e distribuição com objetivos educacionais ou de investigação, não comerciais, desde que seja dado crédito ao autor e editor.

As secções desta dissertação já publicadas por editores para os quais foram transferidos direitos de cópia pelos autores, encontram-se devidamente identificadas ao longo da dissertação e são reproduzidas sob permissão dos editores originais e sujeitas às restrições de cópia impostos pelos mesmos.

To my son Gonalo

Start by doing what is necessary; then do what is possible; and suddenly you are doing the impossible.

Francis of Assisi

Acknowledgments

Foi um longo percurso que enfrentei com o entusiasmo de concretizar o sonho de quem ganha uma bolsa de Doutoramento. Só quem realmente vive ou viveu este momento sabe dar o valor da alegria de tamanha notícia. E como praticamente todas as coisas boas desta vida são para ser divididas com alguém, são muitas as pessoas a quem tenho de agradecer por terem feito parte deste caminho.

Em primeiro lugar, tenho que destacar a Professora Susana Barreiros, que mais uma vez me abriu a porta do seu laboratório e deu-me toda a liberdade para avançar com este projeto. Não posso deixar de lhe dizer que para além de toda a gratidão, é para mim uma pessoa muito especial, alguém que admiro e respeito por todo o trabalho e pela postura ao longo deste tempo que trabalhamos juntas. Obrigada pela partilha de conhecimento, pela paciência (que foi muita) e pela amizade ao longo destes anos.

A ti Alexandre, um muitíssimo obrigada pelo apoio, pela ajuda, pelos ensinamentos, pelas sugestões, por teres acreditado neste trabalho e por acima de tudo pela paciência. Eu sei que não foi fácil ensinar modelação a uma Engenheira Biotecnológica. Acredita que eu também sofri! Mas não recorri a medicação e orgulho-me disso! Hehe! E apesar de algumas das tuas t-shirts camuflarem a tua maturidade, és uma pessoa muito inteligente e que merece ter um lugar de destaque na ciência. Bom, e no meio disto tudo, haverá sempre uma festa que nos vai unir todos os anos!

Ao Professor Carlos Afonso, obrigada por ter aceitado fazer parte deste trabalho. Obrigada pela generosidade, pelos conselhos e pela valiosa ajuda no arranque inicial desta tese. Obrigada pela oportunidade e pela compreensão.

A dois dos impulsionadores deste trabalho, Pedro Vidinha e Nuno Lourenço o meu muito obrigada. Pedro, tu és alguém que ficará para sempre na minha memória e no meu coração, pelas aventuras científicas e não só, e é claro pela tua sabedoria, pela tua vontade de ensinar, de partilhar e de motivar quem trabalha contigo. Nuno, tu foste o “cérebro orgânico” deste trabalho! Obrigada pelas horas que estiveste comigo a desenvolver este projeto! Por me teres recebido tão bem no IST e por tudo o que me ensinaste!

Zé Jorge, o que seria de mim sem ti?! Tu não foste apenas um colega de trabalho, foste e continuas a ser um grande amigo! Apesar do meu ar calmo, eu sei que houve dias em que as coisas não andavam fáceis...eu ponho a culpa em todos os solventes “não verdes” que tivemos que inalar! Viva ao CO₂ e abaixo o éter de petróleo! Obrigada pela paciência que tiveste comigo quando eu entrei no clube das grávidas! Com mais 11 kg e de máscara foi dose, mas no fundo

eu sei que tinhas medo das minhas hormonas! Por isso é que me tratavas bem! Obrigada por tudo! Este trabalho não seria sido a mesma coisa sem ti!

Querida Ana Nunes, tiveste um papel tão importante nesta tese que não posso deixar de dizer o quanto te estou agradecida. A tua paciência, os teus conselhos, a tua ajuda, foram tão preciosas que nem imaginas! Mas acima de tudo és especial porque para além destas qualidades, ainda reúnes outra que é a tua generosidade. Obrigada por tudo do fundo do coração.

Querida Vesna, muito obrigada pela ajuda nos estudos de equilíbrio de fases! Foste sempre tão disponível e atenciosa. Aprendi muito contigo! Agradeço-te todo o tempo que dedicaste ao nosso trabalho.

Rita Craveiro e Carmen Montoya, a vocês só vos tenho a agradecer por tudo! Foram e são as minhas grandes amigas e companheiras desta longa caminhada! Cada uma ao seu estilo, com a autenticidade que vos caracteriza! Temos tantas coisas que ficarão para sempre na nossa memória! O nosso cruzeiro “Preziosa” será sempre um marco nas nossas vidas! Não me esquecerei de tanto brilhante naquelas escadas! Obrigada do fundo do coração pela amizade que temos, pelo bom humor e pelas grandes gargalhadas que demos juntas! Espero que estes momentos durem para sempre! O meu Gonçalo será sempre “vosso sobrinho” de coração!

Aos membros que permaneceram mais tempo comigo no 427: Vera Augusto, Tânia, Diana, Rita Rodrigues, Ricardo e Pedro Lisboa, obrigada pela ajuda sempre que precisei, obrigada pelo companheirismo e pela boa disposição!

Ignácio, Lino Lopez, Sónia Silva, Andreia Pimenta, Margherita, Alhambra, Ana Paninho, Guima e tantos outros que passaram pelo laboratório e pela faculdade ao longo deste trabalho, obrigada a cada pela ajuda e pelos bons momentos que privámos.

Um obrigado muito especial ao Professor Pedro Simões, Professor Marco, Professor Manuel Nunes da Ponte, Professora Paula Branco, D. Conceição, D. Idalina, D. Amélia, Engenheiro Rui Costa, Doutora Carla Brazinha, Professora Isabel Coelho, pela ajuda e pela disponibilidade sempre que precisei ao longo deste trabalho.

Quero agradecer aos meus amigos, em especial a ti Mafalda e a ti Cristina. No outro dia li que uma amizade que dure 7 anos tem grandes probabilidades de durar para sempre...no nosso caso, acredito mesmo! As nossas aventuras davam para uma serie daquelas de muito sucesso. Obrigada por todo o carinho que partilhamos!

Aos meus pais, a quem devo tudo...obrigada por me apoiarem nas minhas decisões, obrigada pelo carinho e dedicação que sempre tiveram comigo. Pelo amor e paciência ao longo destes anos. Vocês são os melhores pais do mundo!

À minha irmã, um grande beijinho por tudo! Obrigada pela amizade que temos uma pela outra, pelo carinho e por todas as horas que temos vivido juntas. Seremos sempre irmãs, de sangue e de coração para todos os momentos da nossa vida! E este para sempre não tem fim.

A ti Pedro, obrigada pelo teu amor e dedicação! Temos o melhor presente que o amor pode dar a duas pessoas: o Gonçalo!

Ao meu filho, que veio preencher o meu coração de alegria e que me ensinou a maior das descobertas: o amor incondicional! És o que eu tenho de mais precioso na vida! És o meu maior tesouro! És o amor da vida da mamã!

Por fim quero agradecer à Fundação para a Ciência e Tecnologia o financiamento para a realização deste trabalho.

OBRIGADA A TODOS!!!!!!!!!!!!!!

Resumo

O objetivo do trabalho apresentado nesta tese foi desenvolver um processo inovador para a separação de enantiómeros de álcoois secundários, combinando a utilização de um líquido iónico (LI) quer como solvente para a realização de resolução cinética enzimática, quer como agente acilante, e a utilização de dióxido de carbono (CO_2) como agente de extracção. Para a aplicação desta estratégia de reacção/separação, foi escolhido o mentol, um composto cada vez mais utilizado em várias indústrias, como a farmacêutica, cosmética ou alimentar.

Com vista à utilização, como agente acilante, de um éster iónico cuja conversão dava lugar à formação de etanol, e devido à necessidade de remover este álcool de modo a deslocar o equilíbrio reaccional no sentido directo, realizou-se um estudo de equilíbrio de fases do sistema etanol/(\pm)-mentol/ CO_2 para pressões entre os 8 e os 10 MPa e temperaturas entre 40 e 50 °C. Observou-se que o CO_2 é mais selectivo para o etanol, sobretudo à pressão mais baixa e temperatura mais elevada testadas, tendo-se obtido factores de separação entre 1.6 e 7.6. Os dados de pressão-temperatura-composição obtidos foram correlacionados com a equação de estado Peng-Robinson, em combinação com a regra de mistura de Mathias-Klotz--Prausnitz. O modelo ajustou-se bem aos dados experimentais, com um desvio médio absoluto total de 3.7%. Estudou-se a resolução do mentol racémico utilizando duas lipases, nomeadamente *de Candida rugosa* (CRL) e *de Candida antarctica* (CALB) imobilizada, e dois agentes ésteres iónicos. Em nenhum dos casos o mentol reagiu. Testou-se assim outro substrato, o (*R,S*)-1-feniletanol, tendo-se obtido baixos valores de conversão não selectiva com a CRL, mas um excesso enantiomérico (*ee*) do substrato de 95%, a 30% de conversão, no caso da CALB.

Experimentou-se seguidamente outros agentes acilantes na resolução do (\pm)-mentol, nomeadamente esteres vinílicos e anidridos ácidos, utilizando várias lipases e fazendo variar outros parâmetros que influenciam a conversão e a enantioseletividade enzimática, como a concentração dos substratos, solvente e temperatura. Um dos agentes acilantes utilizados foi o anidrido propiónico. Fez-se assim um estudo de equilíbrio de fases para o sistema anidrido propiónico/ CO_2 , numa gama de temperatura entre os 35 e os 50 °C. Este estudo revelou que, a 35 °C e pressões a partir de 7 MPa, o sistema se encontra numa só fase para todas as composições. Os estudos de catálise enzimática realizados com o anidrido propiónico revelaram que a reacção não catalizada decorria em elevada extensão, com consequências negativas na enantioseletividade. Mostraram também que era possível reduzir muito o impacto da reacção não catalizada face ao da reacção catalizada pela CRL baixando a temperatura para 4 °C. Os melhores resultados, em condições mais adequadas à combinação com CO_2 supercrítico como

agente de separação pós-reacção, foram obtidos utilizando decanoato de vinilo em vários líquidos iónicos, nomeadamente [bmim][PF₆], [bmim][BF₄], [hmim][PF₆], [omim][PF₆], e [bmim][Tf₂N], o que permitiu alcançar valores de excesso enantiomérico do produto (*ee_p*) superiores a 96%, para cerca de 50% de conversão, com a CRL. Já em *n*-hexano e CO₂ supercrítico, a reacção progredia mais lentamente. Escolheu-se portanto o decanoato de vinilo para testar duas estratégias de separação para o mentol e respectivo produto, decanoato de mentilo. A primeira, envolvendo um sistema combinado IL/scCO₂, e a segunda, recorrendo ao uso de uma membrana seletiva, num processo de pervaporação. Estudos de partição do mentol e do decanoato de mentilo num sistema bifásico IL/scCO₂ mostraram que, a 35 °C e 7.5 MPa, cerca de metade do mentol permanecia na fase de IL, enquanto o decanoato de mentilo se encontrava maioritariamente na fase de CO₂. Os factores de separação obtidos, embora elevados, não evitariam a necessidade de recorrer a vários separadores, com custos associados elevados. No caso da pervaporação, verificou-se que os dois compostos tinham comportamentos semelhantes, passando ambos através da membrana em extensões muito parecidas.

Recorreu-se então de novo a um agente acilante iónico, desta vez um anidrido. Utilizou-se o (*R,S*)-1-feniletanol como substrato, uma vez que já tinha demonstrado bons resultados anteriormente, com a CALB. A aplicação desta metodologia foi levada a cabo utilizando o IL [bmim][PF₆] como solvente, tendo-se obtido um *ee_p* de 80% a cerca de 50% de conversão, às 24 h de reacção. O álcool que não reagiu foi completamente extraído do meio reacional por uma corrente de CO₂ a 180 bar e 37 °C, durante 3 horas, o que permitiu obter (*S*)-1-feniletanol com um *ee* de 87%. Seguidamente, procedeu-se à hidrólise do éster iónico-produto contendo o outro enantiómero, o que permitiu libertar cerca de 30% do (*R*)-1-feniletanol ligado, após 24 h de reacção. Este enantiómero foi também extraído na totalidade com CO₂. Foi assim possível obter os dois enantiómeros do (*R,S*)-1-feniletanol separados.

Com esta última abordagem atingiu-se o objectivo desta tese.

Palavras-chave:

Enantioselectividade, (\pm)-mentol, lipase de *Candida rugosa*, líquidos iónicos, dióxido de carbono supercrítico, solventes verdes, equilíbrio liquido-vapor.

Abstract

The objective of the work presented in this thesis was the development of an innovative approach for the separation of enantiomers of secondary alcohols, combining the use of an ionic liquid (IL) - both as solvent for conducting enzymatic kinetic resolution and as acylating agent - with the use of carbon dioxide (CO₂) as solvent for extraction. Menthol was selected for testing this reaction/separation approach due to the increasing demand for this substance, which is widely used in the pharmaceutical, cosmetics and food industries.

With a view to using an ionic ester as acylating agent, whose conversion led to the release of ethanol, and due to the need to remove this alcohol so as to drive reaction equilibrium forward, a phase equilibrium study was conducted for the ethanol/(±)-menthol/CO₂ system, at pressures between 8 and 10 MPa and temperatures between 40 and 50 °C. It was found that CO₂ is more selective towards ethanol, especially at the lowest pressure and highest temperature tested, leading to separation factors in the range 1.6-7.6. The pressure-temperature-composition data obtained were correlated with the Peng-Robinson equation of state and the Mathias-Klotz-Prausnitz mixing rule. The model fit the experimental results well, with an average absolute deviation (AAD) of 3.7 %.

The resolution of racemic menthol was studied using two lipases, namely lipase from *Candida rugosa* (CRL) and immobilized lipase B from *Candida antarctica* (CALB), and two ionic acylating esters. No reaction was detected in either case. (*R,S*)-1-phenylethanol was used next, and it was found that with CRL low, nonselective, conversion of the alcohol took place, whereas CALB led to an enantiomeric excess (*ee*) of the substrate of 95%, at 30% conversion.

Other acylating agents were tested for the resolution of (±)-menthol, namely vinyl esters and acid anhydrides, using several lipases and varying other parameters that affect conversion and enantioselectivity, such as substrate concentration, solvent and temperature. One such acylating agent was propionic anhydride. It was thus performed a phase equilibrium study on the propionic anhydride/CO₂ system, at temperatures between 35 and 50 °C. This study revealed that, at 35 °C and pressures from 7 MPa, the system is monophasic for all compositions. The enzymatic catalysis studies carried out with propionic anhydride revealed that the extent of noncatalyzed reaction was high, with a negative effect on enantioselectivity. These studies showed also that it was possible to reduce considerably the impact of the noncatalyzed reaction relative to the reaction catalyzed by CRL by lowering temperature to 4 °C. Vinyl decanoate was shown to lead to the best results at conditions amenable to a process combining the use of supercritical CO₂ as agent for post-reaction separation. The use of vinyl decanoate in a number

of IL solvents, namely [bmim][PF₆], [bmim][BF₄], [hmim][PF₆], [omim][PF₆], and [bmim][Tf₂N], led to an enantiomeric excess of product (*ee_p*) values of over 96%, at about 50% conversion, using CRL. In *n*-hexane and supercritical CO₂, reaction progressed more slowly. Vinyl decanoate was thus selected to test two separation approaches for menthol and its product, menthyl decanoate. The first approach involved the use of a combined IL/scCO₂ system, and the second involved the use of a selective membrane for pervaporation. Partitioning studies for menthol and menthyl decanoate in an IL/scCO₂ biphasic system showed that, at 35 °C and 7.5 MPa, about half of the menthol stayed in the IL phase, whereas most of the menthyl decanoate was in the CO₂ phase. The separation factors obtained, although high, would lead to the need for a series of separators, with high associated costs. In the case of pervaporation, it was found that the two compounds behaved similarly, both crossing over the membrane to comparable extents.

An ionic acylating agent was again used, but this time an anhydride. (*R,S*)-1-phenylethanol was used as substrate, since it had already led to good results when using CALB. This methodology was applied using the IL [bmim][PF₆] as solvent, leading to an *ee_p* of 80% at approximately 50% conversion, at 24 h. The unreacted alcohol was completely extracted from the reaction medium by a stream of CO₂ at 180 bar and 37 °C, for 3 h, which allowed to obtain (*S*)-1-phenylethanol with an *ee* of 87%. The hydrolysis of the ionic ester product, holding the other enantiomer, was then conducted, which led to the release of nearly 30% of bound (*R*)-1-phenylethanol, after 24 h of reaction. This enantiomer was also fully extracted with CO₂. It was thus possible to obtain each of the two enantiomers of (*R,S*)-1-phenylethanol separately.

This last approach allowed the fulfilment of the objective of the thesis.

Keywords

Enantioselectivity, (±)-menthol, *Candida rugosa* lipase, ionic liquids, supercritical carbon dioxide, green solvents, vapor liquid equilibrium.

List of Contents

Acknowledgements.....	ix
Resumo.....	xiii
Abstract	xv
List of Contents	xvii
List of Figures.....	xxi
List of Tables.....	xxv
List of Abbreviations, acronyms and symbols	xxvii

Chapter I	1
1. Introduction	3
1.1. Sustainability and green chemistry	3
1.2. Chirality – The concept.....	6
1.3. Menthol – Background, enantiomers and properties	7
1.4. Biocatalysis.....	10
1.4.1. Lipases.....	11
1.4.1.1. <i>Candida rugosa</i> lipase (CRL)	11
1.4.1.2. <i>Candida antarctica</i> lipase B (CAL B)	12
1.4.2. Reaction mechanism of lipases	13
1.5. Enzymatic Kinetic Resolution. Enzyme enantioselectivity	15
1.5.1. Enzymatic Kinetic Resolution of Secondary Alcohols. The Kazlauskas rule.	16
1.6. Biocatalysis in nonaqueous media. Supercritical carbon dioxide and ionic liquids	19
1.6.1. Supercritical fluids. Supercritical carbon dioxide (scCO ₂).....	20
1.6.2. Ionic liquids (ILs)	22
1.7. Resolution of (±)-menthol and relevance of nonaqueous media	24
1.8. Strategies to facilitate the physical separation of enantiomers	26
1.8.1. Dynamic kinetic resolution	26
1.8.2. Postreaction separation strategies. Pervaporation	26
1.8.3. Combined reaction and separation strategies. IL/scCO ₂ systems	27
1.9. Phase equilibrium measurements	29
1.9.1. Methods for phase equilibria at high pressures	30
1.9.2. Phase equilibrium	31
1.9.3. Phase behavior at high pressure	32
1.9.4. Equations of state (EOS) for mixtures.....	33

1.10. High-pressure phase behavior of systems containing CO ₂ , an ionic liquid, and substrates or products of an enzymatic reaction	35
1.11. Aims and structure of the thesis	36
Chapter II	39
2.1. High pressure vapor-liquid equilibrium for the ternary system ethanol/(±)-menthol/carbon dioxide	41
2.1.1. Introduction	41
2.1.2. Experimental section	41
2.1.2.1. Materials	41
2.1.2.2. Apparatus and experimental procedure.....	42
2.1.2.3. Sample analysis	44
2.1.3. Results and discussion	44
2.1.4. Models and parameters	50
2.1.4.1. Correlations.....	50
2.1.5. Conclusions	56
2.2. Experimental determination and modeling of the phase behavior of the carbon dioxide + propionic anhydride system at high pressure	57
2.2.1. Introduction	57
2.2.2. Experimental section	57
2.2.2.1. Materials.....	57
2.2.2.2. Phase equilibrium measurements	57
2.2.3. Results and discussion	58
2.2.4. Thermodynamic modeling.....	60
2.2.5. Conclusions	62
Chapter III	63
3. Resolution of <i>sec</i> -alcohols using ionic acylating esters	65
3.1. Introduction	65
3.2. Experimental section	66
3.2.1. Materials	66
3.2.2. Preparation of ionic acylating agents	66
3.2.3. Enzymatic resolution of (±)-menthol and (<i>R,S</i>) – 1-phenylethanol	67
3.2.4. General procedure for sampling.....	68
3.2.5. Sample analysis	68
3.3. Results and discussion.....	69
3.4. Conclusions	71

Chapter IV	73
4. Reaction and separation of (±)-menthol enantiomers through the combination of nonaqueous media for biocatalysis, extraction, and membrane separation	75
4.1. Introduction	75
4.2. Experimental	76
4.2.1. Materials	76
4.2.2. Synthesis of (-)-menthyl laurate, (±)-menthyl laurate, (-)-menthyl decanoate and (±)-menthyl decanoate	77
4.2.3. Enzymatic assays in n-hexane, in ILs, and in scCO ₂	77
4.2.4. Reaction analysis	78
4.2.5. Partitioning of substrates and product in biphasic IL/scCO ₂ systems.....	78
4.2.5.1. Mixtures of (±)-menthol and vinyl decanoate	78
4.2.6. Pervaporation method	79
4.3. Results and discussion	80
4.3.1. Reactions with vinyl esters	80
4.3.2. Reactions with propionic anhydride	83
4.3.3. Partitioning of substrates and product in IL/CO ₂ systems	85
4.3.4. Pervaporation	86
4.4. Conclusions	87
 Chapter V	 89
5. Enzymatic resolution/separation of sec-alcohols using an ionic anhydride as acylating agent	91
5.1. Introduction	91
5.2. Experimental section	92
5.2.1. Materials	92
5.2.2. Enzymatic reaction/separation experiments	92
5.2.3. Sample analysis	93
5.3. Results and discussion	94
5.4. Conclusions	97
 Chapter VI	 99
6. Conclusions and Final Remarks	101
References.....	105

List of Figures

Figure 1.1 - Stereoisomers of menthol	8
Figure 1.2 - Ribbon diagram of CRL with open and closed states of the lid superimposed. The central mixed L-sheet is light blue and the smaller N-terminal L-sheet is dark blue. Helices which pack against the central L-sheet are dark green. The closed conformation of the lid is yellow and the open conformation is red. The residues forming the catalytic triad are shown in red.	12
Figure 1.3 - Ping-pong bi-bi mechanism. A and B are substrates, P and Q are products, E and F are different configurations of the free enzyme, EA-FP and FB-EQ are transition states.....	13
Figure 1.4 - Catalytic cycle of ester hydrolysis by CRL	14
Figure 1.5 - Plots for enantiomeric excess (<i>ee</i>) of substrate (a) and product (b) vs. conversion for several values of enantiomeric ratio (<i>E</i>)	16
Figure 1.6 - Binding pocket of CRL	17
Figure 1.7 - Prediction of the enantioselectivity of lipases for secondary alcohols as regards the Kazlauskas rule	18
Figure 1.8 - Comparison of the transition state for the fast and slow reacting enantiomers of menthol in the active site of CRL	18
Figure 1.9 - Carbon dioxide pressure-temperature phase diagram.....	21
Figure 1.10 - The separate phases of CO ₂ (liquid and vapour). As temperature and pressure increase (from left to right), the system becomes homogeneous and is called “supercritical fluid”	21
Figure 1.11 - Common structures of ILs used for biocatalysis	23
Figure 1.12 - Methodology for the enzymatic resolution and separation of sec-alcohols. CALB = lipase B from <i>Candida Antarctica</i>	29
Figure 1.13 - Vapour - liquid equilibrium (VLE).....	31
Figure 2.1 - Schematic representation of the VLE apparatus	42
Figure 2.2 - Sapphire tube cell showing a biphasic liquid + vapor system at equilibrium	44
Figure 2.3 - Composition (mole fraction) of CO ₂ in the liquid and vapor phases for the (±)-menthol/CO ₂ binary system at 323 K. This work (×). Sovová <i>et al.</i> (□).....	45
Figure 2.4 - CO ₂ mole fractions at 313 K for several feed compositions of (±)-menthol on a CO ₂ -free basis: (◆) 1.000, (■) 0.750, (▲) 0.500, (✱) 0.250, (●) 0.....	48
Figure 2.5 - Separation factor as a function of pressure at 313 K (Figure 2.5 a) and 323 K (Figure 2.5 b), for several feed compositions of (±)-menthol on a CO ₂ -free basis: (■) 0.750, (▲) 0.500, (✱) 0.250. Lines are just guide-lines.....	49

Figure 2.6 - Separation factor as a function of pressure for a fixed feed composition of (\pm)-menthol on a CO ₂ -free basis of 0.750. (◆) 313 K, (▲) 323 K. Lines are just guide-lines.....	50
Figure 2.7 - Correlation of the pT_{xy} experimental data using the PR-EOS/MKP-MR model, at 313 K (●) and 323 K (■). Points represent experimental data.....	51
Figure 2.8 - pT_{xy} experimental data for the ethanol/(\pm)-menthol/CO ₂ ternary system at 323 K and 8, 9 and 10 MPa. The points are experimental data and lines were obtained by fitting with the PR-EOS/MKP-MR model.....	53
Figure 2.9 - pT_{xy} experimental data for the ethanol/(\pm)-menthol/CO ₂ ternary system at 313 and 323 K, at 8 MPa. The points are experimental data and lines were obtained by fitting with the PR-EOS/MKP-MR model.....	54
Figure 2.10 - pT_{xy} experimental data for the ethanol/(\pm)-menthol/CO ₂ ternary system at 313 K and 9 MPa. The points are experimental data and lines were obtained by fitting with the PR-EOS/MKP-MR model.....	55
Figure 2.11 - A schematic view of the three-phase (L ₁ L ₂ V), system inside the sapphire tube cell.....	55
Figure 2.12- A real view of the three phases (L ₁ L ₂ V), inside the sapphire tube cell.....	55
Figure 2.13 - A view of the sapphire tube cell showing the ethanol/(\pm)-menthol/CO ₂ ternary system as it reaches the three-phase region.....	56
Figure 2.14 - Apparatus used for the phase equilibrium measurements.....	58
Figure 2.15 – VLE data for the CO ₂ /propionic anhydride binary system at 308 K (▲), 313 K (■) and 323 K (●).....	60
Figure 2.16 - Fitting of the pT_{xy} experimental data (symbols) for the CO ₂ /propionic anhydride binary system by the PR-EOS/MKP-MR model (lines) at 308 K (▲), 313 K (■) and 323 K (●).....	62
Figure 3.1 – Preparation of methyl-3-(11-ethoxycarbonylundecyl) imidazolium hexafluorophosphate (a) and 1-methyl-3-(11-ethoxycarbonylundecyl) imidazolium tetrafluoroborate (b).....	67
Figure 3.2 - Scheme for the EKR of (\pm)-menthol in [bmim][PF ₆], using an acylating agent based on the imidazolium cation, using a lipase as biocatalyst.....	69
Figure 3.3 - (<i>R,S</i>)-1-phenylethanol	71
Figure 4.1 - Diagram of the high-pressure apparatus for substrate/product partitioning studies	79
Figure 4.2 - Apparatus used for the pervaporation assays	80
Figure 4.3 - Menthol conversion as a function of reaction time when using CRL and vinyl decanoate as acylating agent, at 37 °C. [enzyme] = 100 mg/mL. ◇, [bmim][PF ₆]. △, [hmim][PF ₆]. x, [bmim][BF ₄]. ○, [omim][PF ₆]. □, [bmim][NTf ₂]. ■, n-hexane. ▲, scCO ₂	82
Figure 4.4 – Concentration of (+)-menthol (white bars) and (–)-menthol (light gray bars), and ee_s (darker gray bars; right Y-axis) as a function of reaction time when using CRL and vinyl decanoate as acylating agent, in [hmim][PF ₆] at 37 °C. [enzyme] = 100 mg/mL. ee_p was >96%	83

Figure 4.5 – Menthol conversion as a function of reaction time when using CRL and propionic anhydride as acylating agent, at 37 °C. [enzyme] = 100 mg/mL. Δ , [hmim][PF₆]. \circ , [omim][PF₆]. \square , [bmim][NTf₂]. \blacktriangle , scCO₂. Inset: ee_p at nearly 50% menthol conversion.....84

Figure 4.6 – Formation of (-)-menthyl propionate (open symbols) and (+)-menthyl propionate (closed symbols) as a function of reaction time when using CRL and propionic anhydride as acylating agent, in n-hexane, at 4 °C (Δ , \blacktriangle) and 37 °C (\circ , \bullet). [enzyme] = 100 mg/mL. The dashed lines represent the consumption of (+)-menthol at 4 °C (x) and 37 °C (+) in the blank without enzyme.....85

Figure 5.1 - Scheme for the EKR of (*R,S*)-1-phenylethanol with the IL bis((1(11-undecanoic acid)-3-methyl)imidazolium hexafluorophosphate) anhydride94

Figure 5.2 - Scheme with the methodology for the enzymatic resolution and separation of (*R,S*)-1- phenylethanol (steps 1 and 2)95

Figure 5.3 - Scheme with the methodology for the enzymatic resolution and separation of (*R,S*)-1- phenylethanol (steps 3 and 4)95

List of Tables

Table 1.1 - The 12 Principles of Green Chemistry	4
Table 1.2 - The 12 Principles of Green Engineering	5
Table 1.3 - Improvements Productively	5
Table 1.4 - E factor in the Chemical Industry	6
Table 1.5 - Comparison of physical properties of gases, supercritical fluids and liquids	20
Table 1.6 - Critical points of some substances	20
Table 1.7 - Measurements of high-pressure phase equilibrium	30
Table 2.1 - Vapor-liquid equilibrium data for the (\pm)-menthol/ CO_2 binary system	45
Table 2.2 - Vapor-liquid equilibrium data for the ethanol (1)/(\pm)-menthol (2)/ CO_2 (3) ternary system	47
Table 2.3 - Pure component physical properties	50
Table 2.4 - Optimized interaction parameters for the (\pm)-menthol / CO_2 binary system at 8, 9 and 10 MPa, at 313 and 323 K, using the PR-EOS/MKP-MR model	51
Table 2.5 - Optimized interaction parameters for the ethanol (1)/(\pm)-menthol (2)/ CO_2 (3) ternary system at the temperatures and pressures indicated, using the PR-EOS/MKP-MR model	52
Table 2.6 - Phase behavior of the CO_2 (1)/propionic anhydride (2) binary system expressed in mole fraction of carbon dioxide (χ_{CO_2})	59
Table 2.7 - Pure component physical properties	61
Table 2.8 - Optimized interaction parameters for the CO_2 /propionic anhydride binary system at 308 K(\blacktriangle), 313 K(\blacksquare) and 323 K (\bullet), using the PR-EOS/MKP-MR model	61
Table 3.1 - Screening of two different ionic acylating agents a) and b) and two different enzymes for the EKR of (\pm)-menthol using as solvent [bmim][PF ₆], under different pressures, at 35 °C	70
Table 4.1 – Effect of enzyme, acylating agent and temperature on the conversion of menthol and the ee of menthyl decanoate and of menthol, at 48 h reaction in n-hexane. [enzyme] = 20 mg/mL	82
Table 4.2 - Partitioning of menthol and menthyl decanoate in [bmim][PF ₆]/ CO_2 systems. P = 7.5 MPa. Results are given as wt.% of total amount of compound used in the experiment	86
Table 4.3 – Permeation of menthol and menthyl decanoate, dissolved in [bmim][BF ₄], through a PERVAP™ 4060 membrane. Results are given as wt.% of total amount of compound that remained in the cell, relative to the total amount used in the experiment	87
Table 5.1 – Results for reactions carried out using Novozym as biocatalyst, bis((1(11-undecanoic acid)-3-methyl)imidazolium hexafluorophosphate) anhydride as acylating agent, and an IL as	

solvent, at 35 °C, as part of a four-step methodology for the separation of (<i>R,S</i>)-1-phenylethanol enantiomers. c = conversion	96
Table 5.2 – Efficiency of the extraction of the separate (<i>R,S</i>)-1-phenylethanol enantiomers using scCO ₂ . The % values given are relative to the amount of alcohol quantified in the IL solvent before hydrolysis ((<i>S</i>)-enantiomer) and after hydrolysis ((<i>R</i>)-enantiomer)	97

List of abbreviations, acronyms and symbols

%	percent
z_i	fraction component i in mixture
μL	microliter
μm	micrometre
a, b	equation of state mixture parameters
AAD	absolute average deviation
atm	atmosphere
BASF	Baden Aniline and Soda Factory
BP	bubble point
BSE	<i>Bacillus subtilis</i> esterase
C	number of components
ca.	<i>circa</i> ; approximately
CALA	<i>Candida antarctica</i> lipase A
CALB	<i>Candida antarctica</i> lipase B
$-\text{CH}_3$	methyl group
CLA	cross-linked aggregates
cm	centimetre
cm^2/s	square centimetre per second
CO_2	carbon dioxide
$-\text{COOH}$	carboxyl
C_R	concentration of (<i>R</i>)-enantiomer
CRL	<i>Candida rugosa</i> lipase
C_S	concentration of (<i>S</i>)-enantiomer
DCC	N,N'-Dicyclohexylcarbodiimide
DES	deep eutectic solvent
DKR	dynamic kinetic resolution
DMAP	4-Dimethylaminopyridine
DMF	dimethylformamide
DP	dew point
E	enantioselectivity
e.g.	<i>exempli gratia</i> ; for example
EC	Enzyme Commission
ee	enantiomeric excess
ee_p	enantiomeric excess of product
ee_s	enantiomeric excess of substrate
EKR	Enzymatic kinetic resolution
EPA	Environmental Protection Agency
eq.	equivalent
<i>et al.</i>	<i>et alli</i> ; and others
Et_2O	diethyl ether
EtOAc	ethyl acetate
F	number of degrees of freedom
FDA	Food and Drug Administration

FID	flame ionization detector
g	gram
GC	gas chromatography
h	hour
H & R	Haarman and Reimer
H ₂ O	water
HPLC	high-pressure liquid chromatography
i.e.	<i>id est</i> ; in other words
IL	ionic liquid
K	degree Kelvin
K	partition coefficient
k, l, λ	binary interaction parameters
KDa	kilodalton
KF	Karl-Fischer
kg	kilogram
mbar	millibar
min	minute
MKP-MR	Mathias-Klotz-Prausnitz mixing rule
mL	millilitre
mm	millimetre
mM	millimolar
mm Hg	millimetre mercury
mmol	milimole
MPa	megapascal
°C	degree Celsius
-OH	hydroxyl group
P	pressure
P	number of phases in equilibrium
Pa	Pascal
P_c	critical pressure
PE	phase equilibrium
PID	proportional-integral-derivative
PR-EOS	Peng-Robinson equation of state
R	universal gas constant
r	number of reaction equilibria relations
RTIL	room temperature ionic liquid
s	second
scCO ₂	supercritical carbon dioxide
SCF	supercritical fluid
T	temperature
t	time
T_c	critical temperature
TSILs	task specific ionic liquids
v/v	volume per volume
VLE	vapor-liquid equilibrium

VOC	volatile organic compound
w/w	weight per weight
wt%	weight percentage
α	separation factor
K	constant
V	molar volume
a	energy parameter
b	co-volume parameter
c	concentration
f	fugacity
i, j	components of the mixture
n	number of data points
x	liquid mole fraction
y	vapor mole fraction
φ	fugacity coefficient
ω	acentric factor

Ionic Liquids

$[(CF_3SO_2)_2N^-]$	bistrifluoromethylsulfonyl imide
[bmim][BF ₄]	1-Butyl-3-methylimidazolium tetrafluoroborate
[bmim][PF ₆]	1-Butyl-3-methylimidazolium hexafluorophosphate
[bmim][Tf ₂ N]	1-Butyl-3-Methylimidazolium bis(trifluoromethanesulfonyl)imide
[EtNH ₃] ⁺ [NO ₃] ⁻	ethylammonium nitrate
[hmim][PF ₆]	1-Hexyl-3-methylimidazolium hexafluorophosphate
[omim][PF ₆]	1-Methyl-3-octylimidazolium hexafluorophosphate

Chapter I

Introduction

1. Introduction

1.1. Sustainability and green chemistry

Over the last decades, chemistry has had a strong impact in our society. Its presence can be perceived in countless products, from fuels to complex drugs in the pharmaceutical industry. However traditional chemistry involves hazardous materials and generates large amounts of dangerous waste. It became essential to create a new approach, and the scientific community has been finding creative ways to minimize human and environmental impact without compromising scientific progress, giving rise to a new area of research called Green Chemistry [1].

Green Chemistry is concerned with the design of chemical products and processes that reduce or eliminate the generation of hazardous substances. Green chemistry is not a cleanup approach, but a prevention approach. A main role of chemistry is to ensure that the next generation of products, materials and energy is more sustainable than the current one. The risk associated with a chemical compound depends both on how dangerous it is (hazard) and on one's contact with it (exposure) (Equation 1.1).

$$\textit{risk} = \textit{hazards} \times \textit{exposure} \quad (1.1)$$

A few years ago, industry and governments were focused on reducing the risk by minimizing exposure. Procedures were created to limit the exposure of workers to hazardous chemicals and to control the release of these products into the environment, in particular, air and water. However, this approach is expensive; it is difficult to establish a safe level of hazardous chemicals, and currently, only a small fraction of the chemicals manufactured are regulated. Green chemistry focuses on reducing or eliminating the hazard. The dangerous materials are eliminated and replaced with non-hazardous ones [1].

In 1983, the United Nations founded the "World Commission on Environment and Development", which was given the task of preparing "A global agenda for change". Later, the publication "Our Common Future" appeared, which interconnects social, cultural and environmental issues and global solutions. It was mentioned that "the environment does not exist as a sphere separated from human's actions, ambitions and needs, and therefore it should not be considered in isolation from human concerns. The environment is where we all live; and

development is what we all do in attempting to improve our lot within that abode. The two are inseparable” [2].

In the early 1990's, Anastas and his colleagues at the US Environmental Protection Agency (EPA) created the concept “Green Chemistry”. Using a simple approach, Anastas and Warner developed and condensed the concepts, objectives and guidelines of green chemistry in twelve principles [3]. Some of these principles appear to be little more than the application of common sense to chemical processes, but the truth is that their combined implementation requires a great effort in the design and development of products and processes. Table 1.1 outlines an early perception of what would make a greener chemical process, or product.

Table 1.1- The 12 Principles of Green Chemistry [3].

1. Prevention	7. Use of Renewable Feedstocks
It is better to prevent waste than to treat or clean up waste after it has been created.	A raw material or feedstock should be renewable rather than depleting whenever technically and economically practicable.
2. Atom Economy	8. Reduce Derivatives
Synthetic methods should be designed to maximize the incorporation of all materials used in the process into the final product.	Unnecessary derivatization (use of blocking groups, protection-deprotection, and temporary modification of physical-chemical processes) should be minimized or avoided if possible, because such steps require additional reagents and can generate waste.
3. Less Hazardous Chemical Synthesis	9. Catalysis
Synthetic methods should be designed to use and generate substances that possess little or no toxicity to human health and the environment.	Catalytic reagents (as selective as possible) are superior to stoichiometric reagents.
4. Designing Safer Chemicals	10. Design for Degradation
Chemical products should be designed so that their toxicity is minimized.	Chemical products should be designed so that at the end of their function they break down into innocuous degradation products and do not persist in the environment.
5. Safer Solvents and Auxiliaries	11. Real-time Analysis for Pollution Prevention
The use of auxiliary substances (such as solvents and separation agents) should be made unnecessary wherever possible and innocuous when used.	Analytical methodologies need to be further developed to allow for real-time, in-process monitoring and control prior to the formation of hazardous substances.
6. Design for Energy Efficiency	12. Inherently Safer Chemistry for Accident Prevention
Energy requirements of chemical processes should be recognized for their environmental and economic impacts and should be minimized.	Substances and the form of a substance used in a chemical process should be chosen to minimize the potential for chemical accidents, including releases, explosions, and fires.

Later, Anastas and Zimmerman, in order to evolve the Principles, suggested 12 more principles, this time from an engineering point of view [4]. Green engineering motivations are related to how to achieve sustainability through science and technology [4]. The 12 Principles of Green Engineering (Table 1.2) offer a new context to be followed by scientists and engineers when they want to create and design new materials, products, systems and processes that are friendly to human health and to the environment [4,5].

Table 1.2 - The 12 Principles of Green Engineering [4].

1. Inherent Rather Than Circumstantial	7. Durability Rather Than Immortality
Designers need to strive to ensure that all materials and energy inputs and outputs are as inherently nonhazardous as possible.	Targeted durability, not immortality, should be a design goal.
2. Prevention Instead of Treatment	8. Meet Need, Minimize Excess
It is better to prevent waste than to treat or clean up waste after it is formed.	Design for unnecessary capacity or capability (e.g., "one size fits all") solutions should be considered a design flaw.
3. Design for Separation	9. Minimize Material Diversity
Separation and purification operations should be designed to minimize energy consumption and materials use.	Material diversity in multicomponent products should be minimized to promote disassembly and value retention.
4. Maximize Efficiency	10. Integrate Material and Energy Flows
Products, processes, and systems should be designed to maximize mass, energy, space, and time efficiency.	Design of products, processes, and systems must include integration and interconnectivity with available energy and materials flows.
5. Output-Pulled Versus Input-Pushed	11. Design for Commercial "Afterlife"
Products, processes and systems should be "output pulled" rather than "input pushed" through the use of energy and materials.	Products, processes, and systems should be designed for performance in a commercial "afterlife."
6. Conserve Complexity	12. Renewable Rather Than Depleting
Embedded entropy and complexity must be viewed as an investment when making design choices on recycle, reuse, or beneficial disposition.	Material and energy inputs should be renewable rather than depleting.

Poliakoff and his colleagues proposed two mnemonics, which aim to highlight the spirit of all the principles described above - Improvements Productively (Table 1.3).

Table 1.3 - Improvements Productively [6].

I – Inherently non-hazardous and safe	P – Prevent wastes
M – Minimize material diversity	R – Renewable materials
P – Prevention instead of treatment	O – Omit derivatisation steps
R – Renewable material and energy inputs	D – Degradable chemical products
O – Output-led design	U – Use of safe synthetic methods
V – Very simple	C – Catalytic reagents
E – Efficient use of mass, energy, space & time	T – Temperature, Pressure ambient
M – Meet the need	I – In-Process monitoring
E – Easy to separate by design	V – Very few auxiliary substrates
N – Networks for exchange of local mass and energy	E – E-factor, maximize feed in product
T – Test the life cycle of the design	L – Low toxicity of chemical products
S – Sustainability throughout product life cycle	Y – Yes, it is safe

After defining Green Chemistry it becomes necessary to compare processes and products in order to reduce waste. It is very important to determine if one method of making a product is better than another, mainly in terms of environmental impact. One such metric is called the E

Factor, or the Environmental Impact Factor. The E factor is the measure of the amount of waste generated while making a product, and is defined by [7][8]:

$$E \text{ factor} = \frac{\text{mass of waste}}{\text{mass of product}} \quad (1.2)$$

The lower the E factor, the less waste is produced. Using Equation 1.2, it is possible to evaluate the dimension of the environmental problems associated with processes carried out in different segments of the chemical industry.

As seen in Table 1.1, the E factor increases radically in the segments of fine chemicals and in the pharmaceutical industry. These processes involve multi-step synthesis and downstream processing, which results in the waste of large amounts of solvents and the generation of by-products. Larger E Factors are also due to the common use of classical stoichiometric reagents instead of catalysts [8].

Table 1.4 – E factor in the Chemical Industry [5]

Industry Segment	Volume (tons/year) ^a	E Factor (kg waste/kg product)
<i>Bulk Chemicals</i>	10 ⁴ -10 ⁶	< 1-5
<i>Fine Chemicals</i>	10 ² -10 ⁴	5 to >50
<i>Pharmaceutical Industry</i>	10-10 ³	25 to >100

^a Annual production world-wide

In order to solve some of these problems, alternatives can be adopted, as for example the use of environmentally compatible solvents, such as water, or alternative solvents, such as supercritical fluids (SCFs) and ionic liquids (ILs), and the use of enzymes as catalysts. These alternatives can bring many benefits in terms of green approaches [9], and will be referred to later.

1.2. Chirality – The concept

The phenomenon of chirality is very common in Nature. The term chirality is related with “mirror-image, non-superimposable molecules”. One molecule is considered as chiral if it can exist as isomers (enantiomers) that are non-superimposable mirror images of each other. Jean Baptist Biot observed for the first time this property in the case of tartaric acid, in 1832. Louis

Pasteur continued this research, with the discovery of molecular chirality and spontaneous resolution [10,11].

Commonly the source of chirality is the asymmetric center, although restricted rotation around axes or planes can be the source of chirality as well. The chiral centers are tetrahedral atoms (usually carbons) that have four different substituents. If one molecule has one asymmetric center, it has one pair of enantiomers. If it has more than one asymmetric center, the pairs of enantiomers will usually increase. Some enantiomers appear alone (only one enantiomer), but others appear in the form of racemic mixtures, with equal amounts of each enantiomer. Enantiomers have identical physical properties, except for the fact that they rotate plane-polarized light in opposite directions. Racemic mixtures are thus optically inactive. The fact that the physical properties of enantiomers are nearly all identical makes the resolution of racemic mixtures very difficult to achieve through conventional methods of separation.

The two enantiomers of a racemic mixture are identified on the basis of their configuration, or their optical rotation. Designations such as *d*, for *dextro*, and *l*, for *levo*, are no longer recommended. In the case of sugars and amino acids, the nomenclature D/L is used. The recommended terms for absolute configuration, according to the 3-dimensional structure of the molecule, are (*R/S*) – *R* from the Latin designation *rectus* (right), and *S* from the Latin *sinister* (left) – and (+/-) for optical rotation. Generally, racemates can be designated as (*R,S*) or (\pm) [12]. Market demand for enantiomerically pure compounds has been growing, especially in the pharmaceutical and agrochemical industries. If only one enantiomer is active for the envisaged application, administering the racemic mixture means delivering 50% of what can be considered an impurity, the effects of which may not be well understood, and may even be harmful. The alternative to using racemic mixtures is to find a way to produce the substance as a pure isomer, or to separate the isomers from the racemic mixture. Both of these options are difficult and expensive. Nevertheless, it is clear that many pharmaceuticals must be administered as pure isomers to produce the desired results with no side effects. This has led to a great effort directed to the synthesis and separation of chiral compounds.

1.3. Menthol – Background, enantiomers and properties

Menthol is the most popular flavor and is the best-selling aroma ingredient in the world. It is used extensively in pharmaceuticals, cosmetics, toothpaste, chewing gum, candies and other products. Normally menthol is associated to the essence of freshness, but menthol owes its

popularity not only to its fresh taste, but also to its cooling effect on the skin and mucous membranes. This is the reason why it is frequently used in the pharmaceutical and cosmetics industries, e.g. in cooling lotions, inhalation and toilet products, deodorants and shower gels [13]. The demand for menthol has been constantly growing due to the continuous development of new products containing menthol. Menthol has an annual production of about 20.000 tons and the current worldwide demand of 25.000 to 30.000 tons per year already exceeds the available supply.

Menthol is a secondary alcohol, namely a terpene. Terpenes are found in essential oils or in the form of their oxygenated derivatives, such as alcohols, aldehydes, ketones, esters or carboxylic acids. The menthol molecule has three chiral centers – C-atoms 1, 2 and 5 – which results in 4 pairs of enantiomers (8 stereoisomers): (±)-menthol, (±)-isomenthol, (±)-neomenthol and (±)-neo-isomenthol (Fig. 1.1).

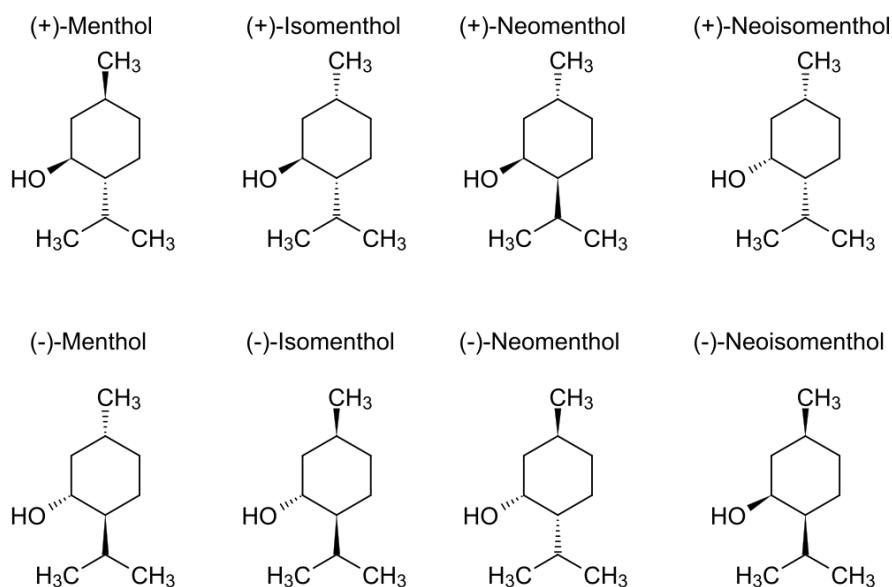


Figure 1.1 - Stereoisomers of menthol [14].

A racemic mixture of menthol contains (-)-(*1R, 2S, 5R*)-menthol and (+)-(*1S, 2R, 5S*)-menthol. Of these two forms, (-)-menthol is the enantiomer that occurs most widely in nature and the one that is mostly referred to as “menthol”. (-)-menthol is perceived to have the most favorable set of characteristics. It has a characteristic peppermint odor and exerts the well-known cooling sensation [13,15].

Menthol can be obtained from nature or produced synthetically. Menthol can be extracted from plants of the *Lamiaceae* family, such as *Mentha*, *Peppermint* and *Mentha arvensis*, as corn mint,

peppermint or other mint oils [13,15]. Most of pure (-)-menthol is obtained by freezing the oil of *Mentha arvensis* to crystallize (-)-menthol. Afterwards (-)-menthol crystals are separated by centrifuging the supernatant liquid (dementholized cornmint oil). Traces of *Mentha arvensis* oil may remain as impurity, which confers a slight peppermint aroma to the menthol crystals [13]. In the last decades, and due to the economic importance of menthol, a considerable effort has been done by several companies to find an efficient synthetic route to produce (-)-menthol. It is not easy to achieve a good yield of pure (-)-menthol through chemical synthesis. In nature, the process is controlled by an enzyme, (-)-methonone reductase, which reduces (-)-menthone to (-)-menthol. Only two processes of chemical synthesis are considerable sustainable at industrial level: the Haarmann & Reimer process (H & R), and the Takasago process [16–18].

The H & R process (also known as Symrise Process) is the market leader, comprising a synthetic route to obtain (-)-menthol from thymol. Thymol is synthesized from m-cresol (of petrochemical origin). The formation of thymol results from the alkylation of m-cresol with propene in the presence of a metal catalyst (aluminium). Then, thymol is hydrogenated to give a mixture of menthol isomers. (±)-menthol is obtained by fractional distillation. The residual mixture is epimerized catalytically (i.e. through a change in configuration of a single chiral center), thus increasing the amount of racemic menthol. The latter is esterified to (±)-menthyl benzoate. The crucial step in the separation of the two enantiomers is crystallization by seeding the concentrate with (-)-menthol. (+)-menthol is recycled back to the distillation cycle. (-)-menthyl benzoate is hydrolyzed to give (-)-menthol. The total yield of (-)-menthol is around 90% [16–18]. In the Takasago process, menthol enriched in (-)-menthol is produced on the scale of 3.000 tons per year. The process is based on an asymmetric synthesis developed by Ryōji Noyori, who won the Nobel Prize for Chemistry in 2001, in recognition for this contribution. In this process, myrcene, a natural monoterpene, reacts with lithium amide, yielding diethylgeranylamine. The crucial step of this process is the isomerization of the latter compound to yield 3R-citronellal enamine, using a chiral ruthenium catalyst. The enamine is hydrolysed to give high purity 3R-(+)-citronellal. Acid hydrolysis of the enamine gives (R)-citronellal, which undergoes zinc catalysed conversion to isopulegol. Finally, hydrogenation over a nickel catalyst gives (-)-menthol [16,17]. Since 2012, BASF has extended to (-)-menthol a production platform starting from citral, in which (+)-(R)-citronellal is converted to (-)-isopulegol, which is then hydrogenated to (-)-menthol (similarly to the Takasago process) [19].

As summarized above, one of the commercial synthetic routes to (-)-menthol involves the use of a chiral catalyst. Enzymes are chiral. The demand for (-)-menthol of superior quality has driven research into the use of enzymatic catalysis as an alternative to processes of chemical synthesis to obtain (-)-menthol.

1.4. Biocatalysis

Enzymes are proteins which catalyze a wide range of biochemical reactions. They are present not only in animals and plants, but also in filamentous fungi, bacteria and yeasts. As any catalyst, biocatalysts increase reaction rates without being consumed, not changing the chemical equilibrium of the reaction. Their major role is the acceleration of the reaction rate by providing alternative reaction paths with more favorable activation energy in comparison with non-catalyzed transformations [20].

Enzymes present some advantages relatively to chemical catalysts, in particular due to their selectivity towards substrate, namely enantioselectivity – preference for one enantiomer – regioselectivity – preference for a given functional group when it is in a specific location on the substrate molecule – and chemoselectivity – preference for one functional group of the substrate over others [21].

The constant interest for enantiomerically pure and specifically functionalized compounds makes biocatalysts particularly attractive for applications in the pharmaceutical, agrochemical and food industries [22].

Typically enzymes exhibit high activity at mild conditions (as regards pressure, temperature and range of pH values), which minimizes problems of product isomerization, racemization or epimerization. Furthermore, biocatalysts can be very efficient, and capable of increasing reaction rates up to 10^{12} [22].

Additionally and from a sustainable point of view, these catalysts are biodegradable and are also considered natural products. Biocatalytic processes are less hazardous and the energy consumed is lower compared with conventional catalysts, especially when heavy-metal catalysts are used. But there may also be disadvantages, such as low stability under more severe conditions, and cost [23].

There are six enzyme classes, based on the type of reaction catalyzed [24]: EC1- Oxidoreductases; EC2 - Transferases; EC3 - Hydrolases; EC4 – Lyases; EC5 – Isomerases; EC6 - Ligases (EC = Enzyme Commission). Of these, hydrolases are the most widely used, accounting for almost 80% of all industrial enzymes. Their applications include household care products, the food and beverages sector, bioenergy, agriculture and feed, technical and pharma. Oxidoreductases come next, but their use is limited by their dependence on cofactors and strategies for recycling these [25].

In this thesis, lipases will be addressed in more detail, given that they were the biocatalysts used during this work. Lipases are a subclass of the esterases, which are hydrolases that catalyze the hydrolysis of ester bonds.

1.4.1. Lipases

Lipases catalyze hydrolysis, alcoholysis, esterification and transesterification of carboxylic acids and esters. They have been used successfully in the detergents, food, paper, and pharmaceutical industries, including applications in the resolution of racemic mixtures and the synthesis of chiral intermediates [26,27] .

In common with other hydrolases, lipases have α / β -hydrolase "fold" (a central hydrophobic sheet, which consists of eight different β chains linked to six α helices), an active site formed by a triad of catalytic residues – Serine (Ser), Aspartic acid (Asp) (or Glutamic acid, Glu) and Histidine (His) – an oxyanion cavity and, in most cases, a hydrophobic "lid" formed by a α helix that covers the active site of the enzyme. The serine residue of the catalytic triad is positioned exactly at the same position as the central β sheet, a highly preserved pentapeptide [28].

Lipases have a high performance in reaction systems that contain an organic and an aqueous phase. The lid that covers the active site is composed by polar amino acids in the external part, and by less polar amino acids in the internal part that faces the active site. The lid is closed when lipases are in contact with aqueous solutions, blocking access of substrate molecules to the active site. Consequently lipase activity in aqueous media is very low. However, in the presence of substrate aggregates in aqueous media that originate a hydrophobic-hydrophilic interface, or in the presence of a hydrophobic solvent, there is a conformational change in the enzyme leading to stabilization of the open lid conformation, allowing access to the active site. This phenomenon is known as interfacial activation [29–31].

Interest in lipases derives from the fact that they accept a great variety of substrates, have high stability, do not require expensive co-factors and can be obtained in high yield from microorganisms, such as fungi and bacteria [32].

1.4.1.1. *Candida rugosa* lipase (CRL)

Candida rugosa lipase (CRL) is one of the enzymes most frequently used in biotransformations, due to its high activity and efficiency in reactions of hydrolysis and esterification.

The yeast *Candida rugosa* (formerly *Candida cylindracea*) is a non-sporogenic, pseudo-filamentous, unicellular and non-pathogenic microorganism. CRL produces at least five isoenzymes that had been very well studied by several authors [33].

Each enzyme has a single polypeptide chain containing 543 amino acids and a molecular weight of 60 kDa, with a well-defined catalytic triad comprising Ser 209, His 449 and Glu 341, and an overarching flap at the active site.

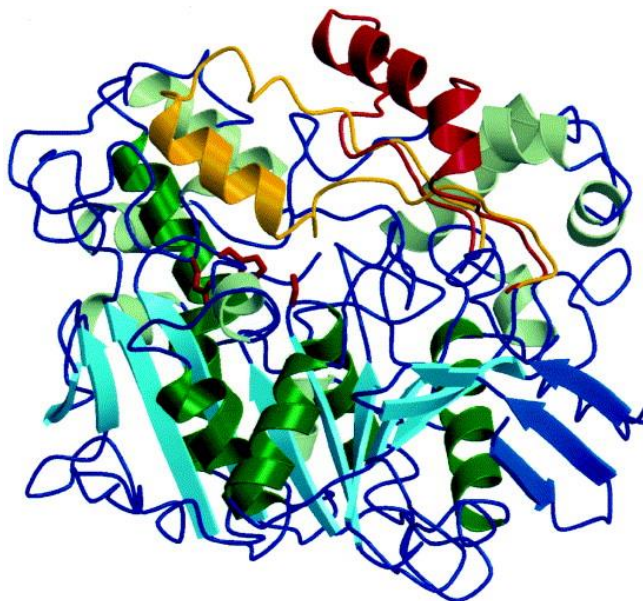


Figure 1.2 - Ribbon diagram of CRL with open and closed states of the lid superimposed. The central mixed L-sheet is light blue and the smaller N-terminal L-sheet is dark blue. Helices which pack against the central L-sheet are dark green. The closed conformation of the lid is yellow and the open conformation is red. The residues forming the catalytic triad are shown in red. Adapted from [34].

1.4.1.2. *Candida antarctica* lipase B (CALB)

Lipase B from *Candida antarctica* (CALB) is one of the most used enzymes in biocatalysis. CALB was isolated from a fungus of the genus Basidiomycetes. The yeast *Candida antarctica* was originally isolated in Antarctica and was subsequently used to produce two variants of lipase, CALB and CALA, which were cloned and expressed in *Aspergillus oryzae*. CALB is highly resistant to extreme conditions (high stability at alkaline pH and very high temperatures) [35,36]. CALB is commonly reported to be a “workhorse” of biocatalysis due to its flexibility in accepting many substrates and to its high activity, when compared to other lipases.

In 1994, Uppenberg *et al.* reported on the three dimensional structure of CALB. This protein has a molecular mass of 33 KDa and a sequence of 317 amino acids. The crystalline structure shows an α / β hydrolase fold with an active site composed of a catalytic triad, formed by residues of

Serine, Histidine and Aspartic acid (Ser 105 – His 224 – Asp 187), common to serine hydrolases [37].

Most lipases have the active site closed, covered by a hydrophobic “lid”. CALB is one of the exceptions. CALB has a hydrophobic helix with five residues ($\alpha 5$ helix), which was identified as a potential “cap”, although later it was found that this “cap” was not involved in any conformational change regulating access to the active site, but rather acts as a lipidic binding surface, attaching the lipase to the oil-water interface [37].

CALB is a well characterized enzyme with many applications. It is marketed as different preparations, in free form or immobilized by physical interactions (adsorption) within a macroporous resin (Novozym[®] 435). In immobilized form, this enzyme is quite stable for long periods of time in the temperature range 60-80 °C, particularly in nonaqueous conditions [38,39].

1.4.2. Reaction mechanism of lipases

The reaction mechanism of lipases is usually described by the ping-pong bi-bi model. This model is said to be followed when the enzyme alternates between two states (ping-pong) and reacts with two substrates to give two products (bi-bi). The first group being transferred is first displaced from substrate (A) by the enzyme (E), to form product (P) and a modified form of the enzyme (F) – the acylenzyme. Next, the second substrate (B) binds to the acylenzyme (F), thereby forming the product (Q) and regenerating the enzyme (E) (Fig. 1.3) [40].



Figure 1.3 - Ping-pong bi-bi mechanism. A and B are substrates, P and Q are products, E and F are different configurations of the free enzyme, EA-FP and FB-EQ are transition states.

The two steps of the reaction mechanism are acylation and deacylation. Acylation starts with the formation of a noncovalent enzyme substrate complex, followed by a nucleophilic attack by the oxygen of Ser to the carbon atom of the carbonyl group of the first substrate (the acylating

agent), yielding the first tetrahedral transition state. A proton is transferred from Ser to His (Asp or Glu must be deprotonated to stabilize the charge developed). The tetrahedral intermediate then collapses, as His releases a proton to reform the double bond on the carbonyl group of the substrate, and the first product is released. In the deacylation step, the second substrate performs a nucleophilic attack on the acylenzyme, and through the action of His, a second tetrahedral intermediate is formed, which collapses to release the second product and return the enzyme to its initial form, ready for another catalytic cycle [41].

Figure 1.4 shows the catalytic mechanism for the hydrolysis of an ester by CRL. The scheme includes the catalytic triad (Ser 209, Glu 341, His 449) and the oxyanion hole, which consists of the backbone of the amino acid residues Gly 123, Glu 124 and Ala 210. The model substrate is methyl acetate. In transesterification, deacylation involves nucleophilic attack by an alcohol instead of water.

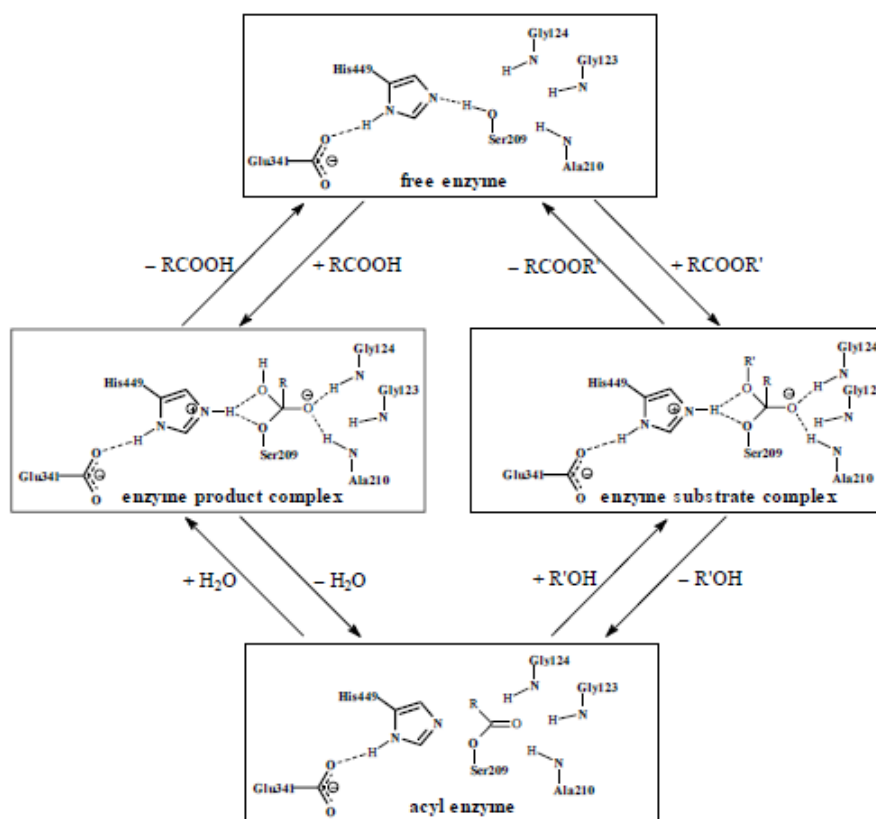


Figure 1.4 - Catalytic cycle of ester hydrolysis by CRL. Adapted from [42].

1.5. Enzymatic Kinetic Resolution. Enzyme enantioselectivity.

Enzymatic kinetic resolution (EKR) is one of the methods used in the resolution of racemic mixtures. The main requirement of this process is that one of the two enantiomers of the racemic mixture react much faster than the other one with a given substrate, as is the case when the activation energies involved are very different [43]. Under these circumstances, at 50% conversion the product formed originates essentially in the fast reacting enantiomer, while the slow reacting enantiomer is essentially not altered. If the reaction is stopped then, the two enantiomers are found in different chemical forms, which facilitates their separation. When the difference in reaction rates of the two enantiomers is less pronounced, the enantiomeric enrichment of both the starting compound and the product formed decrease.

The extent of enantiomeric enrichment can be measured through the enantiomeric excess (*ee*) and the enantiomeric ratio (*E*).

ee is derived from the concentration of the two enantiomers, and can be defined by equation 1.3 [44].

$$ee (\%) = \left| \frac{C_S - C_R}{C_S + C_R} \right| \times 100 \quad (1.3)$$

C_R and C_S are the concentration of the (*R*)- and (*S*)- enantiomers, respectively, of substrate or product.

E can be calculated from the concentrations of the two enantiomers, according to Equation 1.4. This equation is equivalent to equations 1.5 and 1.6 in the case where the biocatalytic reaction is irreversible.

$$E = \frac{\ln(C_S/C_{S0})}{\ln(C_R/C_{R0})} \quad (1.4)$$

$$E = \frac{\ln[1-c(1+ee_p)]}{\ln[1-c(1-ee_p)]} \quad (1.5)$$

$$E = \frac{\ln[(1-c)(1-ee_s)]}{\ln[(1-c)(1+ee_s)]} \quad (1.6)$$

C_{S0} and C_{R0} are the initial concentrations of the (*S*)-enantiomer and the (*R*)-enantiomer, respectively, at the start of reaction, *c* is the conversion, and *ee_p* and *ee_s* are the enantiomeric excess of the product and the substrate, respectively [45].

E is a ratio of the specificity constants of the enzyme for each enantiomer [44]. As such, it is an intrinsic property of the biocatalyst, which responds to factors that affect the binding and catalytic conversion of each enantiomer, such as solvent used, temperature, pH, etc.

When the value of E is lower than 15, enantiomer separation is considered inefficient, for E values between 15 and 30, just efficient, and for E values higher than 30, very efficient [46].

The conversion (c) can be calculated using ee_s and ee_p :

$$c(\%) = \frac{ee_s}{ee_s + ee_p} \times 100 \quad (1.7)$$

The figure below (Fig. 1.5) illustrates the interplay between conversion, ee_s (a) and ee_p (b), for different E values.

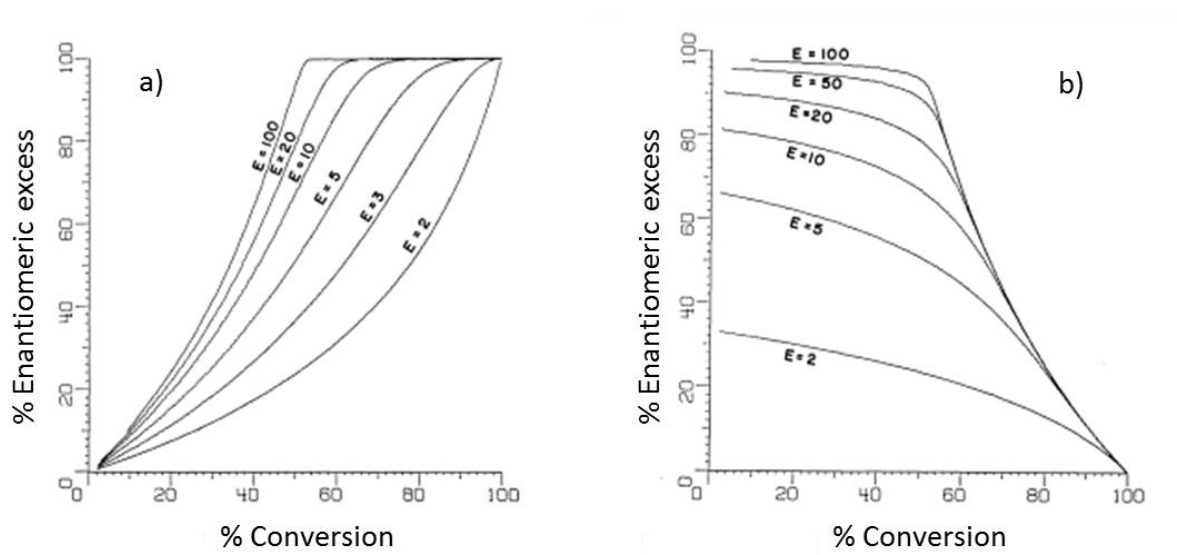


Figure 1.5 - Plots for enantiomeric excess of substrate (a) and product (b) vs. conversion for several values of enantiomeric ratio (E). Adapted from [47].

1.5.1. Enzymatic Kinetic Resolution of Secondary Alcohols. The Kazlauskas Rule.

The synthesis of enantiomerically pure secondary alcohols is very important for the pharmaceutical industry, since these compounds are widely used as intermediates in the production of active pharmaceutical ingredients. The enzymatic kinetic resolution of racemic secondary alcohols is one of the major routes to obtain pure alcohol enantiomers, together with the asymmetric reduction or hydrogenation of prochiral ketones [48].

Kazlauskas and coworkers established a rule for the chiral recognition of secondary alcohols by lipases, based on a model of the enzyme active site with pockets with different sizes [49]. A secondary alcohol contains two different substituents attached to its chiral center. Most of the lipases have two different binding pockets in the area of the alcohol binding site that can accept the two substituents of the secondary alcohol. In the case of CRL, a large binding pocket is positioned at the entrance to the alcohol binding site, whereas a medium size binding pocket is positioned deeper inside the lipase structure (Figure 1.6) [50,51].

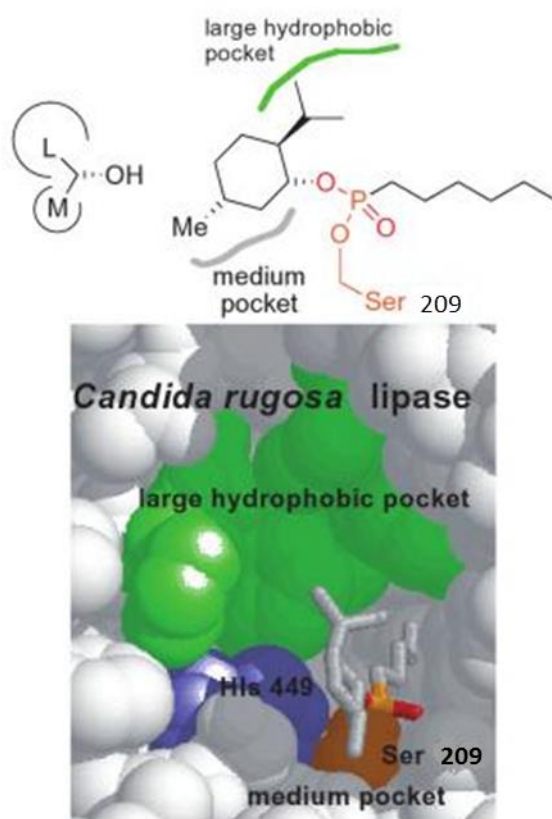


Figure 1.6 - Binding pocket of CRL. Adapted from [51].

The enantiomer which better fits into the active site of the enzyme will react faster (Fig. 1.7). Lipase enantioselectivity is thus seen to originate in the different sizes of the binding pockets. The bigger of the two substituents of a secondary alcohol cannot fit into the medium size-binding pocket and prefers to sit inside the large binding pocket. The Kazlauskas rule thus generally predicts a preference for the (*R*)-enantiomer [49,52,53] due to the difficulty in fitting the larger substituent of the (*S*)-enantiomer into the medium size (smaller) binding pocket.

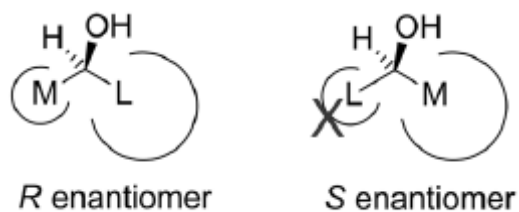


Figure 1.7 - Prediction of the enantioselectivity of lipases towards secondary alcohols as regards the Kazlauskas rule. Adapted from [50].

Figure 1.8 shows how the Kazlauskas rule applies to (\pm)-menthol. The L, M and O substituents assume similar locations in the binding of each enantiomer, but not the hydrogen atom. The enantiomer that reacts faster - menthol (1*R*) - shows the expected hydrogen bonds for catalysis, whereas menthol (1*S*) lacks a key hydrogen bond, in part because the isopropyl substituent pushes the catalytic histidine away [51].

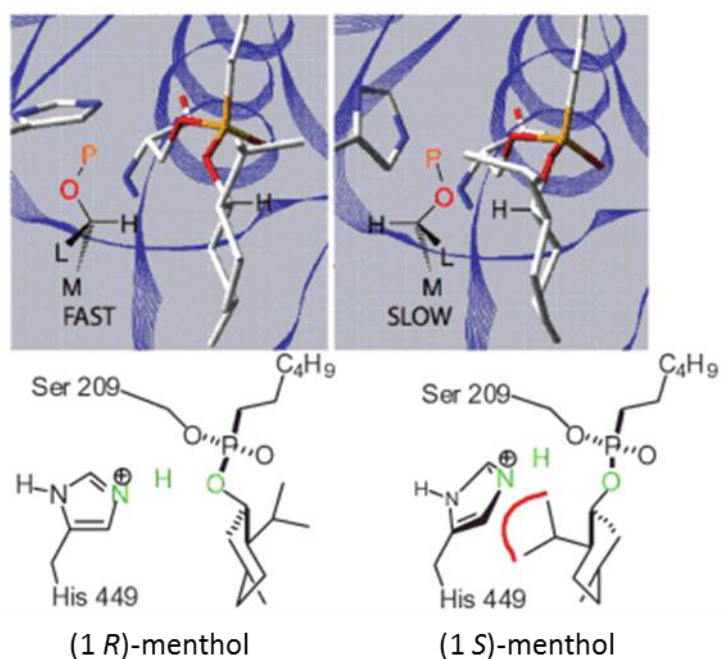


Figure 1.8 - Comparison of the transition state for the fast and slow reacting enantiomers of (\pm)-menthol in the active site of CRL. Adapted from [51].

1.6. Biocatalysis in nonaqueous media. Supercritical carbon dioxide and ionic liquids.

As mentioned earlier, EKR is a well-established, efficient route for the preparation of optically active alcohols. Nevertheless, the separation step can be a drawback. At a laboratory scale, and after preferential conversion of one of the enantiomers into a different chemical compound through e.g. hydrolysis, esterification or transesterification reaction, the two enantiomers that still coexist in the same phase can be separated using chromatographic techniques. Applying these techniques on an industrial scale can be too expensive. This has led to separation strategies such as distillation [54], precipitation [55], sublimation [56], membrane processes [57], crystallization [58], and the use of nonaqueous media such as ionic liquids (ILs) [59] or supercritical CO₂ (scCO₂) [60], as well as combined IL/scCO₂ systems [61].

Biocatalysis offers many benefits as regards sustainable chemistry. A major benefit is the fact that enzymes are biodegradable catalysts. But for a long period of time it was thought that enzymes were restricted to their natural environment, i.e. aqueous reaction media at room temperature and pressure, and physiological pH. However it was found that enzymes can operate with high efficiency in adverse and extreme conditions of temperature, pressure, pH, high salt conditions, the presence of additives and non-natural media [62].

In the mid 80's of the last century, Klibanov and co-workers showed that enzymes were active in dehydrated organic solvents [63]. In such media, enzyme thermal stability was enhanced and selectivity could be altered, to the point of a reversal of enantioselectivity.

These discoveries together with the need for active and selective catalysts to be applied in new product development, such as enriched enantiomeric compounds, contributed to the development of biocatalysis into an area of commercial interest [64].

Organic media, supercritical fluids and ionic liquids are examples of nonaqueous media that have been extensively applied in enzymatic reactions [29,62,65]. Many organic solvents are toxic, flammable, or corrosive. Their volatility contributes to air pollution and in pharmaceutical syntheses a large amount of solvent is used, contributing to hazardous waste streams. Thus the choice of solvent is particularly important, ionic liquids (ILs) and supercritical carbon dioxide (scCO₂) continuing to receive a lot of attention [61,66,67].

1.6.1. Supercritical fluids. Supercritical carbon dioxide (scCO₂)

Supercritical fluids have favourable transport properties, adjustable solvent power and allow the design of a production process with integrated downstream separation of products and unreacted substrates.

As seen in Table 1.5, supercritical fluids have higher diffusivity and lower viscosity than liquids, which facilitates mass transfer and can improve reaction rates. Supercritical fluids also have densities and solvent power that can be similar to those of liquids, which facilitates the dissolution of solutes.

Table 1.5 - Comparison of physical properties of gases, supercritical fluids and liquids [68].

	Diffusivity (cm ² /s)	Density (g/mL)	Viscosity (Pa.s)
Gases	0.1	10 ⁻³	10 ⁻⁵
Supercritical Fluids	10 ⁻³	0.3	10 ⁻⁴
Liquids	5 x 10 ⁻⁶	1	10 ⁻³

Supercritical CO₂ (scCO₂) is the supercritical fluid of choice. CO₂ is available with high purity, it is non-toxic and non-flammable. Its critical pressure is moderate and its critical temperature adequate for work with thermolabile substances. Small changes in pressure close to the critical point lead to significant changes in density, facilitating downstream separation. By simple depressurization of the system, no solvent residues will be found in the final product.

Table 1.6 shows the most commonly used supercritical fluids and their corresponding critical parameters, and helps understand the preference for scCO₂.

Table 1.6 - Critical points of some substances [68].

Solvent	Critical Temperature (<i>T_c</i> , °C)	Critical Pressure (<i>P_c</i> , MPa)
Carbon dioxide	31.1	7.38
Methane	82.6	4.60
Ethane	32.2	4.87
Propane	96.7	4.25
Methanol	239.5	8.08
Ammonia	132.4	11.32
Water	374.0	22.06

Fig. 1.9 shows the P, T conditions at which CO₂ exists as a gas, a liquid, a solid or as a supercritical fluid. The curves represent the temperature and pressure at which two phases coexist in equilibrium (at the triple point, the three phases coexist).

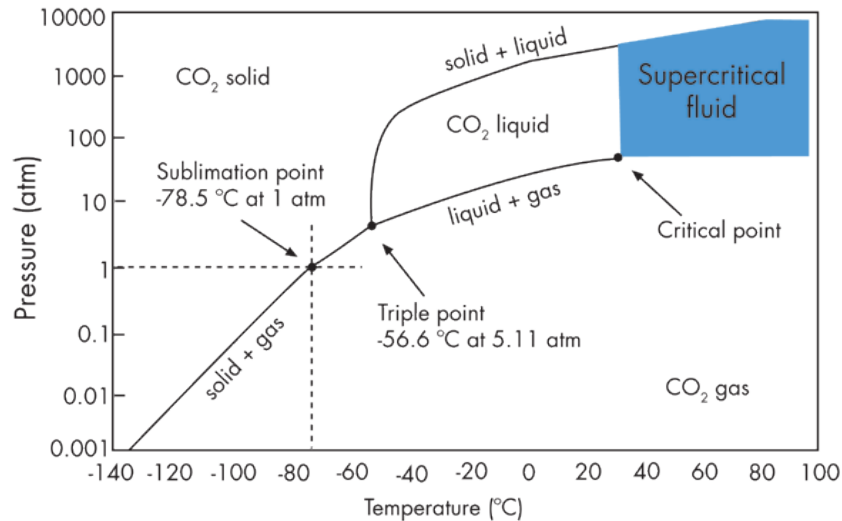


Figure 1.9 – Carbon dioxide pressure-temperature phase diagram.

Moving upwards along the vaporization curve, increasing both temperature and pressure, the liquid becomes less dense due to thermal expansion and the gas becomes denser as the pressure rises. Eventually, the densities of the two phases converge and become identical, the distinction between gas and liquid disappears, and the vaporization curve comes to an end at the critical point.

Fig. 1.10 shows a high pressure cell containing CO₂, as it goes from a two-phase, liquid + gas system, below its critical point, to a supercritical fluid, above the critical point, where the meniscus separating the two phases has disappeared.



Figure 1.10 – The separate phases of CO₂ (liquid and vapour). As temperature and pressure increase (from left to right), the system becomes homogeneous and is called “supercritical fluid”. Adapted from [69].

The first applications of scCO_2 were as solvent for extraction, such as the extraction of caffeine from coffee beans [70], or of oil from corn fiber [71]. ScCO_2 is also an excellent medium for chemical reactions [72–75], dry cleaning [76], synthesis and processing of polymers [77,78], and separation processes, such as the separation of fatty acids [79] and enantiomers (in this case, CO_2 is used as a solvent in supercritical fluid chromatography [80]). Since Randolph *et al.* reported on the use of scCO_2 for enzymatic reactions in 1985 [81], this solvent has been extensively used in biocatalysis [65,82–84]. The combination of a sustainable and clean technology, such as biocatalysis, with a green/natural solvent, such as scCO_2 , allows the implementation of processes with lower environmental impact, and also leads to products considered as natural, and thereby with a significant increase in market value [85].

In some cases, lower enzyme catalytic activities have been reported in scCO_2 , which have been attributed to the formation of carbonic acid or the formation of carbamates with amine groups on the enzyme [86]. As with other supercritical fluids, the use of scCO_2 involves the need for high pressure equipment and considerable energy costs that must be considered when envisaging commercial applications [83,87].

1.6.2. Ionic liquids (ILs)

Room temperature ionic liquids (RTILs, or simply ILs) are organic salts that are liquid at, or slightly above, room temperature, and are made up of an anion and a cation. The term “designer solvents” is commonly applied to ILs, due to their extremely versatility: through the combination of different cations and ions, ILs can be obtained with very different physical and chemical properties, such as melting point, viscosity, density, solvation ability, and hydrophobicity [88]. ILs also have excellent thermal stability and are not readily flammable [68]. One of the most important characteristics of ILs is their negligible vapour pressure, which means that they are essentially non-volatile and can be completely recycled [89]. This is a great advantage over volatile organic compounds (VOCs).

The first materials that would now be recognized as ILs were observed as far back as the mid-19th century, during a Friedel-Crafts reaction [90]. Later in 1914, Paul Walden published a paper with the synthesis of ethylammonium nitrate, $[\text{EtNH}_3]^+ [\text{NO}_3]^-$, described as the first RTIL [91]. In 1948, Hurley and Wier developed, for electroplating, an aluminium-based IL with chloroaluminate ions [92]. The research involving ILs continued, but only focused on electrochemical applications. Seddon and Hussen, in the 1980s, started to use chloroaluminate melts as nonaqueous polar solvents in the field of transition metal complexes [93]. At the end

of the 1990s, ILs became one of the most promising chemicals as solvents, with recognized potential as “green” media.

Nowadays, a challenging task is to have ILs comprising more stable and hydrophobic anions. Some good examples of these anions are bistrifluoromethylsulfonyl imide $[(CF_3SO_2)_2N^-]$, sugars, amino acids, alkylsulfates and alkylphosphates. Choline is a common cation, as well as imidazolium, pyridinium, ammonium, phosphonium, while common anions include, tetrafluoroborate (BF_4^-), hexafluorophosphate (PF_6^-), and halides, as shown in Figure 1.11. It is to be noted that some cations and/or anions are biodegradable (e.g. cholinium and ammonium-based ionic liquids), which is a very favorable characteristic for many applications.

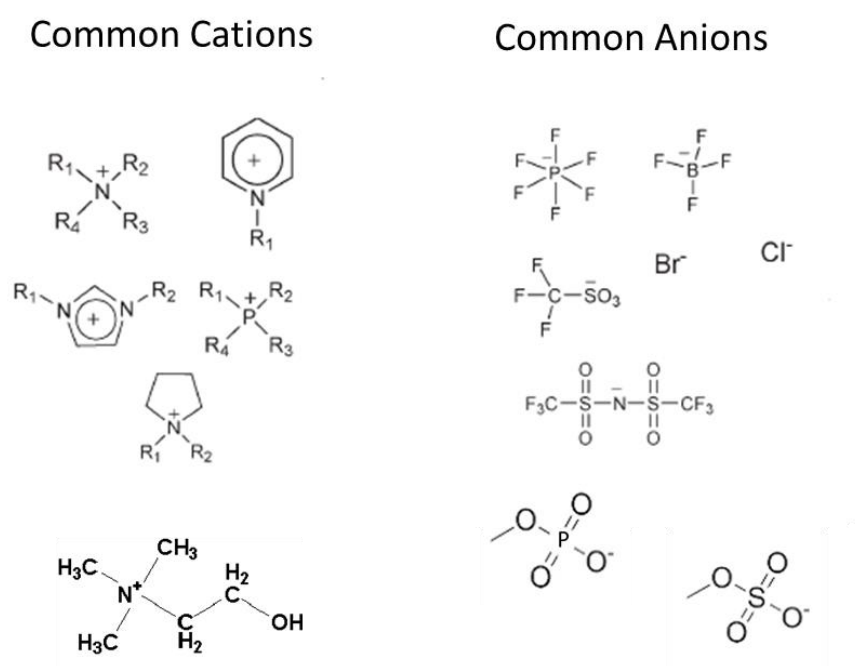


Figure 1.11 - Common structures of ILs. Adapted from [94].

ILs now play an important role as solvents for biocatalysis. It is known that polar organic solvents, such as methanol or DMF, can inactivate enzymes. However, ILs have a polarity similar to these solvents but many of them do not inactivate enzymes, as is the case of 1-butyl-3-methyl-imidazolium hexafluorophosphate ($[bmim][PF_6]$) and 1-butyl-3-methyl-imidazolium tetrafluoroborate $[bmim][BF_4]$. One argument that is used to analyze these effects is water activity (a_w). a_w is a concentration corrected for interactions between water and other components. Enzymes need water to express their activity, but do not need to be in aqueous media to be active, as the early studies by Klivanov showed [95]. When an enzyme with a given hydration is placed in a hydrophilic solvent, it may lose some of its water to the solvent and

change its level of hydration to a value yielding a catalytic activity below optimal. Hydrophobic solvents, on the other hand, have low water stripping ability and the water molecules that hydrate the enzyme do not have a tendency to partition to the solvent. The water stripping effect is avoided if solvent and enzyme are at the same a_w . Another important finding is that at the same a_w , the hydration of an enzyme is practically the same in all the solvents [96].

The analysis of the water stripping effects of ILs is based on the assumption that the hydrophobicity of the IL depends mostly on the cation, whereas the anion is responsible for the interaction of the IL with the water molecules. This latter effect may lead to water stripping effects in media where a_w is not controlled [97]. But there are cases when enzyme hydration cannot explain the effect of ILs on enzymes, as seen in studies with ILs with anions such as acetate, nitrate, trifluoroacetate [98]. The negative impact of such ILs on enzymes has been attributed to the fact that those anions are more nucleophilic than $[\text{PF}_6]^-$ and can coordinate strongly to positively charged sites on the enzyme structure, leading to conformational changes on the enzyme. On the other hand, ILs are reported to have a protective effect on enzymes, as in studies with CRL in $[\text{bmim}][\text{PF}_6]$ and $[\text{omim}][\text{PF}_6]$, where enzyme activity was higher than in organic media, as well as enzyme stability, with good enzyme recyclability and selectivity [98–100].

But there are also disadvantages associated with the use of ILs. One of them is the cost. There is also the question of how green these solvents are. In some cases, their synthesis uses reagents that are considered toxic. On the other hand, environmental effect and toxicity studies showed that in general, the toxicity of ILs depends on both ions and that the effect of the cation alkyl chain length is very strong, although the type of anion also affects the overall toxicity. The prediction of the impact of ILs on human health and environment is under constant research [101,102]. On the other hand, some ILs are viscous and this can lead to mass-transfer limitations in extraction and reaction processes [103].

1.7. Resolution of (±)-menthol and relevance of nonaqueous media

One of the most widely used biocatalysts for the enzymatic kinetic resolution of secondary alcohols, and particularly (±)-menthol, is *Candida rugosa* lipase (CRL) [104–114].

Stereoselective reactions of (±)-menthol using acid anhydrides as acylating agents, namely acetic, propionic, and butyric anhydride, have been successfully performed with CRL [104–110].

The most commonly used solvents for menthol conversion comprised a variety of hydrophobic organic solvents, especially *n*-hexane and cyclohexane [104–109], as well as ILs, such as [bmim][PF₆] and [bmim][BF₄] [108,110], as well as scCO₂ [111].

Xu *et al.* reported on efficient enantioselective esterification by CRL using an acid anhydride as acyl donor in fed-batch mode in cyclohexane [104]. Wu *et al.* reported on the effect of different menthol:acid anhydride molar ratios on the enantioselective synthesis of menthyl propionate and menthyl butyrate in *n*-hexane. The authors obtained an *ee* of 87% for menthyl butyrate and an *ee* of 67% for menthyl propionate after 24 h of reaction, using CRL [105]. Yuan *et al.* looked at the performance of CRL in the enantioselective esterification of (±)-menthol, using propionic anhydride as acylating agent in ILs and organic solvents. The enzyme showed comparable conversion, yield and enantioselectivity in [bmim][PF₆] and *n*-hexane, although in IL medium less acid anhydride was required to achieve higher (±)-menthol conversion and enantioselectivity [108]. The authors obtained an *ee_p* > 88 % for (-)-menthyl propionate. They mentioned higher stability of CRL after long-term incubation in IL. Wang *et al.* studied the resolution of (±)-menthol in cyclohexane, using CRL immobilized on DEAE-Sephadex and several acylating agents, valeric acid yielding an *ee_p* > 95 %. Shimada *et al.* also used acids as acylating agents, namely oleic, linoleic and α-linoleic acid, obtaining an *ee* of (-)-menthyl oleate of 88% after 32h of reaction in a solvent-free system [112]. Using scCO₂, the results were not very encouraging. Michor *et al.* reported on the transesterification of (±)-menthol with isopropenylacetate, triacetin and *n*-butyl acetate. They used several enzymes as catalysts and obtained high enantioselectivity when using lipase AY30 from *Candida rugosa* (Amano), although reaction rates were very low [111].

The resolution of racemic (±)-menthol has been carried out using mostly commercial preparations of CRL. Other approaches include that of Vorlová *et al.*, who used one of the isoenzymes present in commercial CRL lipase preparations to hydrolyze (±)-menthyl benzoate, obtaining (-)-menthol with > 99% enantiomeric excess (*ee*), at nearly 50% conversion. The authors found that the enzyme also allowed efficient resolution of (±)-menthyl acetate and (±)-menthyl valerate. The reactions were performed in sodium phosphate buffer [113]. Chen *et al.* used also an isoenzyme of CRL to perform the resolution of (±)-menthol in *n*-hexane via esterification with triacetin, and obtained (-)-menthyl acetate with 94% *ee* at 48% conversion [114].

The selective transesterification of L-menthol from an 8 isomer mixture was studied by Brady *et al.* Vinyl acetate was used as an acylating agent and *Pseudomonas fluorescens* lipase (Amano AK) was selected as a suitable selective biocatalyst. An enantiomeric excess of L-menthol above

95% and a conversion of 30% (DL-menthol) was achieved [115]. Zheng *et al.* showed that *Bacillus subtilis* exhibits a high hydrolytic activity and an excellent enantioselectivity towards l-menthyl ester. The authors obtained an ee_p of 98% and a 49% conversion in only 3 hours [116]. A recombinant esterase cloned from *Bacillus subtilis*, in the form of cross-linked enzyme aggregates (CLA-BSE), was used in the kinetic resolution of DL-menthyl acetate to produce L-menthol with an $ee_p > 94\%$ at a conversion of 40% [117]. Gong *et al.* used directed evolution to create a thermostable mutant of *Bacillus subtilis* esterase for the production of l-menthol through enantioselective hydrolysis of dl-menthyl acetate [118]. Following the same approach, a recombinant lipase from *Pseudomonas alcaligenes* was used for the resolution of dl-menthyl propionate to produce l-menthol with very high enantioselectivity [119].

1.8. Strategies to facilitate the physical separation of enantiomers.

1.8.1. Dynamic kinetic resolution.

The main problem with EKR is that the chemical yield is limited to 50%. This can be overcome by combining EKR with *in situ* racemisation of the least reactive enantiomer, in what is called dynamic kinetic resolution (DKR) [66].

Chemical catalysts are usually used for racemization. For this process to be effective, the enzyme must be very selective for one of the enantiomers. Also the racemization reaction must be faster than the conversion of the slow reacting enantiomer by the enzyme, so that the enzyme is always surrounded by a much higher concentration of its preferred enantiomer. Another condition is that enzyme and chemical catalyst being compatible.

1.8.2. Postreaction separation strategies. Pervaporation.

When DKR is not or cannot be used, an additional, postreaction step is needed to separate/isolate the two enantiomers, already in different chemical forms, such as chromatography, distillation, liquid-liquid extraction, membrane process, among others [120]. The choice of method depends on cost, which is influenced by factors such as the energy involved, and amount of solvent to be used. There are also environmental issues to consider when volatile media are used.

Pervaporation is a separation process in which a mixture of compounds can be separated by partial vaporization through a nonporous membrane. The membrane material is fundamental for the success of the separation in terms of selectivity and permeability [121]. Both organic and inorganic membranes can be used, the choice depending on the compounds to be separated.

During the process, the feed mixture stays in direct contact with one side of the lipophilic membrane. The permeate is removed in a vapor state from the opposite side, with vacuum, and then condensed. The driving force for the transport of the solute through the membrane is a gradient in chemical potential, which is established by applying a difference in partial pressures of the permeates through the membrane [122,123].

Pervaporation is a method with interesting advantages in terms of green character. Normally separation processes involve the use of organic solvents, but in this case that is not necessary, since the membrane acts as a non-miscible solid solvent.

1.8.3. Combined reaction and separation strategies. IL/scCO₂ systems

One of the alternatives for the separation of enantiomers is the use of combined IL/CO₂ systems. In this kind of system, the enzyme is “immobilized” in the IL phase, where the enzymatic transformation occurs. The substrates and products can be carried into and out of the IL by the scCO₂ phase. ScCO₂ is highly soluble in ILs and can thus fluidize the IL phase, facilitating mass transfer. Blanchard and co-workers showed that for example in [bmim][PF₆], one of the solvents used in this thesis, supercritical CO₂ can dissolve to approximately 0.6 mole fraction, while no residue of this IL is detected in the vapor phase [124]. By not dissolving in scCO₂, the IL does not add complexity to the scCO₂ phase and facilitates product recovery. At the end of the process, it is possible to obtain the pure products without the use of organic solvents, in a completely solvent-free form, and the enzyme/IL mixture can be recycled and re-used, in line with the principles of Green Chemistry.

The potential of these biphasic systems lies also in the fact that the use of an IL as co-solvent helps to overcome the limitations of scCO₂ as a solvent. ScCO₂ can dissolve hydrophobic compounds mostly. Through the combination with an IL, both hydrophobic and hydrophilic compounds that can be solubilized in the IL can be processed. By choosing an appropriate IL and reaction strategy, it may be possible to adjust the partitioning of the species involved in the reaction, namely the solutes of interest that can be extracted by scCO₂. By changing the temperature and pressure of scCO₂, its solvation ability can be adjusted so as to allow the fractionation of a mixture of solutes from the reaction mixture [125,126].

This type of approach has been applied to the separation of secondary alcohols. For example, Reetz and co-workers used vinyl laurate as the acylating agent for the resolution of racemic (*R,S*)-1-phenylethanol, using lyophilized and immobilized CALB. The racemic alcohol and the acylating agent were transported into the reactor using scCO_2 as the mobile phase. Inside the reactor, one of the enantiomers was esterified selectively by the enzyme in the IL, and the products were continuously extracted in the scCO_2 flow. The separation of the enantiomers was very efficient, with $ee_s = 98.9\%$ and $ee_p = 99.5\%$ [61].

Lozano and co-workers used immobilized CALB (Novozym 435) together with a chemical catalyst (silica modified with benzenesulphonic acid groups) in three different ILs – [emim][NTf₂], [btma][NTf₂] and [bmim][PF₆] – for the DKR of (*R,S*)-1-phenylethanol. Reaction yield reached 50 % rapidly, and enantioselectivity was $ee_p = 91\text{--}98\%$ [66].

The combination of an IL with scCO_2 can be taken one-step further by using an ionic acylating agent. In this case, in addition to directly contributing to the formation of a two-phase system, as normally exploited in separation processes, the IL plays the key role of chemical anchor to one of the enantiomers, greatly facilitating the physical separation/recovery of the two enantiomers [127]. Lourenço *et al.* applied this approach to the resolution of (*R,S*)-1-phenylethanol by CALB, using [bmim][PF₆] and [bmim][BF₄] as solvents. The authors used two different esters as acylating agents, based on imidazolium cations in different combinations (Fig.1.12) The slow-reacting enantiomer was isolated in 51 % yield, with 80,9% ee , and the fast-reacting enantiomer was isolated in 41.3 % yield and 99.3 % ee [127]. In the transesterification reaction, one of the products formed was ethanol. To shift reaction equilibrium towards product formation, ethanol had to be removed. The ILs are non-volatile, and thus allowed non-reversible transformation by removal of ethanol under reduced pressure.

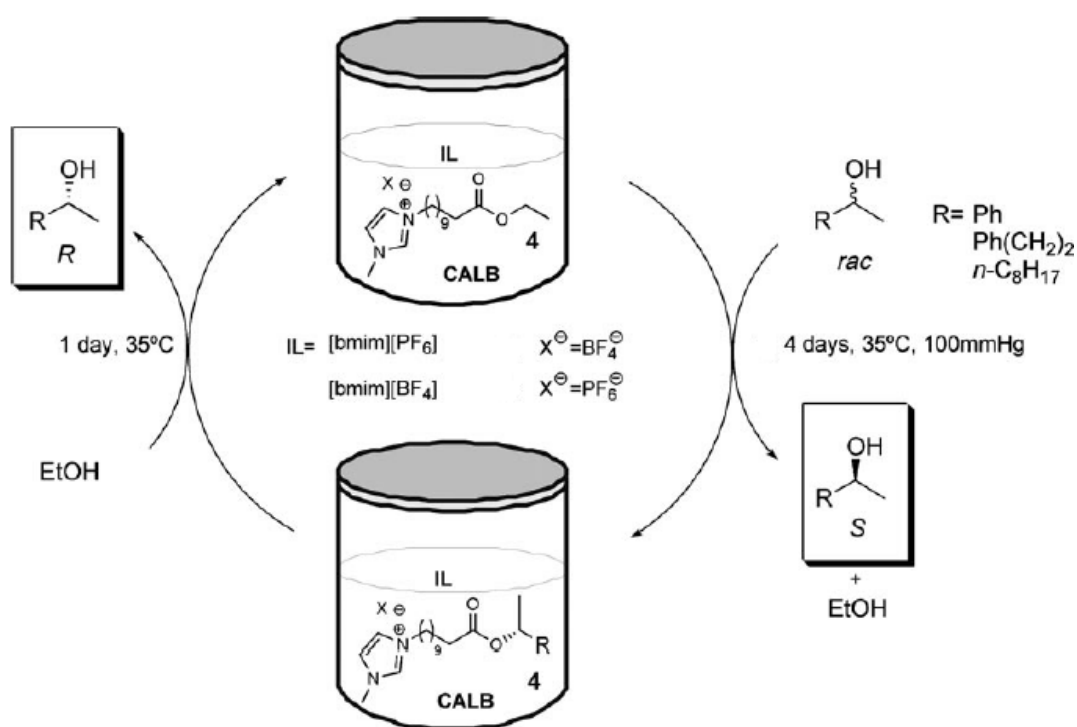


Figure 1.12 - Methodology for the enzymatic resolution and separation of *sec*-alcohols. CALB = lipase B from *Candida antarctica*. Adapted from [127].

Recently Teixeira, *et al.* reported for the first time on the synthesis and application of an anhydride IL as acylating agent in the lipase-catalysed kinetic resolution of different *sec*-alcohols, using acetone as reaction media. The authors used (*R,S*)-1-phenylethanol. The slow-reacting enantiomer was isolated in 58 % yield, with 80 % *ee*, and the fast-reacting enantiomer was isolated in 40 % yield and over 99.9 % *ee* [128].

1.9. Phase equilibrium measurements

Phase equilibrium data is very important for the design and optimization of several industrial processes, such as chemical reactions (e.g. solubility studies and distribution of components in different phases) and separations processes (e.g. distillation, extraction, etc.).

One of the variables that control thermodynamic equilibrium and affect the composition of the coexisting phases is pressure. Thus methods that involve high pressure phase equilibrium, as supercritical fluid applications, gas processing, polymer processing, petroleum reservoir simulations, enhanced oil recovery, carbon capture and storage, refrigeration and heat-pump

cycles, applications of ionic liquids and studies of geological processes, require phase equilibrium data [129]. Consistent data and precise measurements are difficult to achieve, especially when it comes to multicomponent systems.

1.9.1. Methods for phase equilibria at high pressures

There are a wide variety of methods that can be applied in experimental studies of phase equilibrium at high pressure. In this thesis, two main types of methods for the measurement of high-pressure phase equilibrium will be discussed, namely the analytical method, where the compositions of the equilibrium phases are determined, and the synthetic method, where the mixture has to be prepared with precisely known composition. There are many variants of these methods, as shown in the table below.

Table 1.7 - Measurements of high-pressure phase equilibrium [130].

Analytical methods		Synthetic methods	
With sampling	Without sampling	With phase transition	Without phase transition
Isothermal	Spectroscopic	Visual	Isothermal
Isobaric	Gravimetric	Nonvisual	Isobaric
Isobaric/Isothermal	Others		Others

For the selection of the most suitable method, it is necessary to evaluate the experimental data available in the literature and understand the advantages and disadvantages inherent to specific error sources.

In analytical methods, the equilibrium cell is fed with the components of the system to be studied. Experimental conditions such as temperature and pressure are then established. Once equilibrium is achieved, there are two typical ways to determine the composition of the different phases: withdrawing a sample for subsequent analysis, or applying a suitable physicochemical technique for an *in situ* analysis. These methods can be used in systems with more than two components. For example, in a ternary system, when the compositions of all phases in equilibrium are analysed, complete data on tie-lines can be obtained [131].

Synthetic methods consist on the preparation of a mixture with an exact composition and on the observation of phase transitions by changing equilibrium parameters, such as temperature

and pressure. In these methods, no sampling is necessary. Synthetic methods can be applied in situations where analytical methods are not convenient, such as when phase separation is difficult due to similar densities of coexisting phases (near or even at critical points). Synthetic methods are used mainly for binary systems [132]. It is very important to get enough data points for a specific system and a good control of variable parameters such as temperature and pressure [129]. For example, a synthetic visual method is appropriate for a study of cloud-point determinations of IL systems. The phase transitions are identified by visual observation, the appearance or disappearance of a meniscus, or turbidity [133].

1.9.2. Phase equilibrium

Two (or more) phases are in equilibrium when the mass transfer from one phase to another is exactly equal to the transfer in the opposite direction [134].

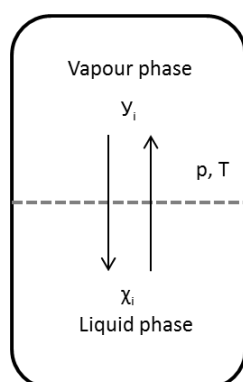


Figure 1.13 - Vapour - liquid equilibrium (VLE). x_i and y_i are the mole fractions of component i in the liquid and vapour phases, respectively.

The Gibbs phase rule is very useful to interpret phase diagrams. This rule elucidates how the operating conditions and restrictions in a process affects the phase equilibrium. The general condition of equilibrium between two phases is that the chemical potential (or fugacity) of each component is the same in each phase. To establish the phase rule, a balance is made for the number of variables and the number of equations between these variables. The difference between the number of intensive variables needed to specify the intensive state of the system and the number of relations between them (equilibria, mass balance relations, reaction equilibria relations and additional relations) is the number of degrees of freedom (or variance), F , of the system. This is the number of variables that must be specified to completely define the intensive state of the system:

$$F = C - P + 2 - r \quad (1.8)$$

C is the number of components, P is the number of phases in equilibrium, and r is the number of reaction equilibria relations and additional relations that exist among the intensive variables. The number of degrees of freedom is the number of independent intensive variables, such as temperature, pressure and composition, which can be varied simultaneously and arbitrarily.

The phase rule is a useful tool for the construction and interpretation of phase diagrams. At a critical point, the physical properties of coexisting phases are identical. So, criticality imposes an additional number of $P - 1$ constraints that reduce the number of degrees of freedom assumed by Eq. 1.8. Therefore, the number of degrees of freedom at a gas-liquid critical point is zero for a system with one component, is one for a system with two components (a line) and is two for a system with three components (a surface) [134].

1.9.3. Phase behavior at high pressure

The calculation of vapour-liquid equilibrium is based on the equality of the fugacity, f , of each component in each phase:

$$f_i^V = f_i^L \quad (1.9)$$

This equality is equivalent to an equality of chemical potentials, but more useful since fugacities can be obtained using equations of state (EOS), as will be discussed later.

At VLE, the amount of component i that is vaporized per unit of time is equal to the amount condensing. This equality means that there is no variation in the composition of the mixture of components in both phases, which are at the same pressure and temperature.

For a pure, ideal gas, the fugacity is equal to the pressure. And for a component i in a mixture of ideal gases, it is equal to its partial pressure, $y_i P$. Because all systems, pure or mixed, approach ideal-gas behavior at very low pressures, the definition of fugacity is completed by the limit:

$$\frac{f_i}{y_i P} \rightarrow 1 \quad \text{as} \quad p \rightarrow 0 \quad (1.10)$$

The main problem is to relate these fugacities to mixture compositions. It is possible analytically to characterize high-pressure VLE using, for the liquid phase, the common thermodynamic

functions: Henry's constant, activity coefficient and partial molar volume. But for multicomponent mixtures, these functions are not useful. The most successful way to describe high-pressure VLE is using the fugacity coefficient, applied to both phases (vapour and liquid). As an example, for a binary liquid mixture with mole fractions x_1 and x_2 , at temperature T and pressure p , in equilibrium with a vapour with mole fractions y_1 and y_2 :

$$f_1^V = f_1^L \quad \text{or} \quad \varphi_1^V y_1 = \varphi_1^L x_1 \quad (1.11)$$

and

$$f_2^V = f_2^L \quad \text{or} \quad \varphi_2^V y_2 = \varphi_2^L x_2 \quad (1.12)$$

where φ is the fugacity coefficient. The equilibrium ratios (K factors) are given by:

$$K_1 \equiv \frac{y_1}{x_1} = \frac{\varphi_1^L}{\varphi_1^V} \quad (1.13)$$

$$K_2 \equiv \frac{y_2}{x_2} = \frac{\varphi_2^L}{\varphi_2^V} \quad (1.14)$$

The fugacity coefficient is a measurement of deviation to the ideal gas behavior. Its value is affected by the chemical nature of the interactions between component i and all the other components of the mixture. Both the fugacity and the fugacity coefficient can be calculated from EOS.

1.9.4. Equations of state (EOS) for mixtures

An EOS is one of the most valuable tools for modelling phase equilibria of multicomponent systems, by providing an algebraic relation between P , V and T . Ideally, the EOS would be valid for the entire range of data values and experimental conditions at which both the vapour and liquid phases exist. Presently there is no EOS that fulfils this requirement, although for many mixtures, approximate equations of state that provide useful results can be used.

An EOS has constants that are based upon pure-component properties, such as acentric factors and critical constants. It was van der Waals who, in 1973, introduced the first EOS, derived from the hypothesis of a finite volume occupied by the constituent molecules.

$$P = \frac{RT}{(V-b)} - \frac{a}{V^2} \quad (1.15)$$

Most of the EOS are based on the original van der Waals type EOS, with two terms which account for contributions of repulsive and of attractive intermolecular forces. This is the most common approach to obtain all the other EOS, such as Redlich-Kwong, Soave modification of Redlich-Kwong, Peng-Robinson, etc.

The equation used in this work was the Peng-Robinson EOS, and thus special attention will be given to it [135]:

$$P = \frac{RT}{V-b} - \frac{a(T)}{V^2+2bV-b^2} \quad (1.16)$$

Where P is the pressure, T is the temperature, V is the molar volume, R is the universal gas constant, a is the energy parameter and b is the co-volume parameter.

Unlike with the van der Waals equation, constant a is now a function of temperature:

$$a(T) = a(T_c)\alpha(T) \quad (1.17)$$

$$a(T_c) = 0.45724 \frac{R^2 T_c^2}{P_c} \quad (1.18)$$

$$\alpha(T) = \left[1 + \beta \left(1 - \sqrt{T/T_c} \right) \right]^2 \quad (1.19)$$

T_c is the critical temperature and β depends on the acentric factor, ω , according to:

$$\beta = 0.37464 + 1.54226\omega - 0.266992\omega^2 \quad (\text{for } 0 \leq \omega \leq 0.5) \quad (1.20)$$

Combining the two equations above yields equation (1.21):

$$a_i(T) = 0.45724 \frac{R^2 T_c^2}{P_c} [1 + (0.37464 + 1.54226\omega - 0.266992\omega^2) \times (1 - \sqrt{T_r})]^2 \quad (1.21)$$

In the Peng Robinson EOS, the parameter b is given by:

$$b = 0.0778 \frac{RT_c}{P_c} \quad (1.22)$$

Parameters for mixtures can be obtained from those for the components using mixing rules. The mixing rules are empirical and have a theoretical basis.

Simple cubic EOS can describe pure fluids reasonably well, but they give satisfactory descriptions only for relatively simple mixtures. It has long been recognized that the source of this difficulty must be the mixing rules. In this work, the parameters a and b used with the Peng Robinson EOS were calculated using the Mathias-Klotz-Prausnitz mixing rule [136]:

Mathias-Klotz-Prausnitz mixing rule

$$a = \sum_{i=1}^N \sum_{j=1}^N x_i x_j \sqrt{a_i a_j} (1 - k_{ij}) + \sum_{i=1}^N x_i \left[\sum_{j=1}^N x_j (\sqrt{a_i a_j} \lambda_{ij})^{1/3} \right]^3 \quad (1.23)$$

$$b = \sum_{i=1}^N \sum_{j=1}^N x_i x_j b_{ij} \quad (1.24)$$

$$b_{ij} = \frac{b_i + b_j}{2} (1 - l_{ij}) \quad (1.25)$$

1.10. High-pressure phase behavior of systems containing CO₂, an ionic liquid, and substrates or products of an enzymatic reaction

VLE data for mixtures containing CO₂ is very important for several applications, particularly for separation processes. As referred earlier, the use of ILs as reaction media may have advantages for enzymatic catalysis because the properties of ILs make possible the development of efficient methods for product separation and recycling. Furthermore, ILs can have a stabilizing effect on enzymes and prevent negative effects of CO₂ [137,138].

In IL/scCO₂ systems, it is important to study the effect of the presence of the IL on the partitioning of the solutes for the vapour or the liquid phase. This depends on the nature of the solutes and of the IL, as well as temperature, pressure, and solute concentrations. Bogel-Lukasik *et al.* performed such a study in the development of an approach for post-reaction separation after conducting an enzyme catalyzed enantioselective transesterification [126]. The authors found that the alcohol substrate had a higher solubility in CO₂ than the products, and that these

solubility differences between substrate and products could be made even larger by choosing an appropriate IL, in this case an IL with the $[\text{PF}_6]$ anion over an IL with the $[\text{N}(\text{CN})_2]$ anion. This allowed the authors to recover >99.99 mol % of unreacted alcohol with very high enantiomeric excess, and with minimal co-extraction of the products.

1.11. Aims and structure of the thesis

The aim of this thesis was to develop an alternative and innovative process for the preparative resolution of secondary alcohols, circumventing the present limitations as regards the physical separation of the two enantiomers, which often involve the use of organic media.

This work started with a focus on (\pm)-menthol as a model, though industrially very relevant compound. The resolution of racemic menthol can be achieved via selective enzymatic transesterification of one of the enantiomers. This yields a mixture of unreacted menthol and a menthol ester.

The selective biotransformation of one enantiomer is just one step of the overall process whose final cost depends heavily on the separation steps that ensue. After the reaction step, if the two enantiomers, now as different chemical entities, still coexist in the same phase, the problem of their physical separation still persists. Normally the separation of the menthol ester from other menthol enantiomers is done by distillation followed by hydrolysis of the menthol ester and crystallization. These are complex and expensive processes, amenable to improvement within the framework of greener approaches.

This work involves a strategy that comprises the use of scCO_2 and ILs. ScCO_2 is an environmentally friendly solvent that works in closed cycle, thereby avoiding concerns on greenhouse effects, and can be separated from substrates and products by simple decompression, which facilitates separation and associated costs. As seen earlier, ILs are extremely versatile substances that can be synthesized to exhibit a series of desired physico-chemical properties. Most ILs have negligible vapor pressure and at normal operation conditions are completely insoluble in scCO_2 , which contributes to facilitated separation processes, and allows recycling.

The methodology for the separation of menthol enantiomers was envisaged to comprise the use of an IL as acylating agent. According to this methodology, racemic menthol would react with the ionic acylating agent, yielding an ionic ester holding (-)-menthol. Because of the ionic character of this ester, it would be insoluble in scCO_2 . (+)-menthol would remain in its original

form. A short chain alcohol would be produced as by-product. Both (+)-menthol and the short chain alcohol by-product would be extracted by scCO₂. By adjusting the temperature and pressure of the scCO₂ stream, the short chain alcohol could be separated from (+)-menthol. Knowledge of relevant vapor-liquid equilibrium phase diagrams would be required for the latter separation process.

Continuous removal of the short chain alcohol would drive the reaction towards the products. Menthol would be recycled back to the reactor and the process would continue until the desired conversion and enantiomeric purity were reached, as monitored in the scCO₂ stream holding (+)-menthol. To recover the product of interest, (-)-menthol, the short chain alcohol (with a make-up contribution to account for losses upon separation) would be recycled back to the reaction vessel, to carry out a transesterification reaction with the ionic ester, thus releasing enantiomerically pure (-)-menthol and regenerating the ionic acylating agent. (-)-menthol would be carried away by scCO₂, and recovered. As before, the continuous removal of one of the products – in this case, (-)-menthol – would drive the reaction forward. The overall output would be the physical separation of the (-) and (+)-isomers of racemic menthol.

In this process, scCO₂ would be used as a carrier of substrates and products to/from the reaction medium, which high concentration of CO₂ would fluidify, thus facilitating mass transfer and promoting higher reaction rates.

This strategy was not possible to implement using (±)-menthol as substrate, due to difficulty in obtaining an adequate ionic acylating agent. However, it was possible to implement it using another secondary alcohol, (*R,S*)-1-phenylethanol, an extensively used model compound for enzymatic resolution studies.

The work on the resolution of (±)-menthol was then mostly carried out using nonionic acylating agents, namely vinyl esters and acid anhydrides.

This thesis is structured in six chapters.

Chapter one provides a general introduction to the work.

Chapter two describes phase equilibrium measurements for the ethanol/(±)-menthol/carbon dioxide system – relevant for the reaction/separation strategy involving ionic acylating agents – and for the propionic anhydride + carbon dioxide binary system, relevant to the work involving the use of acid anhydrides for the resolution of (±)-menthol.

Chapter three reports on the resolution of *sec*-alcohols using ionic acylating esters.

Chapter four deals with the enzymatic resolution of (±)-menthol in organic media, ILs and scCO₂, using vinyl esters and acid anhydrides, and different enzymes. It describes also two different strategies to separate physically the two enantiomers, namely by using a biphasic IL/scCO₂ system, and by using a high pressure membrane separation system.

Chapter I

Chapter five reports on the application of the reaction strategy based on the use of an ionic acylating agent to the resolution of (*R,S*)-1-phenylethanol. This allowed the fulfilment of the initial aim of this thesis, leading to the recovery of the two enantiomers with high enantiomeric purity.

Finally, Chapter six summarizes the main contributions and conclusions drawn from this work.

Chapter II

Phase equilibrium

Part of this chapter was previously published in:

Sílvia Rebocho, Ana V. M. Nunes, Vesna Najdanovic-Visak, Susana Barreiros, Pedro Simões, Alexandre Paiva; High pressure vapor–liquid equilibrium for the ternary system ethanol/(±)-menthol/carbon dioxide, *Journal of Supercritical Fluids*, 92 (2014) 282-287.

2. Phase equilibrium

2.1. High pressure vapor-liquid equilibrium of the ternary system ethanol/(±)-menthol/carbon dioxide

2.1.1. Introduction

An efficient product separation and purification requires phase equilibrium data for the species involved in the reaction. The present work focuses on the phase behavior of the ethanol/(±)-menthol/CO₂ ternary system at high pressure. This data is relevant for the downstream processing with scCO₂ of the reaction mixture resulting from the lipase catalyzed transesterification of (±)-menthol. The reaction proceeds in two steps: acylation, in which enzyme attack on the ester substrate leads to the formation of the acylenzyme and the release of an alcohol – in our case of interest, ethanol – and deacylation, in which (-)-menthol binds to the acylenzyme, and a menthyl ester is released, while the enzyme returns to its initial form. To the best of our knowledge, no experimental data is available in the literature on the phase equilibrium of the ethanol/(±)-menthol/CO₂ ternary system, which is the focus of this work. Vapor-liquid equilibrium (VLE) measurements were performed at two temperatures and three pressures. The data was fitted by the Peng-Robinson equation of state (PR-EOS) [135] with the Mathias-Klotz-Prausnitz mixing rule (MKP-MR) [136], using the program package PE2000 developed by Pfohl *et al.* [139].

2.1.2. Experimental section

2.1.2.1. Materials

(±)-menthol (≥ 98%)(water content ≤0.13% w/w), tridecane (99%) and acetone (≥ 99.5%) were from Sigma- Aldrich. Ethanol (99.9 %) (Water content ≤0.05%w/w) was supplied by Panreac and carbon dioxide (N45) was from Air Liquide. The water content was determined regularly by Karl-Fischer Coulometric titration (Metrohm 831 KF Coulometer).

2.1.2.2. Apparatus and experimental procedure

The apparatus used for VLE measurements, shown in Figure 2.1, comprises a high pressure sapphire tube cell (ca. 30 mL volume) placed inside a thermostatic air bath. Samples were taken both from the liquid and vapor phases.

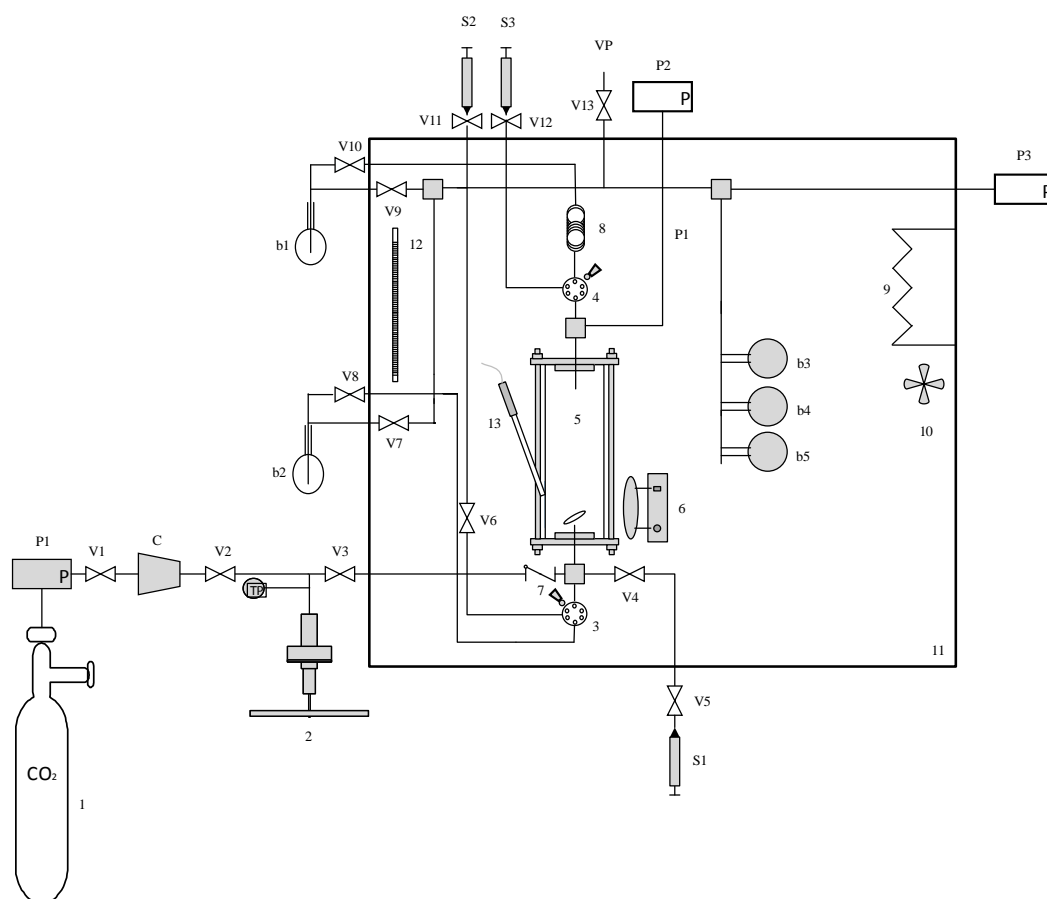


Figure 2.1 - Schematic representation of the VLE apparatus.

Legend:

- 1 - CO₂ cylinder;
- 2 - manual HIP compressor;
- 3 and 4 - HPLC valves;
- 5 - VLE cell;
- 6 - magnetic stirrer;
- 7 - check valve;
- 8 - vapor phase sampling loop;
- 9 - heating resistance;

10 - fan;
11 - air bath;
12 - mercury thermometer;
13 - temperature controller; b1 and b2 - collection cylinders; b3, b4 and b5 - calibrated expansion volume flasks; C - compressor; P1, P2 and P3 - pressure indicators; S1, S2 and S3 - washing syringes; V1 to V13 - valves, VP - vacuum pump.

The apparatus and methodology are described in detail elsewhere [140][141]. Temperature and pressure inside the cell were measured with the mercury thermometer (12) and temperature controller (13), and the pressure indicator P2, respectively. CO₂ was compressed with the compressor (C) and then fed to the cell (through valves V1-V3) to the desired pressure. In each experiment the cell was stirred for 1 h and then allowed to rest for 30 min. Vacuum was then applied to the sampling line. Samples from the gas (top of the cell) and the liquid (bottom of the cell) were taken through two HPLC valves (3 and 4). The compounds dissolved in the liquid and in the gas samples were collected at regular time intervals in the cold traps b1 and b2, kept at a temperature close to zero to ensure the precipitation of all components except CO₂. CO₂ was expanded to the b3, b4 and b5 calibrated flasks, and its amount in each sample was calculated from the measurement of the pressure in the flasks before and after the expansion.

The measurement uncertainties are ± 0.1 K for temperature, and ± 0.07 bar for pressure. The estimated uncertainties in the reproducibility, in mole fractions, had a maximum value of ± 0.004 for the vapor and ± 0.042 for the liquid phase.

A picture of the sapphire tube cell showing the liquid and the vapor phases is given in Figure 2.2:



Figure 2.2 - Sapphire tube cell showing a biphasic liquid + vapor system at equilibrium.

2.1.2.3. Sample analysis

All the samples were analyzed on a gas chromatograph (Trace GC Ultra, Thermo Scientific) equipped with a flame ionization detector (FID) and an auto sampler (Triplus, Thermo Scientific). The compounds were separated in a Thermo TR-Biodiesel (F), 30 m length, 0.25 mm inner diameter, 0.25 μm film thickness capillary column from Thermo Scientific. Helium was used as the carrier gas at a constant flow of 2 mL/min. Oven temperature program: 5 min at 40 $^{\circ}\text{C}$, 40–130 $^{\circ}\text{C}$ at 2 $^{\circ}\text{C}/\text{min}$, and 130 $^{\circ}\text{C}$ for 10 min. A programmable temperature vaporization detector was used: 90–260 $^{\circ}\text{C}$ at 10 $^{\circ}\text{C}/\text{s}$, a transfer time of 3 min, and cleaning at 360 $^{\circ}\text{C}$ with a split of 250 mL/min for 20 min. The detector temperature was 280 $^{\circ}\text{C}$. Tridecane was used as internal standard for GC analysis. Response factors were determined with calibration curves for the pure components. The results presented are the average of duplicate experiments.

2.1.3. Results and discussion

Experimental VLE data for the binary systems (\pm)-menthol/ CO_2 and ethanol/ CO_2 were already reported [142–144]. Nevertheless, for the (\pm)-menthol/ CO_2 system only experimental data for the vapor phase was presented by Sovová *et al.* [142]. Therefore we also measured the liquid

and the vapor phase compositions of the (\pm)-menthol/ CO_2 binary system. The results obtained are given in Table 2.1, which shows good agreement between our experimental results and those of Sovová *et al.* [142], as can be also observed in Figure 2.3, with a maximum value of deviation of $\pm 0.2\%$. Both the solubility of CO_2 in the (\pm)-menthol liquid phase and the solubility of (\pm)-menthol in the CO_2 vapor phase increased sharply with pressure from 8 to 10 MPa. The critical pressure for the mixture at this temperature is expected to be close to 10 MPa.

Table 2.1 – Vapor-liquid equilibrium data for the (\pm)-menthol/ CO_2 binary system.

T (K)	Pressure (MPa)	y_{CO_2}	Source	x_{CO_2}	Source
323	7.96	0.9994	[142]	-	Exp. data
	8.00	0.9984	Exp. data	0.5702	
	9.08	0.9985	[142]	-	
	9.14	0.9975	Exp. data	0.6242	
	10.14	0.9952	[142]	-	
	10.50	0.9941	Exp. data	0.8093	

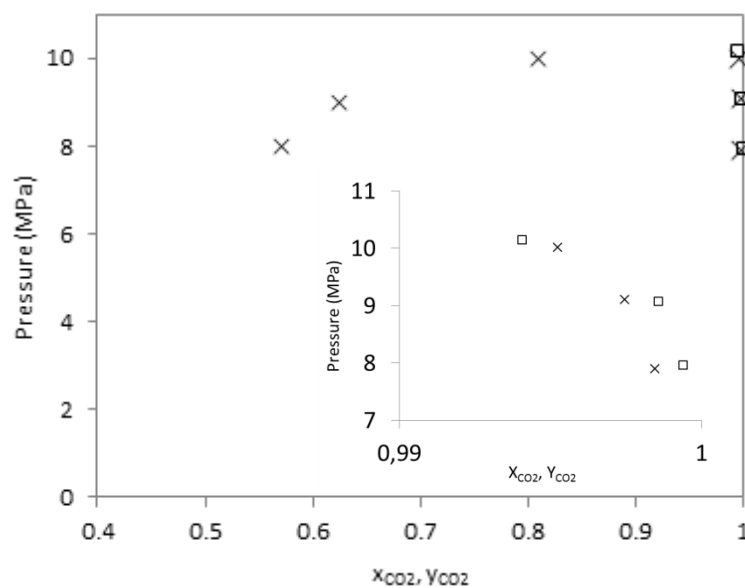


Figure 2.3 - Composition (mole fraction) of CO_2 in the liquid and vapor phases for the (\pm)-menthol/ CO_2 binary system at 323 K. This work (\times). Sovová *et al.* [142] (\square).

Phase equilibrium measurements for the ethanol/(\pm)-menthol/ CO_2 ternary system were performed at 313 and 323 K in the pressure range of 8-10 MPa. Five different feed compositions were studied. In addition to the mole fractions of CO_2 , (\pm)-menthol and ethanol measured at equilibrium in the liquid and vapor phases, the table includes calculated partition coefficients (K) and separation factors (α) (see Equations 2.1 and 2.2, respectively).

Table 2.2 - Vapor-liquid equilibrium data for the ethanol (1)/(±)-menthol (2)/CO₂ (3) ternary system.

T (K)	P (MPa)	(±)- menthol mole fraction in feed*	x_1	x_2	x_3	y_1	y_2	y_3	K_1	K_2	α_{12}
313	8	1	0.0000	0.2728	0.7272	0.0000	0.0010	0.9990	-	0.004	-
		0.750	0.0851	0.1870	0.7279	0.0030	0.0014	0.9956	0.035	0.008	4.7
		0.500	0.1169	0.1061	0.7770	0.0046	0.0009	0.9945	0.039	0.008	4.6
		0.250	0.1334	0.0449	0.8217	0.0144	0.0015	0.9841	0.108	0.033	3.2
		0	0.1550	0.0000	0.8450	0.0185	0.0000	0.9815	0.119	-	-
	9	1	0.0000	0.2007	0.7993	0.0000	0.0131	0.9869	-	0.065	-
		0.750	0.0346	0.1367	0.8287	0.0075	0.0118	0.9807	0.217	0.086	2.5
		0.500	0.0631	0.0649	0.8720	0.0208	0.0131	0.9661	0.330	0.202	1.6
	10	1	0.0000	0.0826	0.9174	0.0000	0.0245	0.9755	-	0.297	-
		0.750	0.0181	0.0536	0.9283	0.0178	0.0332	0.9490	0.983	0.619	1.6
323	8	1	0.0000	0.4298	0.5702	0.0000	0.0016	0.9984	-	0.004	-
		0.750	0.1339	0.3605	0.5056	0.0017	0.0006	0.9977	0.013	0.002	7.6
		0.500	0.2855	0.1933	0.5212	0.0037	0.0005	0.9958	0.013	0.003	5.0
		0.250	0.4454	0.1006	0.4540	0.0083	0.0005	0.9912	0.019	0.005	3.7
		0	0.2984	0.0000	0.7016	0.0190	0.0000	0.9810	0.064	-	-
	9	1	0.0000	0.3758	0.6242	0.0000	0.0022	0.9978	-	0.006	-
		0.750	0.0843	0.1869	0.7288	0.0031	0.0015	0.9954	0.037	0.008	4.6
		0.500	0.2232	0.1625	0.6143	0.0089	0.0018	0.9893	0.040	0.011	3.6
		0.250	0.2808	0.0744	0.6448	0.0168	0.0015	0.9817	0.060	0.020	3.0
		0	0.2331	0.0000	0.7669	0.0352	0.0000	0.9648	0.151	-	-
	10	1	0.0000	0.1907	0.8093	0.0000	0.0048	0.9952	-	-	-
		0.750	0.0848	0.0822	0.8330	0.0180	0.0056	0.9764	0.212	0.068	3.1
		0.500	0.1059	0.0379	0.8562	0.0178	0.0033	0.9789	0.168	0.087	1.9
		0.250	0.1315	0.0367	0.8318	0.0376	0.0059	0.9565	0.286	0.161	1.8

*On a CO₂-free basis.

As shown in Table 2.2, and as expected, (\pm)-menthol and ethanol mole fractions in the vapor phase increase with increasing pressure and decrease with increasing temperature, accompanying the corresponding increase and decrease in CO₂ density, respectively. The effect of pressure for several feed compositions can be observed in Figure 2.4, where the isothermal phase diagram for the pseudo-binary liquid mixture/CO₂ system at 313 K is represented.

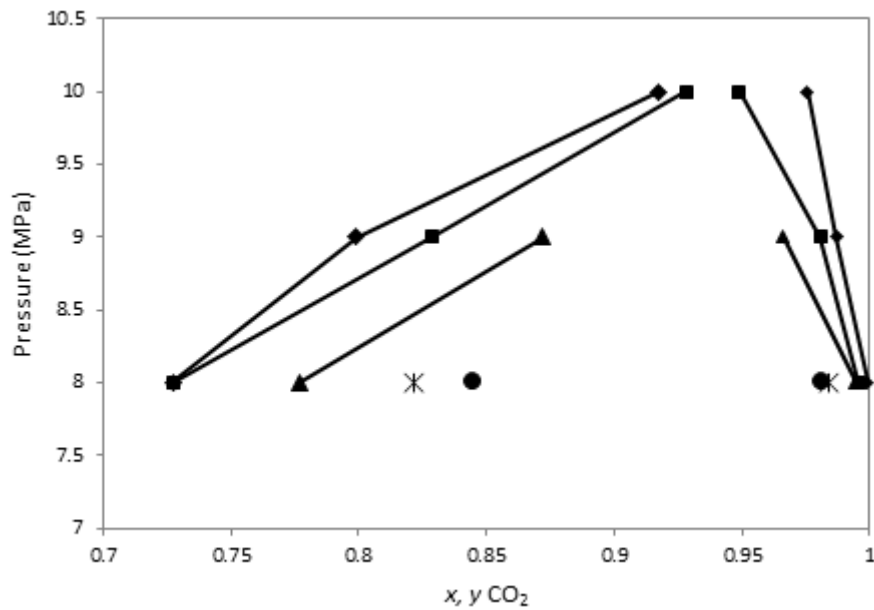


Figure 2.4 - CO₂ mole fractions at 313 K for several feed compositions of (\pm)-menthol on a CO₂-free basis: (◆) 1.000, (■) 0.750, (▲) 0.500, (✱) 0.250, (●) 0.

As shown in Figure 2.4, both the solubility of CO₂ in the liquid mixture phase and the solubility of the liquid mixture in the CO₂ vapor phase increased with the increase in pressure. It is clearly seen that the increase in composition of (\pm)-menthol in the feed causes an enlargement of the two phase region. In fact, the solubility of the liquid in CO₂ decreases as the mole fraction of (\pm)-menthol in the mixture increases, which is due to a higher solubility of ethanol in CO₂ in comparison with (\pm)-menthol.

This difference in solubility can be better observed by the analysis of the partition coefficients and separation factor. The partition coefficient, K , is commonly used to evaluate the distribution of a substance between two phases. It is defined as the ratio of the composition of the substance under study in two phases at equilibrium, given by the following equation:

$$K_i = \frac{y_i}{x_i} \quad (2.1)$$

where y_i and x_i are the mole fractions of component i (ethanol or (\pm)-menthol) in the vapor and in the liquid phase, respectively.

This behavior is more clearly illustrated by calculating the separation factor (α) between the two compounds of interest, which is given by:

$$\alpha = \frac{K_{\text{ethanol}}}{K_{\text{menthol}}} = \frac{y_{\text{ethanol}}/x_{\text{ethanol}}}{y_{\text{menthol}}/x_{\text{menthol}}} \quad (2.2)$$

The ability of scCO₂ to efficiently separate the two compounds of interest, at given conditions of temperature, pressure and feed composition, is measured by the separation factor (α).

Figure 2.5 shows the impact of pressure, temperature and feed composition on α .

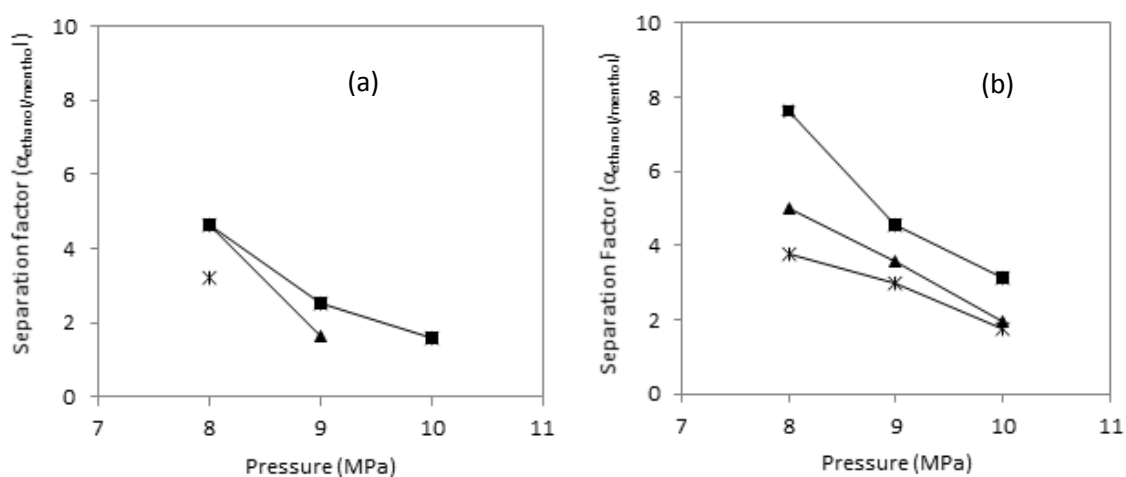


Figure 2.5 - Separation factor as a function of pressure at 313 K (Figure 2.5 a) and 323 K (Figure 2.5 b), for several feed compositions of (\pm)-menthol on a CO₂-free basis: (■) 0.750, (▲) 0.500, (*) 0.250. Lines are just guide-lines.

For both temperatures, the separation factor is higher when the composition of the highest boiling point compound in the feed, (\pm)-menthol, is also higher, i.e. the separation becomes more difficult as the composition of ethanol in the mixture increases. An increase in pressure decreases the selectivity of CO₂ towards ethanol. This behavior can be explained by the increase in the density of CO₂ with pressure, accompanied by an increase in solvation ability that makes it less able to discriminate between solutes.

Temperature has the opposite effect, as shown in Figure 2.6. At fixed pressure, the selectivity of CO₂ towards ethanol increases as temperature increases. Ethanol is more volatile than (\pm)-

menthol, and its vapor pressure changes more pronouncedly with increasing temperature than the vapor pressure of (\pm)-menthol, resulting in an enrichment of the vapor phase in the more volatile compound.

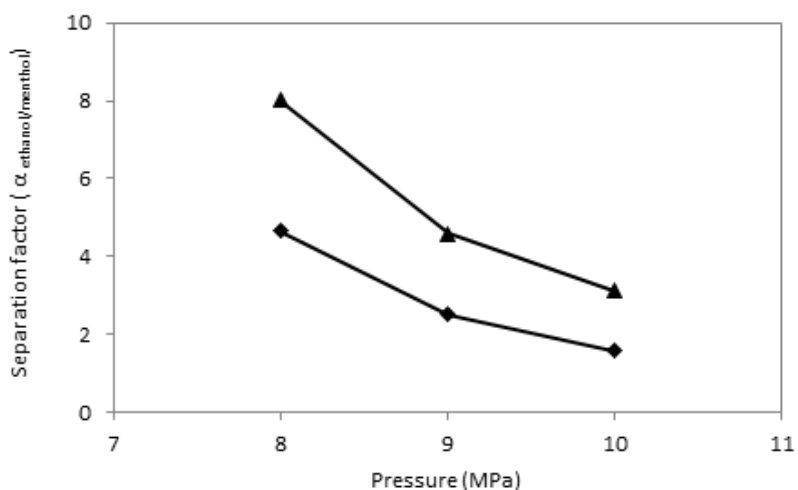


Figure 2.6 - Separation factor as a function of pressure for a fixed feed composition of (\pm)-menthol on a CO₂-free basis of 0.750. (◆) 313 K, (▲) 323 K. Lines are just guide-lines.

2.1.4. Models and parameters

2.1.4.1. Correlations

Experimental results for the binary system (\pm)-menthol/CO₂ mixture were correlated using the Peng-Robinson equation of state (PR-EOS) (see Chapter I Equation 1.16) [135] with the Mathias-Klotz-Prausnitz mixing rule (MKP-MR) (see Chapter I Equations 1.23 and 1.24, respectively) [136].

The correlations were carried out using the program PE 2000 developed by Pfohl *et al.* [139] and the correlated and experimental data were compared in Figure 2.7.

Critical temperature, critical pressure and acentric factor of the pure compounds are presented in Table 2.3.

Table 2.3 - Pure component physical properties [139,145,146].

Compound	T_c (K)	P_c (MPa)	ω
(\pm)- menthol [145]	658	2.71	0.7796
Ethanol [146]	513.9	6.14	0.644
CO ₂ [139]	304.1	7.38	0.239

The obtained binary interaction parameters and the average absolute deviations (AAD) of the calculations are given in Table 2.4

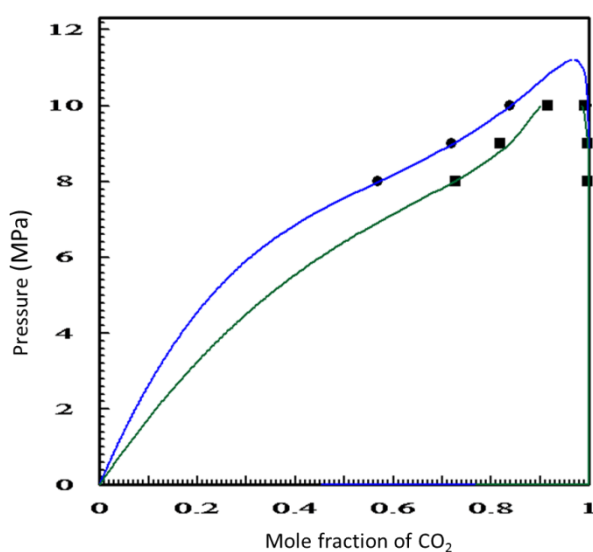


Figure 2.7 - Correlation of the $pTxy$ experimental data using the PR-EOS/MKP-MR model, at 313 K (■) and 323 K (●). Points represent experimental data.

The obtained binary interaction parameters and the average absolute deviations (AAD) of the calculations are given in Table 2. 4.

Table 2.4 - Optimized interaction parameters for the (\pm)-menthol / CO₂ binary system at 8, 9 and 10 MPa, at 313 and 323 K, using the PR-EOS/MKP-MR model.

	313 K	323 K
K_{ij}	0.4950	0.0371
I_{ij}	0.2159	-0.0662
λ_{ij}	0.7016	0.0350
AAD	liq phase: 2.4%	liq phase: 5.9%
	gas phase: 0.9%	gas phase: 0.2%

The Peng-Robinson EOS with the Mathias-Klotz-Prausnitz MR was able to correlate with relatively good accuracy the VLE data for the two temperatures with a total AAD of 4.6%.

The VLE data for the ethanol/(±)-menthol/CO₂ ternary system was fitted with the PR-EOS/MKP-MR model. The critical temperature and pressure, and the acentric factor, ω , of the pure components (Table 3) were used to determine the parameters a_i and b_i used in the correlation of the experimental data. The fitting of the PR-EOS/MKP-MR model was made by finding the best set of interaction parameters that minimized the deviations between the calculated and the experimental data for the liquid and vapor phase compositions. The objective function used to calculate the average absolute deviation (AAD) between the experimental and the correlated data was:

$$AAD = \sqrt{\frac{1}{n} \sum_{i=1}^n (z_i^{exp} - z_i^{EOS})^2} \quad (2.3)$$

with $z = x, y$ and n = number of data points.

The optimized interaction parameters and respective AAD values at selected conditions are given in Table 2.5. The experimental results are compared with those predicted by the model in Figure 2.8 and Figure 2.9. The PR-EOS/MKP-MR model was able to correlate accurately the phase envelope for the ternary system. E.g. at 323 K and 8 MPa, a maximum deviation of 7.5% was obtained for the liquid phase. The total AAD for the four sets of conditions of Table 2.5 was 3.7%.

Table 2.5 - Optimized interaction parameters for the ethanol (1)/(±)-menthol (2)/CO₂ (3) ternary system at the temperatures and pressures indicated, using the PR-EOS/MKP-MR model.

		1-2	1-3	2-3	AAD
313 K 8 MPa	K_{ij}	- 0.0644	0.0076	0.0306	liquid phase: 4.1% gas phase: 0.5%
	I_{ij}	0.0075	0.0063	0.0192	
	λ_{ij}	0.0001	-0.0025	0.0384	
323 K 8 MPa	K_{ij}	-0.0409	0.0425	0.0789	liquid phase: 7.5% gas phase: 0.2%
	I_{ij}	0.0723	-0.0060	0.0619	
	λ_{ij}	-0.0456	0.1077	0.0784	
323 K 9 MPa	K_{ij}	0.1085	0.1075	0.0248	liquid phase: 4.5% gas phase: 0.4%
	I_{ij}	0.1721	0.0331	0.0221	
	λ_{ij}	0.0108	-0.0244	0.0467	
323 K 10 MPa	K_{ij}	- 0.0159	0.0290	-0.0035	liquid phase: 2.8% gas phase: 1.2%
	I_{ij}	-0.0073	0.0860	0.0242	
	λ_{ij}	-0.0665	0.0068	0.0384	

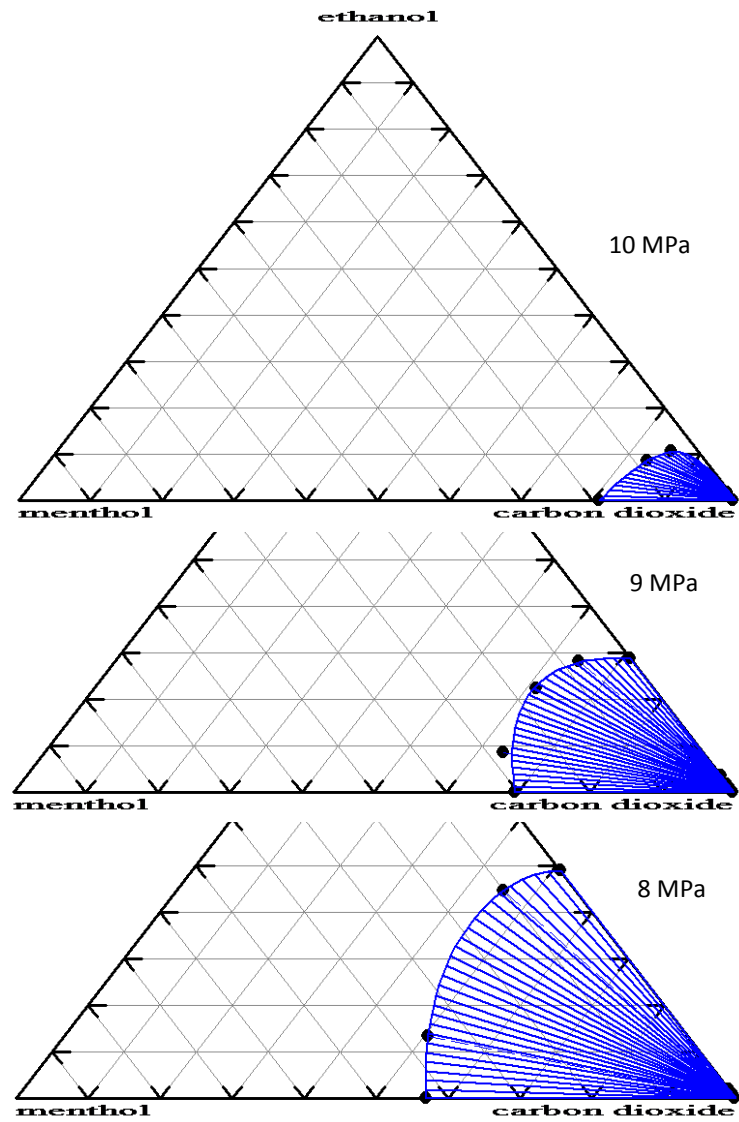


Figure 2.8 - $pTxy$ experimental data for the ethanol/(±)-menthol/CO₂ ternary system at 323 K and 8, 9 and 10 MPa. The points are experimental data and lines were obtained by fitting with the PR-EOS/MKP-MR model.

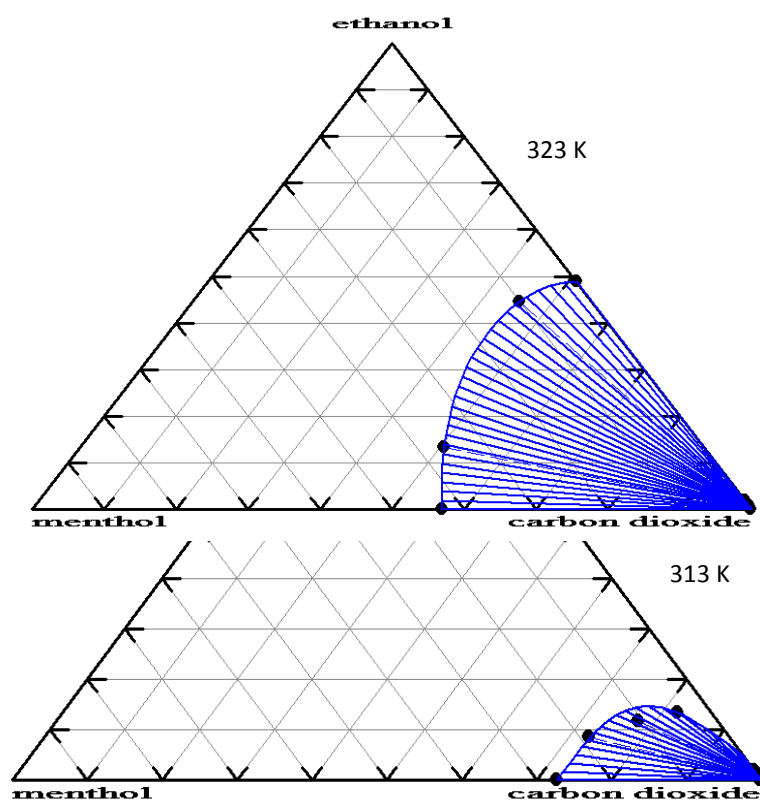


Figure 2.9 - $pTxy$ experimental data for the ethanol/(±)-menthol/CO₂ ternary system at 313 and 323 K, at 8 MPa. The points are experimental data and lines were obtained by fitting with the PR-EOS/MKP-MR model.

At 313 K and 9 MPa, a three-phase region was experimentally observed. The system was left to rest for several hours to ensure that the three phases were in equilibrium. The model was able to predict this behavior, as shown in Figure 2.10. Three phases (L_1L_2V) in equilibrium can be observed distinctly in the diagram by its characteristic triangular surface. Ethanol and (±)-menthol are highly mutually soluble, and at certain conditions CO₂ may act as an anti-solvent, promoting their separation. This result is an upper CO₂-rich vapor phase, an intermediate ethanol-rich liquid phase, and a bottom (±)-menthol-rich liquid phase.

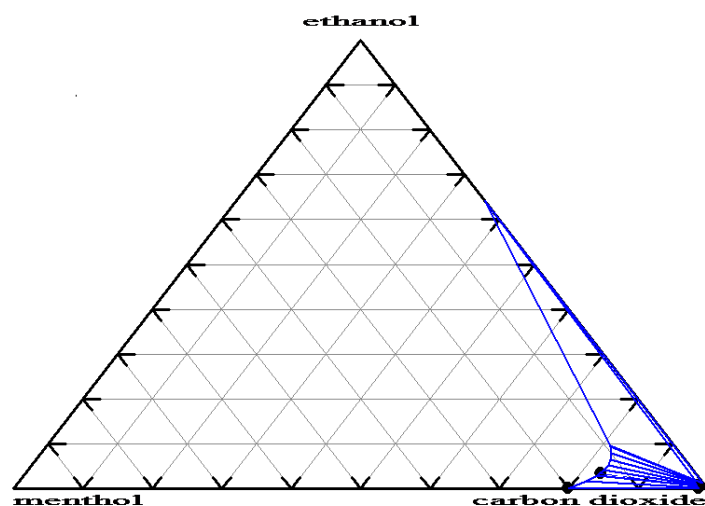


Figure 2.10 - $pTxy$ experimental data for the ethanol/(±)-menthol/ CO_2 ternary system at 313 K and 9 MPa. The points are experimental data and lines were obtained by fitting with the PR-EOS/MKP-MR model.

Figure 2.11 and Figure 2.12 show a schematic and a real view, respectively, of the sapphire tube cell with the three-phase system.

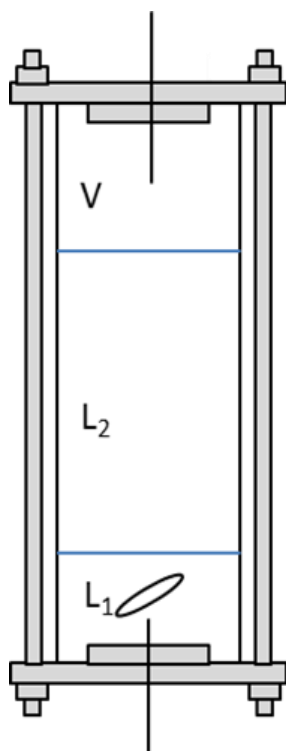


Figure 2.11 - A schematic view of the three-phase (L_1L_2V), system inside the sapphire tube cell.



Figure 2.12- A real view of the three phases (L_1L_2V), inside the sapphire tube cell.

A real view of the sapphire tube cell showing the mixture as it reaches the three-phase equilibrium is shown in Figure 2.13.



Figure 2.13 - A view of the sapphire tube cell showing the ethanol/(\pm)-menthol/ CO_2 ternary system as it reaches the three-phase region.

2.1.5. Conclusions

The experimental data obtained were correlated using the Peng-Robinson equation of state and the Mathias-Klotz-Prausnitz mixing rule. A good correlation was obtained with an average absolute deviation (AAD) of 4.6% for the binary (\pm)-menthol/ CO_2 system, and 3.7 % for the (\pm)-menthol/ethanol/ CO_2 ternary system.

The results obtained show that the selectivity of CO_2 towards ethanol increases with increasing temperature, which indicates that the process is governed by volatility and not CO_2 density. According to the values obtained for the separation factors, the most appropriate conditions to separate ethanol from (\pm)-menthol are lower pressure and higher temperature. Nevertheless, it is important to notice that at these condition the loading of ethanol in CO_2 decreases drastically.

The increase of the amount of (\pm)-menthol in the feed composition results in an increase of the separation factor, which means that as the mixture becomes richer in ethanol, the separation of the two compounds becomes more difficult.

2.2. Experimental determination and modeling of the phase behavior of the carbon dioxide + propionic anhydride binary system at high pressure

2.2.1. Introduction

Propionic anhydride is widely used as acyl donor in enzyme catalyzed enantioselective reactions with secondary alcohols, such as (\pm)-menthol [45,110,147]. The present work focuses on the phase behavior of the CO₂/propionic anhydride binary system at high pressure, which just as the previous study, is relevant for downstream processing with scCO₂ upon menthol conversion. VLE measurements were carried out at three temperatures. The data was fitted by the PR-EOS/MKP-MR model.

2.2.2. Experimental section

2.2.2.1. Materials

Propionic anhydride ($\geq 99\%$ purity) was supplied by Sigma-Aldrich and carbon dioxide (N45) was from Air Liquide.

2.2.2.2. Phase equilibrium measurements

A detailed description of the experimental apparatus was already presented [148], and is shown in Figure 2.14. The high pressure cell is from New Ways of Analytics GmbH, Germany. The cell, equipped with two sapphire windows (one in front and another at the back), allows for visual observation of phase transitions. The sapphire at the back works as a piston, moving inside and along the stainless steel cylinder. This is accomplished by using a hydraulic fluid pump, which allows the internal volume of the cell to be changed in the range 38-70 mL. Temperature is controlled with a PID controller (Eurotherm 221e). This controller combines proportional control

with two additional adjustments, which helps the unit to automatically compensate for changes in the system. The controller is connected to a temperature sensor in direct contact with the fluid mixture inside the cell, and two electrical band heaters. Pressure is measured by an Omega DP41-E230 transducer with an accuracy of 0.05 MPa.

The data points for the CO₂/propionic anhydride binary system were obtained visually by the cloud point method. Depending on the desired composition, given amounts of propionic anhydride and CO₂ were loaded into the cell. CO₂ was added using a manual screw injector, and its amount was controlled by means of the variation of volume per rotation, as described by Podila *et al.* [148].

Briefly, the mixture inside the cell was vigorously stirred using a magnetic stir bar. After achieving the desired temperature, the cell pressure was increased by applying pressure on the back sapphire piston with the help of the hydraulic pump. When a single phase was reached, the system was stirred for 30 min and then the pressure inside the cell was lowered very slowly, until visual observation of new phase formation.

Each data point is the average of two to three measurements.

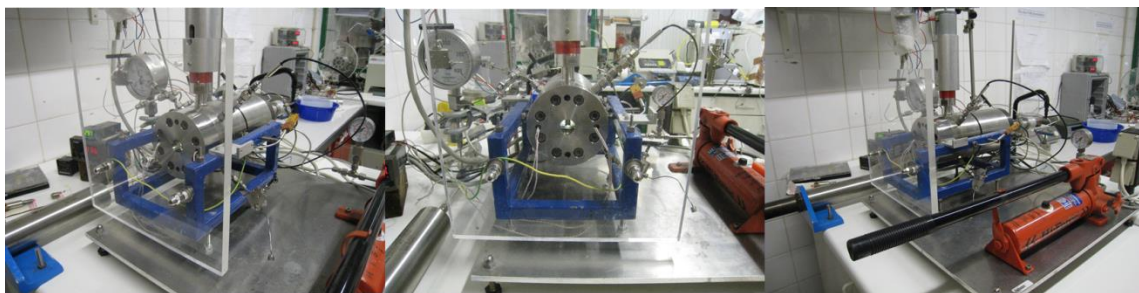


Figure 2.14 - Apparatus used for phase equilibrium measurements.

2.2.3. Results and discussion

Table 2.6 gives the experimental results obtained for the bubble and dew points of the CO₂ + propionic anhydride binary system at 308, 313 and 323 K, and pressures between 5 and 10 MPa.

Table 2.6 – Phase behavior of the CO₂ (1)/propionic anhydride (2) binary system expressed as CO₂ mole fraction (χ_{CO_2}) .

T (K)	P (MPa)	χ_{CO_2}	Phase transition ^a
308	5,21	0,7052	BP
	5,66	0,7625	BP
	6,17	0,8128	BP
	6,21	0,9983	DP
	6,55	0,8578	BP
	7,03	0,9159	BP
	7,17	0,9373	BP
	7,17	0,9974	DP
	7,66	0,9752	BP
	7,72	0,9808	BP
	7,75	0,9885	BP
	7,75	0,9857	BP
	7,76	0,9961	DP
	7,78	0,9926	BP
313	5,66	0,9974	DP
	5,76	0,7052	BP
	6,07	0,9979	DP
	6,34	0,7625	BP
	6,55	0,7934	BP
	6,86	0,8221	BP
	7,24	0,8615	BP
	7,59	0,8985	BP
	7,79	0,9977	DP
	8,00	0,9943	BP
	8,03	0,9373	BP
	8,21	0,9900	DP
	8,30	0,9699	BP
	8,41	0,9839	BP
323	5,55	0,5704	DP
	5,55	0,9942	DP
	6,55	0,6677	DP
	6,55	0,9947	DP
	7,48	0,7625	DP
	8,10	0,8117	DP
	8,59	0,8615	DP
	9,10	0,8985	DP
	9,38	0,9903	DP
	9,38	0,9430	DP
	9,79	0,9752	BP
	9,81	0,9857	BP

^aBP – bubble point; DP – dew point

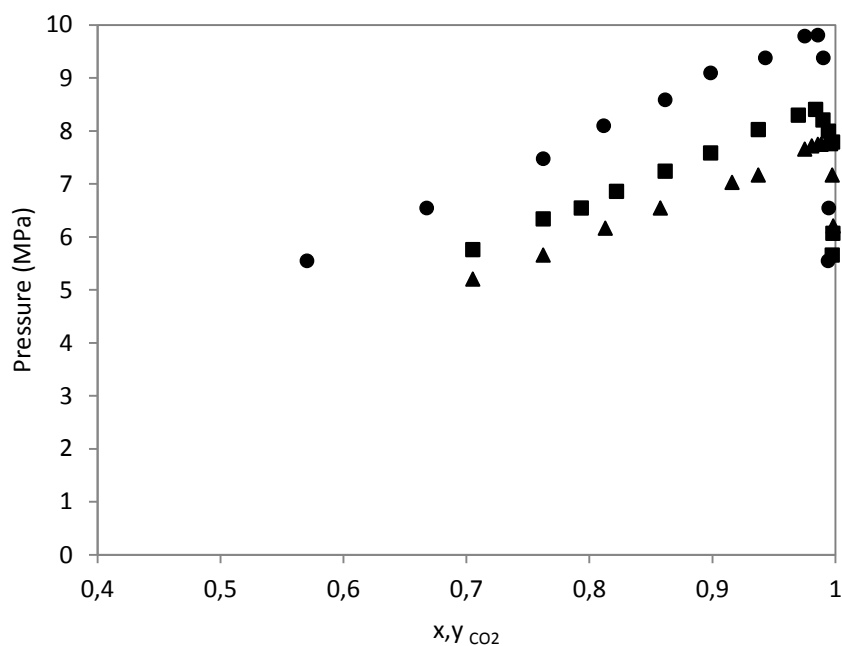


Figure 2.15 – VLE data for the CO₂/propionic anhydride binary system at 308 K (▲), 313 K (■) and 323 K (●).

As expected, the solubility of CO₂ in the propionic anhydride liquid phase as well as the solubility of propionic anhydride in the CO₂ vapor phase increase with an increase in pressure and a decrease in temperature.

To the best of our knowledge, no experimental data is available with which to compare the data generated in this work.

2.2.4. Thermodynamic modeling

The VLE data for the CO₂/propionic anhydride system was fitted with the PR-EOS/MKP-MR model, by finding the best set of interaction parameters that minimized the deviations between the calculated and the experimental data for the liquid and vapor phase compositions. The objective function used to calculate the AAD between the experimental and the correlated data was the same as before (Equation 2.3).

Critical temperature and pressure, as well as acentric factors of the pure components (Table 2.7) were used to determine the parameters a_i and b_i used in the correlation of the experimental data.

Table 2.7 - Pure component physical properties [149].

Compound	T_c (K)	P_c (MPa)	ω
Propionic anhydride	623	3.27	0.560
CO ₂	304.1	7.38	0.239

The optimum binary interaction parameters obtained and the respective AAD values are given in Table 2.8.

Table 2.8 - Optimized interaction parameters for the CO₂/propionic anhydride binary system at 308 K(▲), 313 K(■) and 323 K (●), using the PR-EOS/MKP-MR model.

	308 K	313 K	323 K
K_{ij}	0.0217	-0.1081	-0.4191
I_{ij}	-0.0157	-0.0949	-0.3464
λ_{ij}	0.0301	-0.1555	-0.6083
AAD (%)	liq phase: 0.008%	liq phase: 0.243%	Liq phase: 0.148%
	gas phase: 0.090%	gas phase: 0.155%	Gas phase: 0.366%

As shown in Figure 2.16, the PR-EOS/MKP-MR model gave a good fitting to the $pTxy$ data. A total AAD of 0.21 % was obtained.

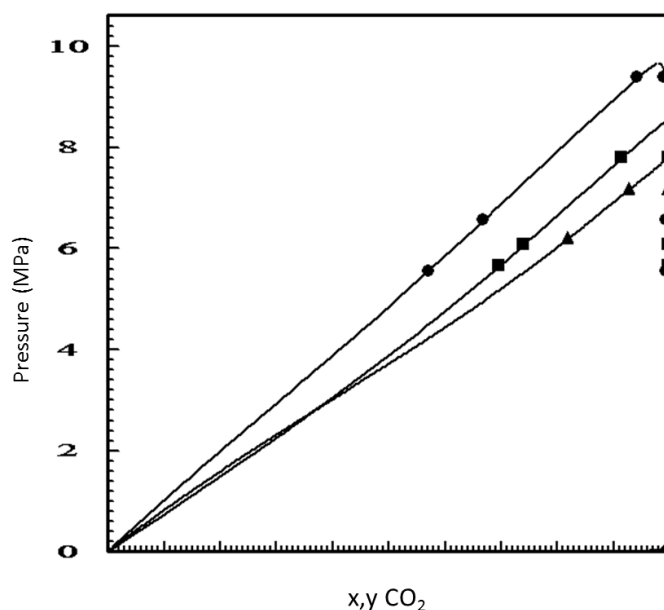


Figure 2.16 - Fitting of the $pTxy$ experimental data (symbols) for the CO_2 /propionic anhydride binary system by the PR-EOS/MKP-MR model (lines) at 308 K (▲), 313 K (■) and 323 K (●).

2.2.5. Conclusions

The phase behavior of the CO_2 /propionic anhydride system was studied at three temperatures (308, 313 and 323 K) that are relevant for enzymatic reaction studies of (\pm)-menthol conversion in scCO_2 , using propionic anhydride as acylating agent.

Although the reaction system of interest was CO_2 + menthol + propionic anhydride, the study of the (CO_2 + propionic anhydride) binary was very important to assess the solubility of the substrate in CO_2 . This information is not available in the literature, unlike what happens with the (menthol + CO_2) binary.

The results obtained show that propionic anhydride is highly soluble in CO_2 at relatively low temperatures. At around 308 K and pressures of 7 MPa and above, the system is monophasic for all compositions.

Chapter III

Resolution of *sec*-alcohols using ionic acylating esters

3. Resolution of *sec*-alcohols using ionic acylating esters

3.1. Introduction

In the last ten years, the use of ILs as solvents for enzymatic kinetic resolution has been the object of much attention. As referred earlier, ILs are very versatile since they can be prepared with many different cation/anion combinations. ILs can dissolve useful amounts of many compounds of interest, most ILs have negligible vapor pressure, and many ILs have been shown to favor enzymatic activity. Additionally IL/scCO₂ systems may allow for greener reaction/separation strategies.

Task specific ionic liquids (TSILs), or functionalized ILs, are synthesized to comply with a set of required chemical, physical and biological properties, and find application in several areas such as organic synthesis, catalysis, and more recently nanoparticle synthesis [128,150,151].

TSILs can be synthesized through several synthetic methods. The synthesis of ILs consists in two steps: the cation synthesis, and the anion exchange. TSILs that have a hydroxyl group appended to an imidazolium cation have been described as efficient vehicles for the substrate of lipase catalyzed kinetic resolution systems [152].

The main objective of the work presented in this chapter is the synthesis and testing of new ionic acylating agents containing an ester moiety, featuring in their structure a methyl-imidazolium unit (ionic) and an alkyl-carboxylic derivative unit (acylating), which can be used in the resolution of (±)-menthol. Based on the work of Lourenço *et al.* [59], the success of the methodology depends essentially on the evaluation of the performance of the chosen ionic acylating agent in the reaction of interest.

Previous studies performed to design new acylating agents [153] showed that one of the critical parameters is the size of the spacer between the permanent cation and the carboxyl group involved in the enzymatic reaction. It was also observed that the cation 1-(11-ethoxy-11-oxoundecan-1-yl)-3-methyl-imidazolium seemed to be the most suitable for the demonstration of the technology [153]. Two different ionic acylating agents, differing in the anion, were thus prepared and tested.

3.2. Experimental section

3.2.1. Materials

Lipase from *Candida rugosa* (CRL; Type VII) from Sigma-Aldrich, Novozym 435 (*Candida antarctica* lipase B - CALB - immobilized within a macroporous resin of poly-methyl methacrylate - Lewatit VP OC 1600) was gently provided by Novozymes (Denmark). (±)-Menthol (≥98% purity) and (*R,S*)-1-phenylethanol (98% purity) were from Sigma-Aldrich. 1-Butyl-3-methylimidazolium hexafluorophosphate [bmim][PF₆] was supplied by Iolitec. Tridecane (99%, Aldrich) was used as external standard and ethyl acetate (EtOAc, ≥ 99.8%, Carlo Erba) was used as solvent, both for GC analysis. Diethyl ether (Et₂O, ≥ 99% purity) was supplied by Sigma-Aldrich.

For the preparation of 1-methyl-3-(11-ethoxycarbonylundecyl)imidazolium tetrafluoroborate and 1-methyl-3-(11-ethoxycarbonylundecyl)imidazolium hexafluorophosphate, all reagents were purchased from Sigma-Aldrich, unless otherwise stated. The ILs based on 1-n-butyl-3-methylimidazolium cation were kindly provided by Solchemar. All ILs were dried under vacuum for 48 h prior to use.

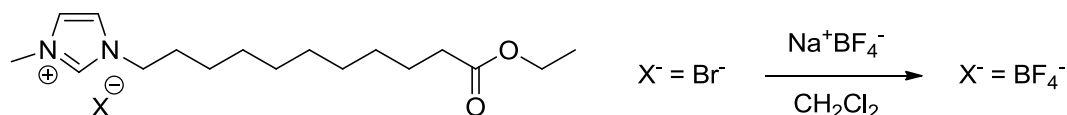
3.2.2. Preparation of ionic acylating agents

Earlier studies by Lourenço and co-workers [59,153,154] were the starting point for the preparation of the envisaged TSILs. The synthesis of the ionic acylating ester was accomplished through chemical reaction between two different halogen-alkyl-esters and the methyl-imidazolium. The ionic compounds formed underwent ion exchange with different salts, to generate the ionic acylating agents for enzymatic reaction assays:

a) Sodium tetrafluoroborate (409.31 mg, 3.72 mmol) was added to a stirred solution of 1-methyl-3-(11-ethoxycarbonylundecyl) imidazolium bromide (previously prepared) (1.16 mg, 3.10 mmol) in 10 mL of dichloromethane. The reaction mixture was stirred at room temperature for 48 h. Then it was filtered and washed with water (3 x 10 mL). The solution was passed through a pipette-sized column filled with silica gel. The solvent was evaporated under reduced pressure [154].

b) Potassium hexafluorophosphate (1.93 mg, 10.49 mmol) was added to a stirred solution of 1-methyl-3-(11-ethoxycarbonylundecyl) imidazolium bromide (previously prepared) (2.63 mg, 6.99 mmol) in 10 mL of dichloromethane. The rest of the procedure was identical to a).

(a)



(b)

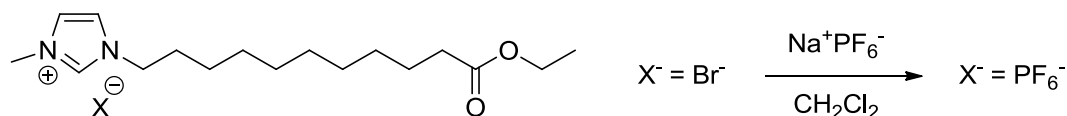


Figure 3.1 – Preparation of methyl-3-(11-ethoxycarbonylundecyl) imidazolium hexafluorophosphate (a) and 1-methyl-3-(11-ethoxycarbonylundecyl) imidazolium tetrafluoroborate (b).

3.2.3. Enzymatic resolution of (±)-menthol and (*R,S*)-1-phenylethanol

Experiments were performed in a plastic tube (10 mL). The alcohol, (±)-menthol/1-phenylethanol (0.065g, 0.414 mmol/ 0.051g, 0.414 mmol) and the ionic acylating agent (0.238 g, 0.414 mmol) were used in a 1:1 molar ratio of. First 1 mL of solvent [bmim][PF₆] was placed in the tube, followed by the alcohol, the enzyme (100 mg of CRL/20 mg of Novozym 435), and finally the ionic acylating agent. The plastic tube was placed in a glass trap attached to a vacuum pump system. The reaction mixture was stirred under reduced pressure (10/100 mm Hg) in a thermostatic water bath, for 96 h.

The reaction mixture was then extracted with Et₂O (3 x 7 mL). The organic phase was passed through a Pasteur pipette filled with silica gel, to remove ILs. Et₂O was evaporated under reduced pressure to give the unreacted (+) enantiomer. The remaining reaction mixture was submitted to reduced pressure for 2 h to remove traces of Et₂O, and then 2.5 equivalents of water were added. The mixture was kept under stirring for 24 h at 35 °C in a thermostatic bath, after which it was again extracted with Et₂O (3 x 7 mL), and the organic phase collected. The

latter was passed through a Pasteur pipette filled with silica gel, and the solvent was evaporated under reduced pressure to give the reacted (-) enantiomer.

3.2.4. General procedure for sampling

Approximately 100 μL (weighed) samples were taken at 0 h, 6 h, 24 h, 48 h, 72 h and 96 h. Samples were treated by dissolving them in 8 mL of EtOAc (less volatile than Et₂O), after which they were passed through a Pasteur pipette filled with silica gel. To the filtered solution was added 1 mL of a 22.5 mM solution of tridecane in EtOAc, to obtain 9 mL of a 2.5 mM tridecane solution that was used for GC analysis.

3.2.5. Sample analysis

All the samples were analyzed on a gas chromatograph (TermoQuest Trace GC 2000 Series) equipped with a flame ionization detector (FID) and an auto sampler (Thermo Finnigan AS 2000). The compounds were separated in a Cyclodex B (10.5% Beta-Cyclodextrin; J&W Scientific) capillary column (0.25 mm I.D. x 30 m with 0.25- μm film). Two different methods were used in the analysis, depending of the reaction. For (\pm)-menthol - oven temperature program: 90 °C for 10 min; 90-140 °C at 1 °C/min. Injection temperature: 200 °C. For (*R,S*)-1-phenylethanol - oven temperature program: 90 °C for 15 min; 90-108 °C at 1 °C/min and 108-220 °C at 30 °C/min for 5 min. For both reactions: Flame ionization detection (FID) and injector temperatures were set at 250 °C. Carrier gas: helium (1 mL/min). Split ratio: 1:50. Response factors were determined with calibration curves for the pure components. The results presented are the average of replicate experiments.

3.3. Results and discussion

Following the strategy previously reported in the literature by Lourenço *et al.* [59], two different imidazolium-based acylating agents bearing the PF_6^- anion (a) or the BF_4^- anion (b) were tested, under different conditions.

The reaction mechanism is shown in Figure 3.2:

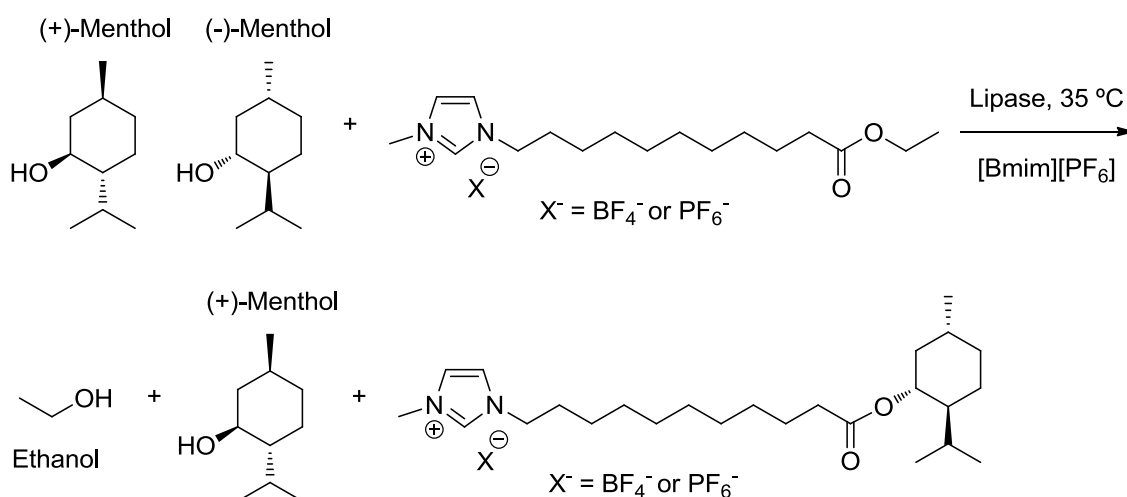


Figure 3.2 - Scheme for the EKR of (±)-menthol in $[\text{bmim}][\text{PF}_6]$, using an acylating agent based on the imidazolium cation, using a lipase as biocatalyst.

Although CRL is an efficient catalyst for the enantioselective conversion of menthol, no conversion was detected, using either of the two ionic acylating agents (Table 3.1).

As mentioned previously, during the transesterification an alcohol is formed, and it is essential to remove it to facilitate the forward reaction. The use of ILs as solvent/acylating agent is very suitable in this case because the non-volatility of ILs allows the easy removal of the alcohol under reduced pressure. But as seen in Table 3.1, changes in reduced pressure or even keeping the system at atmospheric pressure had no effect of reaction conversion.

In order to see if the problem was with the biocatalyst, it was tested another enzyme, Novozym. It was known, and will be referred later, that CALB is capable of nonselective conversion of menthol. However, no conversion was observed with this enzyme either.

Table 3.1 - Screening of two different ionic acylating agents a) and b) and two different enzymes for the EKR of (\pm)-menthol using as solvent [bmim][PF₆], under different pressures, at 35 °C.

Alcohol	Enzyme	Time (days)	Acylating agent	Pressure (mm Hg)	Substrate Conversion (%)	<i>ee</i> _s (%)
(\pm)-menthol	CRL	4	a)	760	no	-
(\pm)-menthol	CRL	4	a)	10	no	-
(\pm)-menthol	CRL	4	a)	100	no	-
(\pm)-menthol	CRL	4	b)	760	no	-
(\pm)-menthol	CRL	4	b)	10	no	-
(\pm)-menthol	CRL	4	b)	100	no	-
(\pm)-menthol	Novozym	4	b)	100	no	-
(<i>R,S</i>)-1-phenylethanol	CRL	4	b)	100	<10	not selective
(<i>R,S</i>)-1-phenylethanol	Novozym	4	b)	100	30	95

These findings suggested that the problem was with the combination ionic acylating agent/menthol. To see which of these two factors was determinant, attention was turned to the alcohol substrate. Thus (\pm)-menthol was replaced with (*R,S*)-1-phenylethanol under the same conditions. As seen in Table 3.1, the results obtained were not satisfactory in the case of CRL, which led to low, nonselective conversion of (*R,S*)-1-phenylethanol. However, conversion was higher in the case of Novozym, and the *ee* of the substrate was considerably high. As expected, carrying out the reaction at normal pressure led to low conversion due to the presence of the product ethanol.

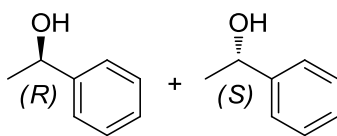


Figure 3.3 - (*R,S*)-1-phenylethanol.

3.4. Conclusions

The main goal was to achieve the resolution of racemic menthol using an ionic acylating agent that formed a covalent compound with (-)-menthol, thus facilitating the removal of nonreacted substrate. However, this strategy did not work. Good results were obtained for a different alcohol – 1-phenylethanol – and a different enzyme – immobilized CALB (Novozym).

The results obtained indicate that it is difficult for both enzymes to convert menthol with the ionic acylating agents tested. They also suggest that menthol is more of a problem than the acylating agent, as indicated by the fact that the latter led to good results using 1-phenylethanol and CALB, and to measurable conversion using 1-phenylethanol and CRL.

The ionic acylating agents used have an imidazolium ring bound to a long alkyl chain bearing the carbonyl group. The imidazolium ring may hinder the access of the alcohol to the enzyme active site. On the other hand, the –OH group of menthol (Figure 3.2) has lower flexibility than the –OH group of (*R/S*)-1-phenylethanol (Figure 3.3), and additionally is in close proximity to freely rotating –CH₃ groups. Combined, these features may be behind the difficulty in achieving the enzymatic conversion of menthol using the ionic acylating agents.

The approach based on the use of ionic acylating agents will be resumed later on, with different ionic acylating agents, but using CALB and (*R,S*)-1-phenylethanol.

Chapter IV

**Reaction and separation of (\pm)-menthol enantiomers
through the combination of nonaqueous media for
biocatalysis, extraction, and membrane separation**

4. Reaction and separation of (\pm)-menthol enantiomers through the combination of nonaqueous media for biocatalysis, extraction, and membrane separation

4.1. Introduction

The conversion of one enantiomer of a racemic mixture into a different chemical species facilitates the separation of the two enantiomers but does not in itself accomplish that separation, i.e. the downstream processing to obtain a pure component needs to be addressed. Over the past two decades, ionic liquids (ILs) have gained great attention from the scientific community, and the number of reports in the literature has grown exponentially on many applications, which include biocatalysis [155]. ILs have negligible vapour pressure, which is a considerable advantage over organic solvents. Also through a judicious choice of anion and cation, ILs can be synthesized to meet requirements as regards properties and function.

The utility of the combination of ILs and supercritical fluids, such as environmentally friendly supercritical carbon dioxide (scCO₂), in the context of biocatalysis was highlighted by a number of researchers [60,61,156]. E.g. the reaction can take place in the IL phase, and the solutes of interest can be extracted by scCO₂. Because ILs are virtually insoluble in scCO₂, no solvent is lost to the supercritical phase. By changing the temperature and pressure of scCO₂, its solvation ability can be adjusted so as to allow the fractionation of a mixture of solutes from a reaction mixture [125,157].

We describe two approaches to separate the two enantiomers of (\pm)-menthol. Anhydrides and vinyl esters conveniently make the acylation reaction irreversible, and have been commonly used in the enzymatic resolution of (\pm)-menthol [104-110,115,116]. We used these two types of acyl donors. The solvent is another experimental parameter of relevance for enzyme activity and selectivity. As seen also earlier, the most common nonaqueous media used in the resolution of racemic (\pm)-menthol are hydrophobic organic solvents, in particular *n*-hexane [105,107-109,114], although ILs 1-butyl-3-methyl-imidazolium hexafluorophosphate ([bmim][PF₆]) and 1-butyl-3-methyl-imidazolium tetrafluoroborate ([bmim][BF₄]) have also been used [108,110]. There is also a report using scCO₂ as reaction medium [111]. We thus tested several ILs in addition to [bmim][PF₆] and [bmim][BF₄] as reaction media, and used also *n*-hexane and scCO₂ for comparison. Attention was paid to the amount of water present, since water can hydrolyze

the acylating substrates, as well as new esters formed, reducing the efficiency of the process. As noted early on [105], acid anhydrides can react with (\pm)-menthol to a considerable extent without added catalyst, producing equal amounts of the (-)- and the (+)-menthol derived esters. We thus performed reactions at sub-ambient temperatures.

The possibility to use scCO₂ to separate unreacted (-)-menthol, the (-)-menthol derived ester and unreacted acylating agent from the IL medium was assessed for a methodology based on the use of vinyl decanoate as acylating agent. The results obtained showed the need for a different separation strategy, and led to the application of high pressure membrane separation.

4.2. Experimental

4.2.1. Materials

Immobilized lipases from *Candida antarctica* (Novozym 435), *Rhizomucor miehei* (Lipozyme RM), *Thermomyces lanuginosus* (Lipozyme TL) were from Novozymes, and lipases from *Candida rugosa* (CRL; Type VII), and from *Pseudomonas cepacia* were from Sigma-Aldrich. (\pm)-Menthol ($\geq 98\%$), vinyl decanoate (95%), propionic anhydride ($\geq 99\%$), tridecane ($\geq 99\%$), propionic acid ($\geq 99.5\%$), lauric acid (99%), decanoic acid ($\geq 99\%$), dichloromethane ($\geq 99\%$), 4-dimethylaminopyridine (DMAP; $\geq 99\%$), and dicyclohexylcarbodiimide (DCC; $\geq 99\%$) were from Sigma-Aldrich, butyric anhydride ($\geq 99.5\%$) was from Merck, acetic anhydride ($\geq 98\%$) and vinyl laurate ($\geq 99.0\%$) were from Fluka, ethyl acetate ($\geq 99.8\%$) was from Carlo Erba, silica gel 60M was from Macherey-Nagel. The ILs [bmim][PF₆], [bmim][BF₄], 1-hexyl-3-methyl-imidazolium hexafluorophosphate ([hmim][PF₆]), 1-octyl-3-methyl-imidazolium hexafluorophosphate [omim][PF₆], and 1-butyl-3-methyl-imidazolium bis(trifluoromethylsulfonyl)imide ([bmim][Tf₂N]) were from Iolitech. Before use, ILs were dried under vacuum while stirring, for 48 h. All other solvents and substrates were dried with molecular sieves.

The membranes used in the pervaporation method were PERVAPTM 4060, by Sulzer Chemtech, and PDMS from Pervatech, both with top layer material polydimethylsiloxane (PDMS).

4.2.2. Synthesis of (–)-menthyl laurate, (±)-menthyl laurate, (–)-menthyl decanoate and (±)-menthyl decanoate

We followed a protocol described by Gordo *et al.*[158]. In the case of (–)-menthyl laurate, to a solution of lauric acid (220.5 mg, 1.1 mmol, 1.25 eq) in dry dichloromethane (3 mL), DCC (230 mg, 1.1 mmol, 1.25 eq) was added. After 1 h, (–)-menthol (138.1 mg, 0.875 mmol, 1 eq) and DMAP (12.5 mg, 0.10 mmol, 0.125 eq) were added. The reaction was completed after 2 h. The mixture was filtered, and the filtrate was washed with water. The organic layer was dried with anhydrous sodium sulphate, filtered, and concentrated under reduced pressure. The product was purified by flash chromatography using a mixture of *n*-hexane and dichloromethane (9:1 v/v) as washing solvent. The filtrate obtained was concentrated using a rotary evaporator. An identical procedure was followed for the synthesis of (±)-menthyl laurate, using (±)-menthol. In the case of (–)-menthyl decanoate, to a solution of decanoic acid (172.26 mg, 1.1 mmol, 1.25 eq) in dry dichloromethane (3 mL), DCC (230 mg, 1.1 mmol, 1.25 eq) was added. The procedure continued as indicated above, and was similarly applied to the synthesis of (±)-menthyl decanoate.

4.2.3. Enzymatic assays in *n*-hexane, in ILs, and in scCO₂

Reactions were normally carried out with an equimolar (ca. 300 mM) mixture of (±)-menthol and acylating agent, with varying amounts of enzyme, in stoppered glass vials or in a variable volume, high pressure, stainless steel cell equipped with a sapphire window (reactions in scCO₂) placed in a thermostatic bath. Acyl donor addition marked the start of reaction. Periodically, samples were taken for GC analysis. In the case of reactions in *n*-hexane (reaction volume of 5 mL; tridecane used as internal standard), 100 µL samples were taken from the reaction mixture, diluted with 500 µL of solvent, and passed through 0.20 µL pore syringe filters. In the case of reactions in ILs (reaction volume of 2 mL), 100 µL samples were taken and dissolved in 8 mL of ethyl acetate. This mixture was passed through a pipette-sized column filled with silica gel, to remove the IL. To the solution obtained was added 1 mL of a 22.5 mM solution of tridecane (used as external standard) in ethyl acetate, for GC analysis. In the case of reactions in scCO₂ (reaction volume of 10 mL; tridecane used as internal standard; pressure of 150 bar), samples were taken onto a calibrated, 150 µL loop, whose contents bubbled through 500 µL of *n*-hexane in a flask. Pressure was restored to its original value by moving the piston. *n*-Hexane was also

used to wash the loop circuit and collected in the same flask, up to the mark of 2 mL. Reactions were done in duplicate, together with a blank (no enzyme).

4.2.4. Reaction analysis

Reaction conversion and *ee* were measured by GC analysis performed with a Trace 2000 Series Unicam gas chromatograph equipped with a Cyclodex B (10.5% Beta-Cyclodextrin, 0.25 mm I.D. x 30 m with 0.25 - μ m film) fused silica capillary column from J&W Scientific, with a flame ionization detector (FID) and an auto sampler (Thermo Finnigan AS 2000). Oven temperature program (reaction with anhydrides): 90 °C for 10 min; 90-140 °C at 1 °C /min. Oven temperature program (reaction with vinyl esters): 90 °C for 10 min; 90-180 °C at 1 °C /min. Injection temperature: 200 °C. Flame ionization detection (FID) temperature: 250 °C. Carrier gas: helium (1 mL/min). Split ratio: 1:50.

4.2.5. Partitioning of substrates and product in biphasic IL/scCO₂ systems

4.2.5.1. Mixtures of (±)-menthol + menthyl decanoate

To simulate post-reaction separation, reactions were performed in 2 mL of [bmim][PF₆] with (±)-menthol (ca. 300 mM) on a 1:0.6 ratio relative to vinyl decanoate, and enzyme (200 mg of CRL), at 37 °C. Samples were taken and confirmed that after 24 h, all the acylating agent had been converted, thus yielding an approximately equimolar mixture of menthol and menthyl decanoate. The reaction mixture in [bmim][PF₆] was placed in a high pressure, stainless steel, variable volume, visual cell. The high-pressure apparatus and the experimental technique used were similar to those described in Chapter II, with some modifications (Fig. 4.1).

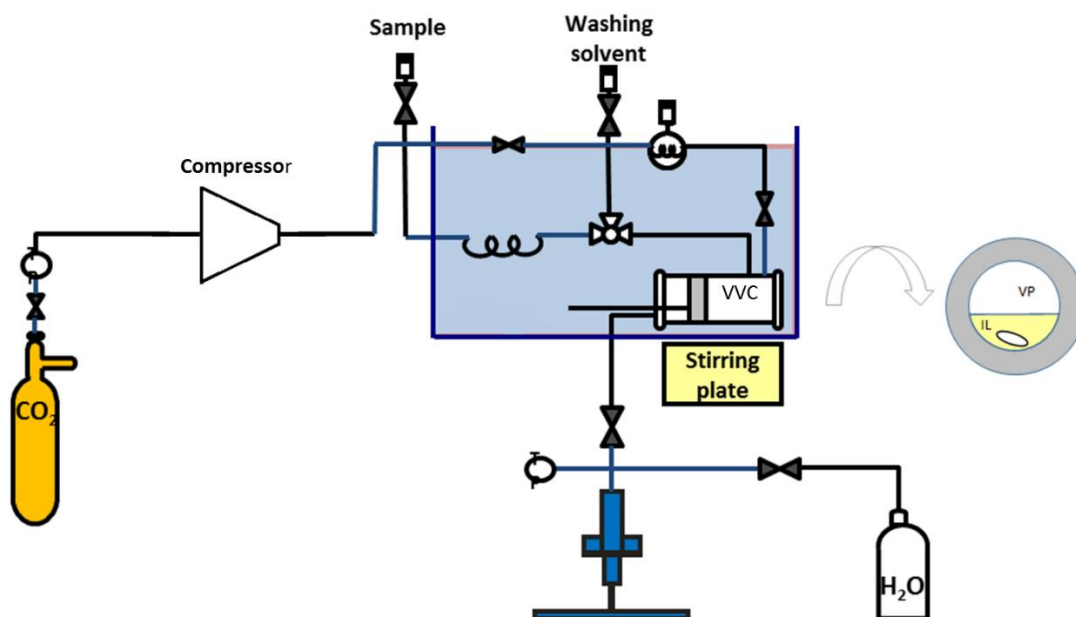


Figure 4.1 – Schematic of the high-pressure apparatus for substrate/product partitioning studies.

The cell was placed in a thermostatic bath and its volume was set to 10 mL using the piston acted upon by the water pressure generator. The cell was pressurized with CO₂ to the desired pressure, keeping its volume constant. The mixture was stirred. Samples were taken at one-hour intervals, in a total of 4 at each pressure and temperature selected.

Samples were taken with a 250 μ L loop and bubbled through 500 μ L of a solution of ethyl acetate with a known concentration of tridecane (external standard), in an eppendorf. The loop was washed with 1 mL of ethyl acetate and this solution was collected in the same eppendorf, which was taken for GC analysis.

Experiments were carried out at 35, 40 and 50 $^{\circ}$ C, and 7.5 MPa. It was assumed that the volume of the CO₂ phase, which initially was set at 8 mL (10 mL minus the volume of IL phase) decreased by 0.25 mL with every sample taken.

4.2.6. Pervaporation method

Preliminary tests were performed with PervapTM 4060 and PDMS Pervatech membranes. These were soaked in in two different ILs, namely [bmim][BF₄] and [bmim][PF₆], and it was observed that in [bmim][PF₆] the membrane floated whereas in [bmim][BF₄] the membrane was

submerged. Thus assays with the substrate/product mixture were only carried out with the PERVAP™ 4060 membrane in [bmim][BF₄].

Experiments were first performed with menthol, and then with a mixture of menthol and menthyl decanoate. An approximately equimolar mixture of menthol and menthyl decanoate was generated as indicated above, in 10 mL of *n*-hexane, using 1 g CRL ([enzyme] = 100 mg/mL), at 37 °C. The solvent was then evaporated, and [bmim][BF₄] was added. The apparatus used is shown schematically in Fig. 4.2. The membrane cell had approximately 20 mL maximum. The membrane was supported on a perforated stainless steel disk. The feed solution volume used was approximately 4.5 mL, which was sufficient to cover all the membrane. The system provides a radial feed flow over the membrane surface. The temperature of the feed stream was controlled at approximately 70 °C down to the condenser, immersed in liquid nitrogen, where the permeate was collected for 22 h. The downstream pressure was controlled at 2.5 ± 0.2 mbar, using a vacuum pump.

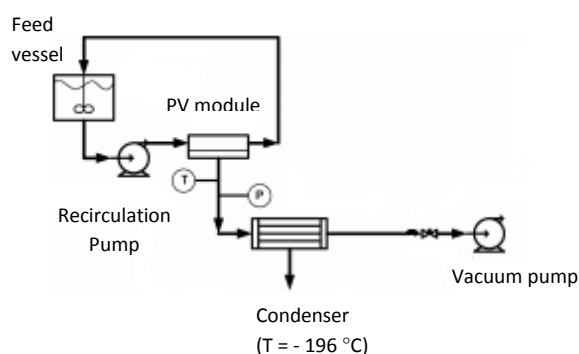


Figure 4.2 - Apparatus used for the pervaporation assays. Adapted from [123].

4.3. Results and discussion

4.3.1. Reactions with vinyl esters.

As seen earlier, vinyl esters conveniently make the transesterification reaction irreversible. E.g. Brady *et al.* have used vinyl acetate in the resolution of (±)-menthol [115]. Aiming at setting up an approach that might facilitate the separate recovery of the two (±)-menthol isomers through the combination of an IL with scCO₂, we selected vinyl esters with higher carbon chain lengths [60,61]. A pre-screening of acylating agent, temperature and enzyme led to the results shown

in Table 1. At 37 °C, CRL was highly enantioselective when using vinyl decanoate or vinyl laurate, although reactions were slower when using the latter ester. Increasing temperature did not make reaction with any of the two vinyl esters faster, possibly due to a negative effect on enzyme activity. Nor did it bring any improvement in enantioselectivity. The normal boiling point of *n*-hexane is 69 °C and thus the data reported at 50 °C for this solvent is affected by a comparatively larger error. Nonetheless, the results obtained indicate that it is more advantageous to work at 37 °C. Of the other enzymes tested in addition to CRL, Lipozyme TL (TL), Lipozyme RM (RM) and *Pseudomonas cepacia* lipase led to very low menthol conversions when using vinyl decanoate. The performance of Novozym 435 (435) was better, but no selectivity was observed. This finding agrees with the observation of Michor *et al.* for a different acylating agent [111].

We next looked at the performance of CRL in different ILs and in scCO₂. All the ILs selected comprise a 1-methyl-3-alkyl-imidazolium cation, a weak hydrogen-bond donor, and have similar polarity as regards the empirical parameter of solvent polarity E_N^T , related to the ability of the solvent to interact with the strong hydrogen-bond acceptor center of a standard dye [159]. The coordination strengths of the anions [PF₆][−], [BF₄][−], and [NTf₂][−] are also comparable [155]. These anions do not form strong hydrogen bonds with proteins, allowing them to maintain their structural integrity [160]. As shown in Figure 4.3, reaction progress was less favorable in scCO₂ than in the other solvents assayed, suggesting that scCO₂ might play a more advantageous role as solvent for extraction than for reaction. The enzyme had a better performance in the ILs, which led to very similar values of menthol conversion at 24 h of reaction, within the experimental error associated to the measurements. The same was true for 6 h of reaction. During this time period, the reaction progressed almost twice or three times as fast in ILs than in *n*-hexane or in scCO₂, respectively. After 6 h of reaction, menthol conversion continued to increase, although at a much slower rate. In all ILs, the reaction was highly enantioselective, as illustrated in Figure 4.4 for [hmim][PF₆].

Table 4.1 – Effect of enzyme, acylating agent and temperature on the conversion of menthol and the *ee* of menthyl decanoate and of menthol, at 48 h reaction in *n*-hexane. [enzyme] = 20 mg/mL.

Enzyme	Acylating agent	T (°C)	Menthol	
			conversion (%)	<i>ee_P</i> (%)
CRL	vinyl decanoate	37	44	>96%
CRL	vinyl laurate	37	31	>96%
CRL	vinyl decanoate	50	34	>90%
CRL	vinyl laurate	50	22	>90%
TL	vinyl decanoate	37	< 10 %	nd
RM	vinyl decanoate	37	< 10 %	nd
PS	vinyl decanoate	37	< 10 %	nd
435	vinyl decanoate	37	18	not selective

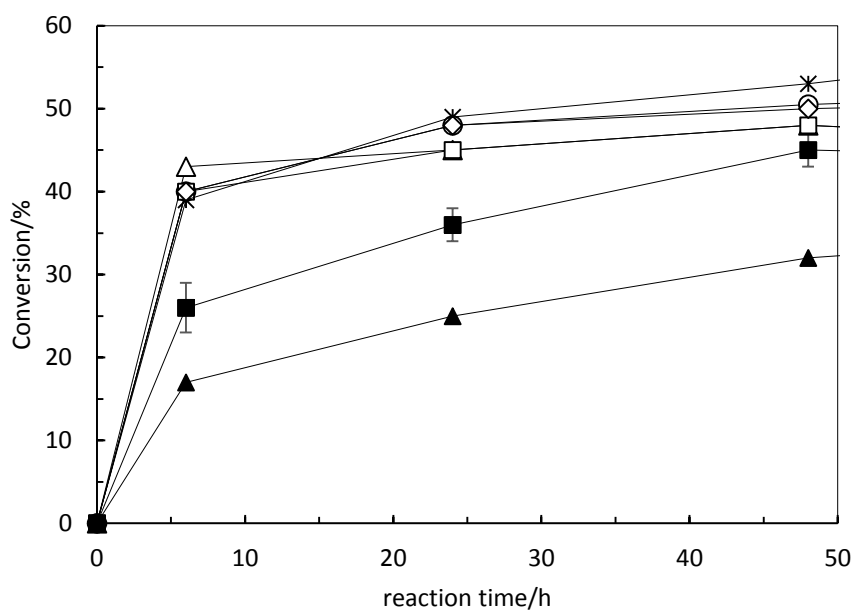


Figure 4.3 – Menthol conversion as a function of reaction time when using CRL and vinyl decanoate as acylating agent, at 37 °C. [enzyme] = 100 mg/mL. ◇, [bmim][PF₆]. △, [hmim][PF₆]. ×, [bmim][BF₄]. ○, [omim][PF₆]. □, [bmim][NTf₂]. ■, *n*-hexane. ▲, sCCO₂.

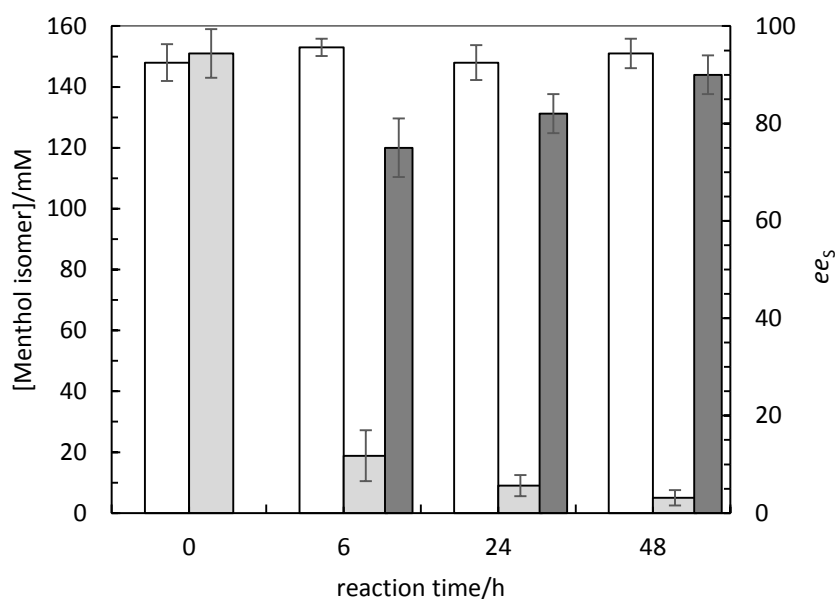


Figure 4.4 – Concentration of (+)-menthol (white bars) and (–)-menthol (light gray bars), and ee_s (darker gray bars; right Y-axis) as a function of reaction time when using CRL and vinyl decanoate as acylating agent, in [hmim][PF₆] at 37 °C. [enzyme] = 100 mg/mL. ee_P was >96%.

4.3.2. Reactions with propionic anhydride.

As with vinyl esters, the use of anhydrides also makes reactions irreversible, an approach often used in the resolution of (±)-menthol [104–110,112]. Yuan *et al.* [108] and Zhang *et al.* [110] studied the esterification of (±)-menthol with propionic anhydride in [bmim][PF₆] and [bmim][BF₄]. We looked at the behavior of CRL also in [hmim][PF₆], [omim][PF₆] and [bmim][Tf₂N], as shown in Figure 4.5, together with the results obtained in scCO₂. In this case, the performance of the enzyme in scCO₂ was very similar to that in ILs, showing that scCO₂ does not have a deleterious effect on the enzyme, as might be hypothesized based on the results obtained when using vinyl decanoate.

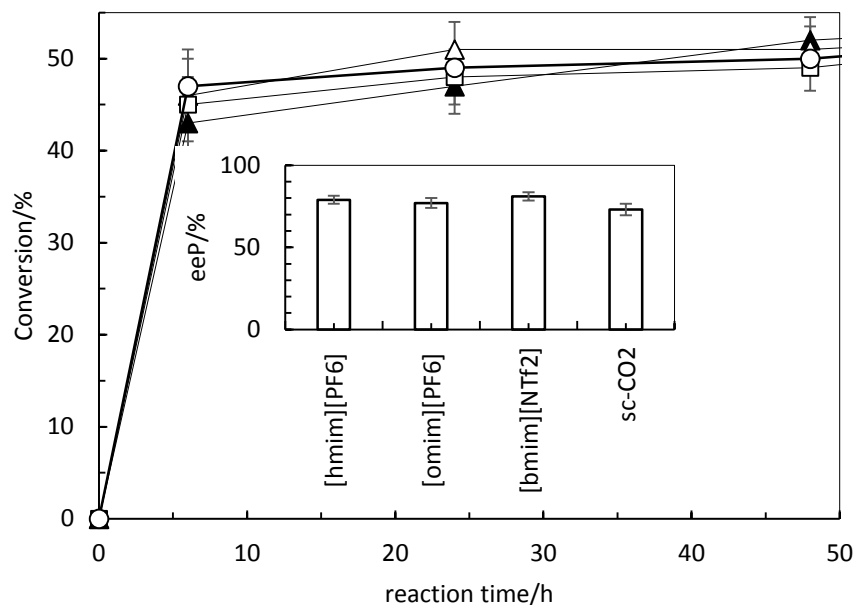


Figure 4.5 – Menthol conversion as a function of reaction time when using CRL and propionic anhydride as acylating agent, at 37 °C. [enzyme] = 100 mg/mL. \triangle , [hmim][PF₆]. \circ , [omim][PF₆]. \square , [bmim][NTf₂]. \blacktriangle , scCO₂. Inset: ee_P at nearly 50% menthol conversion.

As seen from the inset of Figure 4.5, ee_P was lower than in the case of reactions with the vinyl ester. The drawback, as referred earlier, is the extent of the uncatalyzed reaction when using acid anhydrides [105]. In our study, this led to about 30% conversion of menthol to form equal amounts of the two menthyl esters at 37 °C. As illustrated in Figure 4.6, lowering the temperature had a considerable effect on the enantioselectivity of the process. At the conditions depicted in the figure, the conversion of menthol reached similar values at 4 and 37 °C. However, at 4 °C the enzymatic reaction represented a much larger contribution to the overall transformation than the unselective chemical conversion, making the overall reaction highly enantioselective. As seen in the figure, the amount of (+)-menthyl propionate produced is very low at 4 °C.

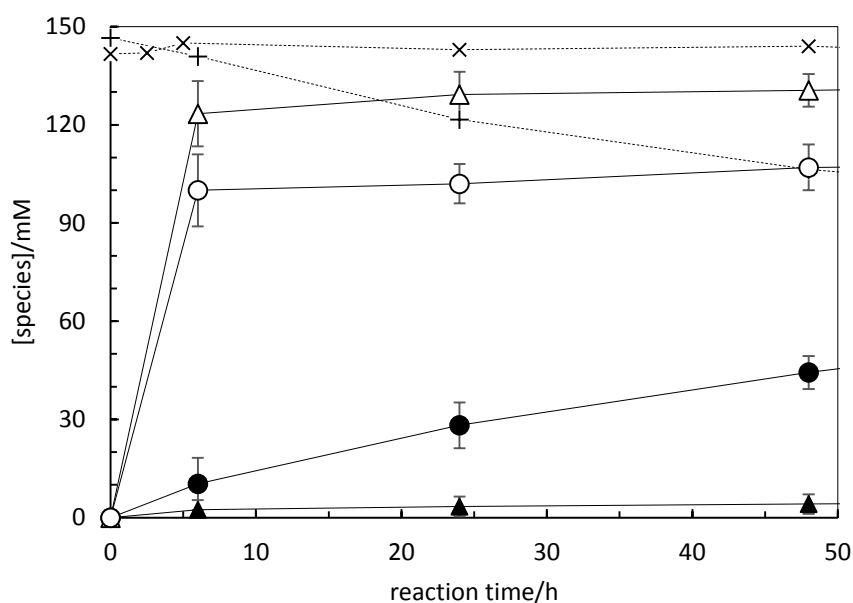


Figure 4.6 – Formation of (-)-menthyl propionate (open symbols) and (+)-menthyl propionate (closed symbols) as a function of reaction time when using CRL and propionic anhydride as acylating agent, in *n*-hexane, at 4 °C (△,▲) and 37 °C (○,●). [enzyme] = 100 mg/mL. The dashed lines represent the consumption of (+)-menthol at 4 °C (x) and 37 °C (+) in the blank without enzyme.

4.3.3. Partitioning of substrates and product in IL/CO₂ systems

As mentioned earlier, the ILs tested led to similar results as regards reaction conversion and enantioselectivity. The solubility of CO₂ is high in ILs with hexafluorophosphate anions [161]. It is also known that scCO₂ can dissolve up to approximately 0.6 mole fraction in [bmim][PF₆], while no IL is detected in the vapor phase [124]. We thus selected [bmim][PF₆] for partitioning experiments. To determine the ability of scCO₂ to fractionate the reaction products, phase partitioning experiments were carried out with a mixture of menthol + menthyl decanoate (Table 4.2). Experiments were carried out at 7.5 MPa. As seen in Chapter 3.1, due to the higher density of scCO₂ at higher pressures [124], the solubility of menthol in CO₂ increases drastically. At pressure of about 10 MPa, the system is near the critical region. In fact, preliminary experiments carried out at 9 MPa showed that more than 95 wt. % of menthol was in the gas phase.

Table 4.2 - Partitioning of menthol and menthyl decanoate in [bmim][PF₆]/CO₂ systems. P = 7.5 MPa. Results are given for the vapor phase, as wt.% of total amount of compound used in the experiment.

Temperature (°C)	menthol (%)	menthyl decanoate (%)
35	43	>95
40	41	>95
50	36	59

The results show that almost all of the menthyl decanoate is in the vapor phase at 35 °C. At constant pressure, an increase in temperature brings about a decrease in the density of CO₂, which may explain why at the highest temperature the solubility of both compounds decreases. This effect is more pronounced at 50 °C.

Adequate conversion and high enantioselectivity can be achieved using a menthol to acylating agent molar ratio higher than 1, as done in this study and as done by others authors [104]. Therefore, the problem lies in the partitioning of menthol and menthyl decanoate in IL/CO₂ systems. The results show that a good separation can be achieved, with a theoretical separation factor of 27. Nevertheless complete separation cannot be attained, it only being possible to obtain a product with a maximum purity of 70% in the gas phase.

4.3.4. Pervaporation

This method uses a membrane that acts as a selective barrier for the components of a liquid mixture. The component that passes through the membrane is recovered in the gas phase, and condensed. Table 4.3 shows results of experiments performed with just menthol – first line – and with the mixture. Measurement of the amounts recovered in the trap closed the mass balance with reasonable approximation.

Table 4.3 – Permeation of menthol and menthyl decanoate, dissolved in [bmim][BF₄], through a PERVAP™ 4060 membrane. Results are given as wt.% of total amount of compound that remained in the cell, relative to the total amount used in the experiment.

Time (h)	Temperature (°C)	Pressure (mbar)	menthol (%)	(-)-menthyl decanoate (%)
5	70	3.5 ± 0.1	70	-
22	70	2.5 ± 0.2	55	37

The membrane used is hydrophobic, and is normally used to recover aroma from aqueous solutions. It is known that pervaporation processes have to operate with a relatively low downstream pressure, to ensure sufficient driving force for the transport of the target compounds across the membrane [162-164]. Both compounds have high boiling points, and therefore the lowest pressure possible was used. However, and as shown in the table, a reasonable percentage of menthol passed through the membrane, and the same was true for the reaction product, whose presence appears to have facilitated the extraction of menthol from the IL.

4.4. Conclusions

Enantioselective conversion of menthol was performed using vinyl esters and acid anhydrides, in organic media, scCO₂ and in different ILs. In the case of acid anhydrides, nonselective, uncatalyzed, reaction occurs and leads to a decrease in selectivity, which can be counteracted by lowering temperature. Vinyl esters, namely vinyl decanoate, led to *ee_p* > 96% at approximately 50% conversion. Thus this system was used as a model to implement a separation strategy based on the use of IL/CO₂ systems. It was expected that the alcohol would have less of a tendency to partition to the vapor phase, compared to the ester. Data on the partitioning of the relevant solutes revealed that the affinity of menthol and menthyl decanoate for CO₂ was indeed different. However, the separation factors obtained make the envisaged separation strategy difficult, requiring a number of separators. Another postreaction strategy was studied, namely pervaporation. The results obtained showed that both the alcohol and the ester product passed

through the membrane, in a proportion that makes unsuitable a separation method based on this methodology.

Chapter V

**Enzymatic resolution/separation of *sec*-alcohols
using an ionic anhydride as acylating agent**

5. Enzymatic resolution/separation of *sec*-alcohols using an ionic anhydride as acylating agent

5.1. Introduction

The use of enzymatic catalysts in the resolution of *sec*-alcohols is an efficient method to separate the two enantiomers, based on the conversion of one of the enantiomers into a different chemical species. However, the subsequent physical separation of the two enantiomers often involves a series of steps. Here we address this challenge using sustainable chemistry approaches, with (*R,S*)-1-phenylethanol as model. This compound is used as synthetic intermediate in the fine chemicals and pharmaceutical industries, and as a chiral building block for pharmaceuticals, agrochemicals and natural products. In particular, (*R*)-1-phenylethanol is usually used as fragrance in the cosmetics industry because of its gentle floral odor [165,166]. In this work, CRL and Novozym 435 - Immobilized *Candida antarctica* lipase B (CALB) – were tested as regards enantioselective conversion of (*R,S*)-1-phenylethanol into the corresponding ester, leaving unreacted (*S*)-1-phenylethanol. The reaction was carried out in an IL solvent. The acylating agent was an ionic acid anhydride that yields an ionic (*R*)-1-phenylethanol derived ester. The ionic character of the latter species is a key factor in the separation of the two alcohol enantiomers [59][128]. Due to the high viscosity of the ionic acylating agent, a different, less viscous, commonly used IL was used as solvent for the enzymatic reaction.

ScCO₂ is highly soluble in IL media, while the reverse is generally not true. In this work, scCO₂ was used to perform the post-reaction separation, instead of organic media. Thus after the (*R*)-enantiomer was converted into an ionic species, a stream of scCO₂ was passed continuously through the IL to selectively extract unreacted (*S*)-1-phenylethanol. The ionic (*R*)-1-phenylethanol derived ester, which is insoluble in scCO₂, remained in the IL solvent. The recovery of (*S*)-1-phenylethanol was straightforward by depressurization of the scCO₂ stream. Water was then added to the IL, to hydrolyze the ionic (*R*)-1-phenylethanol derived ester, yielding (*R*)-phenylethanol. ScCO₂ was again used, this time to extract (*R*)-1-phenylethanol. At the end of the process, both enantiomers of (*R,S*)-1-phenylethanol were obtained with high enantiomeric purity.

5.2. Experimental section

5.2.1. Materials

Lipase from *Candida rugosa* (CRL; Type VII) from Sigma-Aldrich, Novozym 435 (*Candida antarctica* lipase B (CALB), immobilized within a macroporous resin of poly-(methyl methacrylate) – Lewatit VP OC 1600) was gently provided by Novozymes (Denmark). Prior to use, the enzyme was treated according to a procedure described in the literature [128]: 30 mg of Novozym 435 were soaked in 1 mL of *n*-hexane for 1 h. The particles were filtered out and washed three times with acetone (3 x 0.5 mL). After the filtration, the enzyme was washed again with *n*-hexane and dried for 24 h at room temperature.

(±)-Menthol (≥98% purity) and (*R,S*)-1-phenylethanol (98% purity) were from Sigma-Aldrich and bis((1(11-undecanoic acid)-3-methyl)imidazolium hexafluorophosphate) anhydride (acylating agent) was prepared as described in detail elsewhere [128]. The ILs used as solvent in the reaction were 1-butyl-3-methylimidazolium hexafluorophosphate [bmim][PF₆] and 1-butyl-3-methylimidazolium tetrafluoroborate [bmim][BF₄], supplied by Iolitec. Tridecane (99%, Aldrich) was used as external standard and ethyl acetate (≥ 99.8%, Carlo Erba) was used as solvent, both for GC analysis. Carbon dioxide (N45) was from Air Liquide. Ethanol absolute anhydrous (99.9%) was from Carlo Erba. Before use, ILs were dried under vacuum while stirring, for 48 h. All other solvents and substrates were dried with molecular sieves. The water content of the reaction mixture was determined regularly by Karl-Fischer Coulometric titration (Metrohm 831 KF Coulometer).

5.2.2. Enzymatic reaction/separation experiments

Reactions with (±)-menthol were performed in 5 mL glass flasks. The alcohol and the ionic anhydride acylating agent were used in a molar ratio of 1:1 (0.5:1 ratio of each enantiomer of the alcohol to the acylating agent). To 1 mL of IL [bmim][PF₆] were added the alcohol, the enzyme (100 mg of CRL), and finally the ionic anhydride. The reaction mixture was stirred in a thermostatic water bath (35 °C) for 72 h.

Approximately 100 µL (weighed) samples were taken at 0 h, 6 h, 24 h, 48 h, 72 h and 96 h, and dissolved in 8 mL of ethyl acetate. This mixture was passed through a pipette-sized column filled with silica gel, to remove the IL. To the solution obtained was added 1 mL of a 22.5 mM solution of tridecane (used as external standard) in ethyl acetate, for GC analysis.

Based on the previous knowledge that Novozym 435 was effective in the resolution of (*R,S*)-1-phenylethanol using the ionic anhydride, experiments were performed directly in a stainless steel cell. The experimental procedure was identical to that described above, but Novozym 435 (30 mg) was used instead of CRL. Reactions were carried out for 24 or 48 h. After this time, sampling of the IL phase indicated that the desired conversion was reached. CO₂ was then flown through the IL phase in the cell, using an HPLC pump at a flow rate of 6-8 mL/min (T = 37 °C and P = 180 bar). A constant exit flow was maintained under these conditions for a given time. The stream of CO₂ passed through a cold trap, which was afterwards washed with ethyl acetate and analyzed by GC.

After the extraction of all the (*S*)-1-phenylethanol with scCO₂, 3 equivalents of water were added. After 24 h of reaction, the ionic species was converted so as to release (*R*)-1-phenylethanol. The method for the extraction of (*R*)-1-phenylethanol and the experimental conditions used were the same as for (*S*)-1-phenylethanol.

5.2.3. Sample analysis

All the samples were analyzed on a gas chromatograph (TermoQuest Trace GC 2000 Series) equipped with a flame ionization detector (FID) and an auto sampler (Thermo Finnigan AS 2000). The compounds were separated in a Cyclodex B (10.5% Beta-Cyclodextrin; J&W Scientific) capillary column (0.25 mm I.D. x 30 m with 0.25- μm film). It was used two different methods for analysis, depending of the reaction. For (±)-menthol: the oven temperature program: 90 °C for 10 min; 90-140 °C at 1 °C/min. Injection temperature: 200 °C. For (*R,S*)-1-phenylethanol: the oven temperature program: 90 °C for 15 min; 90-108 °C at 1 °C/min and 108-220 °C at 30 °C/min for 5 min. Flame ionization detection (FID) temperature: 250 °C. Carrier gas: helium (1 mL/min). Split ratio: 1:50. For both reactions: Flame ionization detection (FID) and injector temperatures were set at 250 °C. Carrier gas: helium (1 mL/min). Split ratio: 1:50. Tridecane was used as internal standard for GC analysis. Response factors were determined with calibration curves for the pure components. The results presented are the average of duplicate experiments.

5.3. Results and discussion

The reaction mechanism for (*R,S*)-1-phenylethanol with the IL bis((1(11-undecanoic acid)-3-methyl)imidazolium hexafluorophosphate) anhydride is shown in Figure 5.1:

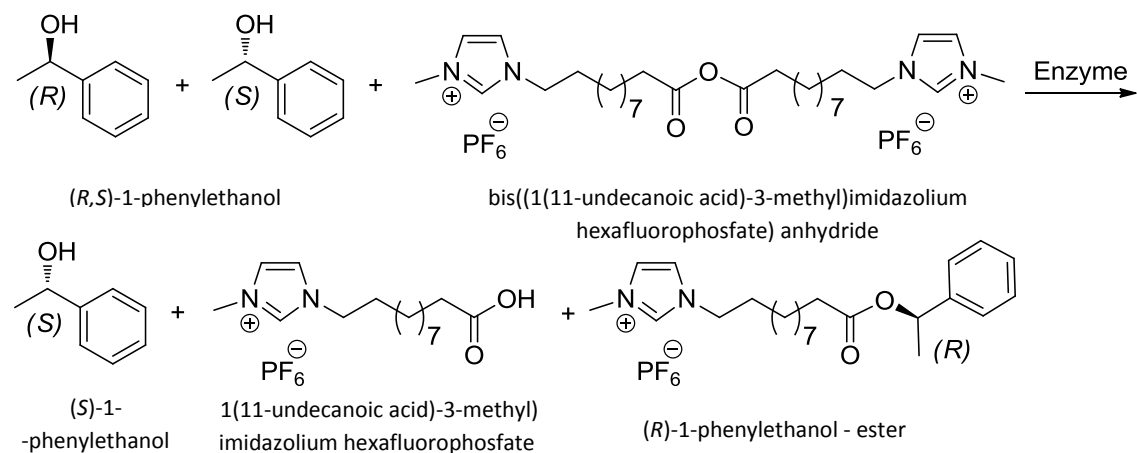


Figure 5.1 - Scheme for the EKR of (*R,S*)-1-phenylethanol with the IL bis((1(11-undecanoic acid)-3-methyl)imidazolium hexafluorophosphate) anhydride.

Using CRL, it was not possible to carry out the reaction/separation procedure envisaged. No conversion of the substrate took place. A similar result had already been obtained using ionic acylating esters, as described in Chapter III. This approach was however successful using Novozym. The reaction/separation methodology is based on a four-step method detailed in Figures 5.2 and 5.3. In Step 1, (*R*)-1-phenylethanol reacts with the ionic anhydride, forming an ionic ester and an ionic acid, and leaving (*S*)-1-phenylethanol unaltered. In Step 2, (*S*)-1-phenylethanol is entirely extracted with scCO_2 . The (*R*)-enantiomer, which is in ionic form and therefore not soluble in CO_2 , remains in the IL solvent. In Step 3, upon addition of water, the ionic ester holding (*R*)-1-phenylethanol releases the latter with formation of ionic acid. The hydrolysis of the remaining ionic anhydride leads to the formation of yet more acid. Finally (Step 4), (*R*)-1-phenylethanol is extracted with scCO_2 .

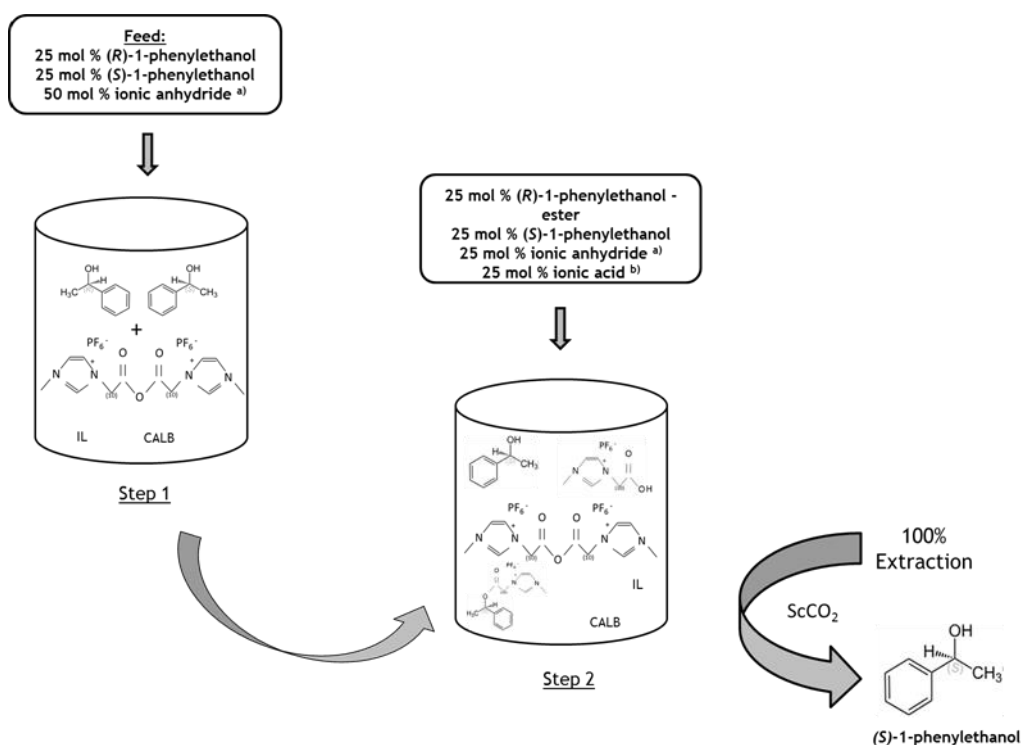


Figure 5.2 - Scheme with the methodology for the enzymatic resolution and separation of (*R,S*)-1-phenylethanol (steps 1 and 2) ^{a, b}.

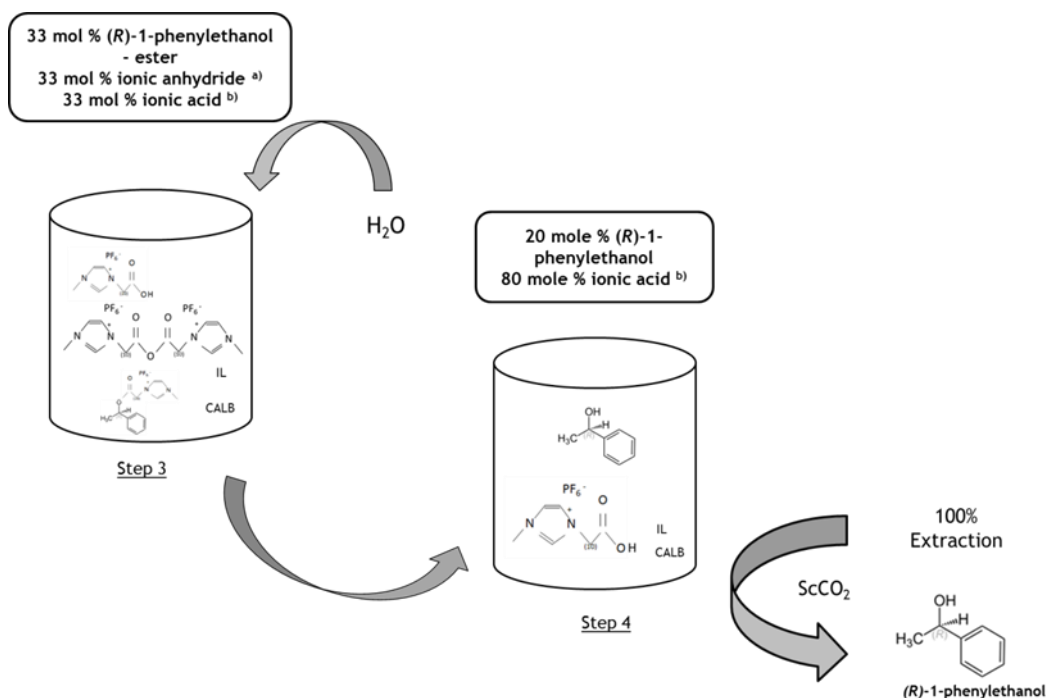


Figure 5.3 - Scheme with the methodology for the enzymatic resolution and separation of (*R,S*)-1-phenylethanol (steps 3 and 4)

^a Bis((1(11-undecanoic acid)-3-methyl) imidazolium hexafluorophosphate) anhydride

^b 1(11-undecanoic acid)-3-methylimidazolium hexafluorophosphate

The results obtained are shown in Tables 5.1. and 5.2.

Table 5.1 – Results for reactions carried out using Novozym 435 as biocatalyst, bis((1(11-undecanoic acid)-3-methyl)imidazolium hexafluorophosphate) anhydride as acylating agent, and an IL as solvent, at 35 °C, as part of a four-step methodology for the separation of (*R,S*)-1-phenylethanol enantiomers. *c* = conversion of (*R,S*)-1-phenylethanol.

Time (h)	[bmim][PF ₆]			[bmim][BF ₄]		
	<i>ee_s</i> (%)	<i>ee_p</i> (%)	<i>c</i> (%)	<i>ee_s</i> (%)	<i>ee_p</i> (%)	<i>c</i> (%)
6	64	79	45	34	50	40
24	80	87	48.5	44	69	39
48	-	-	-	52	70	43

As seen in Table 5.1, better results were obtained in [bmim][PF₆] than in [bmim][BF₄]. In [bmim][PF₆], at 24h of reaction, 94 % of the (*R*)-enantiomer was converted into the ionic ester while only 3 % of the (*S*)-enantiomer was converted. These results are similar to those obtained by Teixeira *et al.* [128] who implemented this reaction/separation strategy using acetone as solvent. After 13 h of reaction, these authors obtained the (*S*)-enantiomer with *ee_s* of 88%.

As seen in Table 5.2, after the hydrolysis reaction, and upon 3 h of extraction with scCO₂, virtually all of the unreacted alcohol was recovered in the CO₂ stream.

After the complete extraction of the unreacted alcohol, water was added to the IL reaction medium to hydrolyze the ionic ester product, thus yielding (*R*)-1-phenylethanol. However, the hydrolysis reaction fell short of the envisaged objective which was the release of the total amount of (*R*)-enantiomer in the form of ionic ester. The yield in (*R*)-1-phenylethanol was approximately 30% after 24 h of hydrolysis, which compares with 40% obtained by Teixeira *et al.* [128]. Nevertheless once again scCO₂ was used to extract the nonionic species, i.e. (*R*)-1-phenylethanol with traces of the (*S*)-enantiomer. As shown in Table 5.2, the extraction efficiency was higher than 99%, meaning that all of the alcohol was extracted from the reaction medium. It is envisaged that subsequent hydrolysis reactions, followed by scCO₂ extractions, would release the remaining phenylethanol until complete recovery of the (*R*)-enantiomer was achieved.

Table 5.2 – Efficiency of the extraction of (*R,S*)-1-phenylethanol enantiomers using scCO₂. The % values given are relative to the amount of alcohol quantified in the IL solvent before hydrolysis ((*S*)-enantiomer) and after hydrolysis ((*R*)-enantiomer).

Time (h)	Conditions			1-phenylethanol enantiomer (wt. %)	
	Pressure (bar)	Temperature (° C)	Flow-rate (mL/min)	Before hydrolysis	After hydrolysis
1.5	140	37	2-4	23	-
2	160	37	4-6	3	-
3	180	37	6-8	<1	<1

5.4. Conclusions

CRL was not able to catalyze the conversion of menthol using an ionic anhydride as acylating agent. On the other hand, using CALB and a different secondary alcohol – (*R,S*)-1-phenylethanol – it was possible to implement a reaction/separation process based on selective enzymatic conversion of one enantiomer into an ionic compound, making possible the extraction of the unreacted enantiomer with a green solvent - CO₂. Upon addition of water, the (*R*)-enantiomer was released, to be also extracted with CO₂. Both enantiomers were obtained in high enantiomeric purity. However, as noted earlier, the hydrolysis step still needs to be optimized.

Chapter VI

Conclusions and Final Remarks

6. Conclusions and final remarks

The main objective of the work carried out within this thesis was the implementation of a methodology for the separation of enantiomers of *sec*-alcohols, based on a sustainable approach. The strategy devised involved enzymatic catalysis for turning one of the enantiomers into a different chemical entity. It also involved the use of an ionic acylating agent to ensure that the enantiomer preferentially converted by the enzyme was trapped in a form not amenable to extraction by supercritical carbon dioxide. Supercritical carbon dioxide could thus be used to extract the slow reacting enantiomer, together with a short chain alcohol formed in the acylation step, avoiding the use of organic media for that purpose, and at the same time driving reaction equilibrium in the forward direction. The two entities extracted could then be separated by varying the solvation ability of CO₂, through changes in the temperature and pressure of the fluid. To circumvent mass transfer difficulties due to the high viscosity of the ionic acylating agent, another ionic liquid, with lower viscosity, could be used as solvent. To the ionic liquid medium, holding the enantiomer of interest bound within an ionic compound, the short chain alcohol, formerly removed, would be added to perform the deacylation step, thereby releasing the enantiomer of interest for extraction by CO₂, at the same time reforming the ionic acylating agent.

As suggested by the various steps referred above, the success of this methodology depends on many factors, such as enzyme enantioselectivity, reactivity towards the substrates, the partitioning of chemical species between the ionic liquid medium and CO₂, temperature, pressure, etc.

(±)-Menthol appeared to be a good candidate to implement the envisaged approach. It is widely used in a number of industries, namely pharmaceutical, food and cosmetics, and market demand is increasing.

Initially it was intended to use an ionic acylating ester that would release ethanol upon binding of the fast reacting enantiomer. This led to a study of the phase equilibrium of the (±)-menthol/ethanol/CO₂ system, as required to implement the post-reaction separation strategy. It was concluded that the separation of menthol and ethanol is more favorable at lower pressure and higher temperature. However, it was found that when using *Candida rugosa* lipase (CRL), known to catalyze enantioselective conversion of (±)-menthol, the reaction did not take place with either of the two ionic esters prepared. Similar results were obtained when using immobilized *Candida antarctica* lipase B (CALB). This led to the use of a different substrate (*R,S*)-

1-phenylethanol – whose reaction with the ionic acylating ester CRL was able to catalyze, although nonselectively, and reaching very low reaction conversion values. CALB, on the other hand, led to high conversion of (*R,S*)-1-phenylethanol, as well as high enantioselectivity. The difficulties encountered may have to do with the position of the –OH on the menthol molecule, which makes it less flexible than the –OH group of phenylethanol, as well as the geometry of the two ionic acylating agents tested, whose imidazolium ring might hinder access to the enzyme active site, upon binding of its carbonyl group to the latter.

This led to a different reaction approach, involving the use of vinyl esters and acid anhydrides, which makes reactions irreversible. Both types of acylating agents had already been used to convert menthol with good selectivity. A phase behavior study of the CO₂/propionic anhydride system was conducted that showed the substrate to be highly soluble in CO₂ at the conditions envisaged for carrying out the enzymatic reaction. A screening of enzymes was conducted that revealed CRL to be the best option as regards reaction conversion and selectivity. Studies were also conducted where several experimental parameters were varied, which showed that when using vinyl decanoate in a number of ionic liquids, (–)-menthyl decanoate could be obtained with an enantiomeric excess > 96%, at nearly 50% conversion, at 37 °C, both *n*-hexane and CO₂ leading to worse results. Propionic anhydride also led to highly selective reactions, but at a sufficiently low temperature – 4 °C – to make the extent of the nonselective, uncatalyzed reaction, a small contribution compared to the extent of the enantioselective, enzymatic contribution.

Based on the results obtained, it was decided to follow up on the strategy comprising the use of vinyl decanoate, and combine it with the use of CO₂ as solvent for extraction, given that the reaction in CO₂ had not progressed as well as in ionic liquids. Partitioning studies for menthol and menthyl decanoate in biphasic LI/scCO₂ media revealed that at 35 °C and 7.5 MPa, about half of the menthol remained in the lower, IL phase, most of the menthyl decanoate being found in the upper phase. This could form the basis of a separation strategy, but the values of the separation factors obtained would imply a series of steps – separators – making the economy of the process unfavorable. This led to the consideration of another separation strategy, namely pervaporation. Given the choice of a hydrophobic membrane, it was expected that menthol would have less of a tendency to get across the membrane and thus remain in the ionic liquid. However, both menthol and menthyl decanoate were able to cross over. Later, the separation of these two species was accomplished using a eutectic mixture as solvent, instead on an ionic liquid. But lack of success with (±)-menthol at the time led to the use of (*R,S*)-1-phenylethanol.

Again, an ionic acylating agent was used, this time an anhydride, using immobilized CALB that had already been shown to catalyze the conversion of (*R,S*)-1-phenylethanol through reaction with an ionic acylating ester. Using the ionic anhydride in an ionic liquid medium, it was possible to reach nearly 50% conversion in 24 h, and obtain unreacted substrate with *ee* of 87%, and a product with *ee* of 80%. CO₂ efficiently extracted the nonacylated menthol. Hydrolysis of the ionic species holding (–)-menthol led to the release of the latter, which was also efficiently extracted with CO₂. It was thus possible to implement the reaction/separation strategy envisaged at the start of this work.

As noted earlier, full hydrolysis of the ionic species holding (–)-menthol was difficult. This limitation should be addressed before applying the reaction/separation strategy described to other *sec*-alcohols, possibly through the synthesis of different ionic anhydrides.

Modeling studies might elucidate the difficulty in applying this approach to menthol.

The very good separation of menthol and menthyl decanoate achieved later on by a different member of our group, when using a eutectic solvent (results not shown), and the fact that eutectic mixtures can also be used for enzymatic reactions, suggest that applying the reaction/separation strategy described to eutectic mixture/CO₂ binary systems holds promise.

References

- [1] J. Tao, R. Kazlauskas, *Biocatalysis for green chemistry and chemical process development*, John Wiley & Sons, Inc., 2011.
- [2] C.Brundtland, *Report of the World Commission on Environment and Development: Our Common Future*, (1987).
- [3] P.T. Anastas, J.C. Warner, *Green Chemistry: Theory and Practice*, 1998.
- [4] P.T. Anastas, J.B. Zimmerman, *Design Through the 12 Principles Green Engineering*, *Environ. Sci. Technol.* 37 (2003) 94A–101A.
- [5] R. A. Sheldon, *Fundamentals of green chemistry: efficiency in reaction design*, *Chem. Soc. Rev.* 41 (2012) 1437.
- [6] S.Y. Tanq, R.A. Bourne, R.L. Smith, M. Poliakoff, *The 24 Principles of Green Engineering and Green Chemistry: "IMPROVEMENTS PRODUCTIVELY,"* *Green Chem.* 10 (2008) 268–269.
- [7] M. Koel, M. Kaljurand, *Green Analytical Chemistry*, 2010.
- [8] R. A. Sheldon, *The E Factor: fifteen years on*, *Green Chem.* 9 (2007) 1273.
- [9] J.M. Woodley, *New opportunities for biocatalysis: making pharmaceutical processes greener*, *Trends Biotechnol.* 26 (2008) 321–7.
- [10] H.D. Flack, *Louis Pasteurs discovery of molecular chirality and spontaneous resolution in 1848, together with a complete review of his crystallographic and chemical work*, *Acta Crystallogr. Sect. A Found. Crystallogr.* 65 (2009) 371–389.
- [11] J. Gal, *Molecular chirality: language, history, and significance*, *Top Curr Chem.* 340 (2013) 1–20.
- [12] J. McConathy, M.J. Owens, *Stereochemistry in Drug Action*, *Prim. Care Companion J. Clin. Psychiatry.* 5 (2003) 70–73.
- [13] R. Eccles, *Menthol and related cooling compounds.*, *J. Pharm. Pharmacol.* 46 (1994).
- [14] <https://en.wikipedia.org/wiki/Menthol>, page consulted September, 2015.

- [15] N. Galeotti, L. M. Di Cessani, Mannelli, G. Mazzanti, A. Bartolini, C. Ghelardini, Menthol: a natural analgesic compound, *Neurosci. Lett.* 322 (2002) 145–148.
- [16] J.C. Leffingwell, R.E. Shackelford, Laevo-menthol-syntheses and organoleptic properties, *Cosmet. Perfum.* 89 (1974) 69–89.
- [17] R. Hopp, Menthol: its origins, chemistry, physiology and toxicological properties, *Rec. Adv. Tob. Sci.* 19 (1993) 3–46.
- [18] B.M. Lawrence, *Mint: the genus Mentha*, CRC Press, 2006.
- [19] <https://www.basf.com/us/en/company/news-and-media/science-around-us/the-cool-freshness-of-menthol.html>, page consulted September, 2015.
- [20] J. Ottosson, J.C. Rotticci-Mulder, D. Rotticci, K. Hult, Rational design of enantioselective enzymes requires considerations of entropy, *Protein Sci.* 10 (2001) 1769–1774.
- [21] A.M. Klibanov, Improving enzymes by using them in organic solvents, *Nature* 409 (2001) 241–246.
- [22] G. Carrea, S. Riva, Properties and Synthetic Applications of Enzymes in Organic Solvents, *Angew. Chem. Int. Ed. Engl.* 39 (2000) 2226–2254.
- [23] A. Illanes, Enzyme biocatalysis: Principles and applications, *Enzym. Biocatal. Princ. Appl.* (2008) 1–391.
- [24] M. Bänziger, G.J. Griffiths, J.F. McGarrity, A facile synthesis of (2R,3E)-4-iodobut-3-en-2-ol and (2S,3E)-4-iodobut-3-en-2-yl chloroacetate, *Tetrahedron: Asymmetry.* 4 (1993) 723–726.
- [25] S. H. Krishna, Developments and trends in enzyme catalysis in nonconventional media, *Biotechnol. Adv.* 20 (2002) 239–267.
- [26] L. Ragupathy, B. Pluhar, U. Ziener, H. Keller, R. Dyllick-Brenzinger, K. Landfester, Enzymatic aminolysis of lactones in aqueous miniemulsion: Catalysis through a novel pathway, *J. Mol. Catal. B Enzym.* 62 (2010) 270–276.
- [27] U.T. Bornscheuer, Lipase-catalyzed synthesis of monoacylglycerols, *Enzym. Microb. Technol.* 17 (1995) 578–586.
- [28] K.E. Jaeger, M.T. Reetz, Microbial lipases form versatile tools for biotechnology, *Trends Biotechnol.* 16 (1998) 396–403.

- [29] J.M.S. Cabral, M.R. Aires-Barros, M. Gama, Engenharia Enzimática, Lidel, Lisboa, 2003.
- [30] Y. -D. Shin, J.-H. Kim, T.-K. Kim, S.-H. Kim, Y.-H. Lee, Esterification of hydrophobic substrates by lipase in the cyclodextrin induced emulsion reaction system, *Enzyme Microb. Technol.* 30 (2002) 835–842.
- [31] R. Verger, “Interfacial activation” of lipases: Facts and artifacts, *Trends Biotechnol.* 15 (1997) 32–38.
- [32] K.-E. Jaeger, T. Eggert, Lipases for biotechnology, *Curr. Opin. Biotechnol.* 13 (2002) 390 – 397.
- [33] J.A. Mancheño, M.A. Pernas, M.J. Martínez, B. Ochoa, M.L. Rúa, J.A. Hermoso, Structural Insights into the Lipase/esterase Behavior in the *Candida rugosa* Lipases Family: Crystal Structure of the Lipase 2 Isoenzyme at 1.97 Å Resolution, *J. Mol. Biol.* 332 (2003) 1059–1069.
- [34] M. Cygler, J.D. Schrag, Structure and conformational flexibility of *Candida rugosa* lipase., *Biochim. Biophys. Acta.* 1441 (1999) 205–14.
- [35] H.S. Seo, S.E. Kim, K.Y. Han, J.S. Park, Y.H. Kim, S.J. Sim, J. Lee, Functional fusion mutant of *Candida antarctica* lipase B (CalB) expressed in *Escherichia coli*, *Biochim. Biophys. Acta - Proteins Proteomics.* 1794 (2009) 519–525.
- [36] I. Høegh, S. Patkar, T. Halkier, M.T. Hansen, Two lipases from *Candida antarctica* : cloning and expression in *Aspergillus oryzae*, *Can. J. Bot.* 73 (1995) 869–875.
- [37] J. Uppenberg, M.T. Hansen, S. Patkar, T.A. Jones, The sequence, crystal structure determination and refinement of two crystal forms of lipase B from *Candida antarctica*, *Structure* 2 (1994) 293–308.
- [38] N. Zhang, W.-C. Suen, W. Windsor, L. Xiao, V. Madison, A. Zaks, Improving tolerance of *Candida antarctica* lipase B towards irreversible thermal inactivation through directed evolution, *Protein Eng.* 16 (2003) 599–605.
- [39] O. Kirk, M.W. Christensen, Lipases from *Candida antarctica*: Unique biocatalysts from a unique origin, *Org. Process Res. Dev.* 6 (2002) 446–451.
- [40] R. K. Murray, D.K. Granner, P.A. Mayes, V.W. Rodwell, Harper’s Illustrated Biochemistry, 26th Edition, 2003.

- [41] H.C. Kwon, D.Y. Shin, J.H. Lee, S.W. Kim, J.W. Kang, Molecular modeling and its experimental verification for the catalytic mechanism of *Candida antarctica* lipase B., *J. Microbiol. Biotechnol.* 17 (2007) 1098–1105.
- [42] P. Monecke, R. Friedemann, S. Naumann, R. Csuk, Molecular Modelling Studies on the Catalytic Mechanism of *Candida Rugosa* Lipase, *J. Mol. Model.* 4 (1998) 395–404.
- [43] A. Ghanem, H.Y. Aboul-Enein, Application of lipases in kinetic resolution of racemates, *Chirality* 17 (2005) 1–15.
- [44] A.J.J. Straathof, J.A. Jongejan, The enantiomeric ratio: Origin, determination and prediction, *Enzyme Microb. Technol.* 21 (1997) 559–571.
- [45] Z. Lü, Y. Chu, Y. Han, Y. Wang, J. Liu, Enzymatic esterification of DL-menthol with propionic acid by lipase from *Candida cylindracea*, *J. Chem. Technol. Biotechnol.* 80 (2005) 1365–1370.
- [46] C.S.Chen, S.H. Wu, G. Girdaukas, C.J. Sih, Quantitative-analysis of biochemical kinetic resolution of enantiomers. 2. Enzyme-catalyzed esterifications in water organic-solvent biphasic systems, *J. Am. Chem. Soc.* 109 (1987) 2812–2817.
- [47] A. Hollaender, A.I. Laskin, P. Rogers, *Basic Biology of New Developments in Biotechnology*, 1st Edition, Plenum Press, New York and London, 1983.
- [48] K.E. Holt-Tiffin, C.J. Cobley, Asymmetric Routes to Chiral Secondary Alcohols, *Pharm. Technol.* 34 (2010) 6–13.
- [49] R.J. Kazlauskas, A.N.E. Weissfloch, A.T. Rappaport, L.A. Cuccia, A rule to predict which enantiomer of a secondary alcohol reacts faster in reactions catalysed by cholesterol esterase, lipase from *Pseudomonas cepacia*, and lipase from *Candida rugosa*, *J. Org. Chem.* 56 (1991) 2656–2665.
- [50] B. Min, J. Park, Y.-K. Sim, S. Jung, S.-H. Kim, J.K. Song, B.T. Kim, S.Y. Park, J. Yun, S. Park, H. Lee, Hydrogen-Bonding-Driven Enantioselective Resolution against the Kazlauskas Rule To Afford γ -Amino Alcohols by *Candida rugosa* Lipase, *ChemBioChem.* 16 (2015) 77–82.
- [51] S. Lutz, U.T. Bornscheuer, *Protein Engineering Handbook*, WILEY-VCH, 2012.
- [52] A.O. Magnusson, M. Takwa, A. Hamberg, K. Hult, An S-selective lipase was created by rational redesign and the enantioselectivity increased with temperature, *Angew. Chemie - Int. Ed.* 44 (2005) 4582–4585.

- [53] D. Rotticci, F. Haeffner, C. Orrenius, T. Norin, K. Hult, Molecular recognition of sec-alcohol enantiomers by *Candida antarctica* lipase B, *J. Mol. Catal. B-Enzymatic*. 5 (1998) 267–272.
- [54] I. Markovits, G. Egri, E. Fogassy, Nonlinearity in optical resolution via distillation applying mixtures of resolving agents, *Chirality*. 14 (2002) 674–6.
- [55] M. Okudomi, M. Nogawa, N. Chihara, M. Kaneko, K. Matsumoto, Enzyme-mediated enantioselective hydrolysis of soluble polymer-supported dendritic carbonates, *Tetrahedron Lett.* 49 (2008) 6642–6645.
- [56] N.M.T. Lourenço, S. Barreiros, C.A.M. Afonso, Enzymatic resolution of Indinavir precursor in ionic liquids with reuse of biocatalyst and media by product sublimation, *Green Chem.* 9 (2007) 734.
- [57] R.M.C. Viegas, C.A.M. Afonso, J.G. Crespo, I.M. Coelho, Racemic resolution of propranolol in membrane contactors: Modelling and process optimisation, *J. Memb. Sci.* 305 (2007) 203–214.
- [58] J.H. Chaaban, K. Dam-Johansen, T. Skovby, S. Kiil, Separation of enantiomers by continuous preferential crystallization: Experimental realization using a coupled crystallizer configuration, *Org. Process Res. Dev.* 17 (2013) 1010–1020.
- [59] N.M.T. Lourenço, C.A.M. Afonso, One-Pot Enzymatic Resolution and Separation of sec-Alcohols Based on Ionic Acylating Agents, *Angew. Chemie Int. Ed.* 46 (2007) 8178–8181.
- [60] A. Paiva, P. Vidinha, M. Angelova, S. Rebocho, S. Barreiros, G. Brunner, Biocatalytic separation of (*R*, *S*)-1-phenylethanol enantiomers and fractionation of reaction products with supercritical carbon dioxide, *J. Supercrit. Fluids.* 55 (2011) 963–970.
- [61] M.T. Reetz, W. Wiesenhöfer, G. Franciò, W. Leitner, Continuous Flow Enzymatic Kinetic Resolution and Enantiomer Separation using Ionic Liquid/Supercritical Carbon Dioxide Media, *Adv. Synth. Catal.* 345 (2003) 1221–1228.
- [62] M.H. Vermue, J. Tramper, Biocatalysis in non-conventional media: Medium engineering aspects (Technical Report), *Pure Appl. Chem.* 67 (1995) 345–373.
- [63] A. Zaks, A.M. Klibanov, Enzyme-catalyzed processes in organic solvents., *Proc. Natl. Acad. Sci. U. S. A.* 82 (1985) 3192–3196.
- [64] P. Halling, L. Kvittingen, Why did biocatalysis in organic media not take off in the 1930s?, *Trends Biotechnol.* 17 (1999) 343–344.

- [65] S. Cantone, U. Hanefeld, A. Basso, Biocatalysis in non-conventional media—ionic liquids, supercritical fluids and the gas phase, *Green Chem.* 9 (2007) 954.
- [66] P. Lozano, T. De Diego, M. Larnicol, M. Vaultier, J.L. Iborra, Chemoenzymatic dynamic kinetic resolution of rac-1-phenylethanol in ionic liquids and ionic liquids/supercritical carbon dioxide systems., *Biotechnol. Lett.* 28 (2006) 1559–1565.
- [67] P. Lozano, T. De Diego, C. Mira, K. Montague, M. Vaultier, J.L. Iborra, Long term continuous chemoenzymatic dynamic kinetic resolution of rac-1-phenylethanol using ionic liquids and supercritical carbon dioxide, *Green Chem.* 11 (2009) 538.
- [68] W. Leitner, P.G. Jessop, *Handbook of green chemistry, Volume 4: Supercritical Solvents*, WILEY-VCH, 2010.
- [69] <http://www1.chem.leeds.ac.uk//People/CMR/whatarescf.html>, page consulted September, 2015.
- [70] R. Fukuzato, *Science and Technology of Supercritical Fluids*, S. Saito, Japan, 1996.
- [71] R. A. Moreau, M.J. Powell, K.B. Hicks, Extraction and Quantitative Analysis of Oil from Commercial Corn Fiber, *J. Agric. Food Chem.* 44 (1996) 2149–2154.
- [72] E. Bogel-Lukasik, I. Fonseca, R. Bogel-Lukasik, Y.A. Tarasenko, M.N. da Ponte, A. Paiva, G. Brunner, Phase equilibrium-driven selective hydrogenation of limonene in high-pressure carbon dioxide, *Green Chem.* 9 (2007) 427–430.
- [73] P.G. Jessop, Y. Hsiao, T. Ikariya, R. Noyori, Homogeneous Catalysis in Supercritical Fluids: Hydrogenation of Supercritical Carbon Dioxide to Formic Acid, Alkyl Formates, and Formamides, *J. Am. Chem. Soc.* 118 (1996) 344–355.
- [74] T. Matsuda, K. Watanabe, T. Harada, K. Nakamura, Enzymatic reactions in supercritical CO₂: carboxylation, asymmetric reduction and esterification, *Catal. Today.* 96 (2004) 103–111.
- [75] J.R. Hyde, B. Walsh, J. Singh, M. Poliakoff, Continuous hydrogenation reactions in supercritical CO₂ “without gases”, *Green Chem.* 7 (2005) 357–361.
- [76] M. Sousa, M.J. Melo, T. Casimiro, A. Aguiar-Ricardo, The art of CO₂ for art conservation: a green approach to antique textile cleaning, *Green Chem.* 9 (2007) 943–947.
- [77] J.L. Kendall, D.A. Canelas, J.L. Young, J.M. DeSimone, Polymerizations in Supercritical Carbon Dioxide, *Chem. Rev.* 99 (1999) 543–563.

- [78] Y. Wang, R.N. Dave, R. Pfeffer, Polymer coating/encapsulation of nanoparticles using a supercritical anti-solvent process, *J. Supercrit. Fluids*. 28 (2004) 85–99.
- [79] F.J. Senorans, E. Ibanez, Analysis of fatty acids in foods by supercritical fluid chromatography, *Anal. Chim. Acta*. 465 (2002) 131–144.
- [80] K.W. Phinney, L.C. Sander, Additive concentration effects on enantioselective separations in supercritical fluid chromatography, *Chirality* 15 (2003) 287–294.
- [81] T.W. Randolph, H.W. Blanch, J.M. Prausnitz, C.R. Wilke, Enzymatic catalysis in a supercritical fluid, *Biotechnol. Lett.* 7 (1985) 325–328.
- [82] H.R. Hobbs, N.R. Thomas, Biocatalysis in supercritical fluids, in fluoruous solvents, and under solvent-free conditions, *Chem. Rev.* 107 (2007) 2786–2820.
- [83] T. Matsuda, T. Harada, K. Nakamura, Biocatalysis in Supercritical CO₂, *Curr. Org. Chem.* 9 (2005) 299–315.
- [84] A.J. Mesiano, E.J. Beckman, A.J. Russell, Supercritical Biocatalysis, *Chem. Rev.* 99 (1999) 623–633.
- [85] M.V. Oliveira, S.F. Rebocho, A.S. Ribeiro, E.A. Macedo, J.M. Loureiro, Kinetic modelling of decyl acetate synthesis by immobilized lipase-catalysed transesterification of vinyl acetate with decanol in supercritical carbon dioxide, *J. Supercrit. Fluids*. 50 (2009) 138–145.
- [86] S. V. Kamat, E.J. Beckman, A.J. Russell, Enzyme Activity in Supercritical Fluids, *Crit. Rev. Biotechnol.* 15 (1995) 41–71.
- [87] M. Habulin, M. Primožič, Ž. Knez, Supercritical fluids as solvents for enzymatic reactions, *Acta Chim. Slov.* 54 (2007) 667–677.
- [88] K.V. Bhaskar, First title: Ionic liquids-useful reaction green solvents for the future Second title: ionic liquids are the replacements for environmentally damaging solvents in a wide range of chemical processes, *J. Biomed. Pharm. Res.* 1 (2012) 7–12.
- [89] T.L. Greaves, C.J. Drummond, Ionic liquids as amphiphile self-assembly media, *Chem. Soc. Rev.* 37 (2008) 1709–1726.
- [90] J.S. Wilkes, A short history of ionic liquids—from molten salts to neoteric solvents, *Green Chem.* 4 (2002) 73–80.

- [91] P. Walden, Molecular weights and electrical conductivity of several fused salts., Bull. l'Academie Imp. Des Sci. St.-Petersbg. (1914) 405–422.
- [92] P. Wasserscheid, W. Keim, Ionic Liquids-New “Solutions” for Transition Metal Catalysis, Angew. Chem. Int. Ed. Engl. 39 (2000) 3772–3789.
- [93] T.B. Scheffler, C.L. Hussey, K.R. Seddon, C.M. Kear, P.D. Armitage, Molybdenum chloro complexes in room-temperature chloroaluminate ionic liquids: stabilization of hexachloromolybdate(2-) and hexachloromolybdate(3-), Inorg. Chem. 22 (1983) 2099–2100.
- [94] M.D. Joshi, J.L. Anderson, Recent advances of ionic liquids in separation science and mass spectrometry, RSC Adv. 2 (2012) 5470.
- [95] A. Zaks, A. M. Klivanov, The effect of water on enzyme action in organic media., J. Biol. Chem. 263 (1988) 8017–8021.
- [96] R.H. Valivety, P.J. Halling, A.R. Macrae, Reaction rate with suspended lipase catalyst shows similar dependence on water activity in different organic solvents., Biochim. Biophys. Acta. 1118 (1992) 218–222.
- [97] H. Zhao, Effect of ions and other compatible solutes on enzyme activity, and its implication for biocatalysis using ionic liquids, J. Mol. Catal. B Enzym. 37 (2005) 16–25.
- [98] J.L. Kaar, A.M. Jesionowski, J. A. Berberich, R. Moulton, A.J. Russell, Impact of ionic liquid physical properties on lipase activity and stability, J. Am. Chem. Soc. 125 (2003) 4125–4131.
- [99] O. Ulbert, T. Fráter, K. Bélafi-Bakó, L. Gubicza, Enhanced enantioselectivity of *Candida rugosa* lipase in ionic liquids as compared to organic solvents, J. Mol. Catal. B Enzym. 31 (2004) 39–45.
- [100] R.A. Sheldon, R.M. Lau, M.J. Sordedraeger, F. van Rantwijk, K.R. Seddon, Biocatalysis in ionic liquids, Green Chem. 4 (2002) 147–151.
- [101] R.F. Frade, C.A. Afonso, Impact of ionic liquids in environment and humans: an overview, Hum. Exp. Toxicol. 29 (2010) 1038–54.
- [102] T.P.T. Pham, C.-W. Cho, Y.-S. Yun, Environmental fate and toxicity of ionic liquids: a review, Water Res. 44 (2010) 352–72.
- [103] Z. Yang, W. Pan, Ionic liquids: Green solvents for nonaqueous biocatalysis, Enzyme Microb. Technol. 37 (2005) 19–28.

- [104] J.-H. Xu, T. Kawamoto, A. Tanaka, Efficient kinetic resolution of dl-menthol by lipase catalyzed enantioselective esterification with acid anhydride in fed-batch reactor, *Appl. Microbiol. Biotechnol.* 43 (1995) 402–407..
- [105] W.-H. Wu, C.C. Akoh, R.S. Phillips, Lipase-catalyzed stereoselective esterification of DL-menthol in organic solvents using acid anhydrides as acylating agents, *Enzyme Microb. Technol.* 18 (1996) 536–539.
- [106] D.-L. Wang, A. Nag, G.-C. Lee, J.-F. Shaw, Factors affecting the resolution of dl-menthol by immobilized lipase-catalyzed esterification in organic solvent., *J. Agric. Food Chem.* 50 (2002) 262–265.
- [107] S. Bai, Z. Guo, W. Liu, Y. Sun, Resolution of (\pm)-menthol by immobilized *Candida rugosa* lipase on superparamagnetic nanoparticles, *Food Chem.* 96 (2006) 1–7.
- [108] Y. Yuan, S. Bai, Y. Sun, Comparison of lipase-catalyzed enantioselective esterification of (\pm)-menthol in ionic liquids and organic solvents, *Food Chem.* 97 (2006) 324–330.
- [109] S.S. Othman, M. Basri, M.Z. Hussein, M.B. Abdul Rahman, R.N.Z.A. Rahman, A.B. Salleh, H. Jasmani, Production of highly enantioselective (–)-menthyl butyrate using *Candida rugosa* lipase immobilized on epoxy-activated supports, *Food Chem.* 106 (2008) 437–443.
- [110] D.-H. Zhang, S. Bai, M.-Y. Ren, Y. Sun, Optimization of lipase-catalyzed enantioselective esterification of (\pm)-menthol in ionic liquid, *Food Chem.* 109 (2008) 72–80.
- [111] H. Michor, R. Marr, T. Gamse, T. Schilling, E. Klingsbichel, H. Schwab, Enzymatic catalysis in supercritical carbon dioxide: Comparison of different lipases and a novel esterase, *Biotechnol. Lett.* 18 (1996) 79–84.
- [112] Y. Shimada, Y. Hirota, T. Baba, S. Kato, A. Sugihara, S. Moriyama, Y. Tominaga, T. Terai, Enzymatic synthesis of L-menthyl esters in organic solvent-free system, *J. Am. Oil Chem. Soc.* 76 (1999) 1139–1142.
- [113] S. Vorlova, U.T. Bornscheuer, I. Gatfield, J.-M. Hilmer, H.-J. Bertram, R.D. Schmid, Enantioselective Hydrolysis of d , l -Menthyl Benzoate, *Adv. Synth. Catal.* 1 (2002) 1152–1155.
- [114] H.-C. Chen, Y.-T. Liang, J.-H. Chen, C. Chang, C.-J. Shieh, Optimization of immobilized *Candida rugosa* lipase LIP2-catalyzed resolution to produce l -menthyl acetate, *Biocatal. Biotransformation.* 27 (2009) 296–302.
- [115] D. Brady, S. Reddy, B. Mboniswa, L.H. Steenkamp, A.L. Rousseau, C.J. Parkinson, J. Chaplin, R.K. Mitra, T. Moutlana, S.F. Marais, N.S. Gardiner, Biocatalytic enantiomeric

resolution of l-menthol from an eight isomeric menthol mixture through transesterification, *J. Mol. Catal. B Enzym.* 75 (2012) 1–10.

- [116] G.-W. Zheng, H.-L. Yu, J.-D. Zhang, J.-H. Xu, Enzymatic Production of l-Menthol by a High Substrate Concentration Tolerable Esterase from Newly Isolated *Bacillus subtilis* ECU0554, *Adv. Synth. Catal.* 351 (2009) 405–414.
- [117] G.-W. Zheng, H.-L. Yu, C.-X. Li, J. Pan, J.-H. Xu, Immobilization of *Bacillus subtilis* esterase by simple cross-linking for enzymatic resolution of dl-menthyl acetate, *J. Mol. Catal. B Enzym.* 70 (2011) 138–143.
- [118] Y. Gong, G.-C. Xu, G.-W. Zheng, C.-X. Li, J.-H. Xu, A thermostable variant of *Bacillus subtilis* esterase: Characterization and application for resolving dl-menthyl acetate, *J. Mol. Catal. B Enzym.* 109 (2014) 1–8.
- [119] H. Chen, J. Wu, L. Yang, G. Xu, Characterization and structure basis of *Pseudomonas alcaligenes* lipase's enantioference towards d,l-menthyl propionate, *J. Mol. Catal. B Enzym.* 102 (2014) 81–87.
- [120] R. Lovlin, M. Vakily, F. Jamali, Rapid, sensitive and direct chiral high-performance liquid chromatographic method for ketoprofen enantiomers, *J. Chromatogr. B Biomed. Sci. Appl.* 679 (1996) 196–198.
- [121] A. Basile, A. Figoli, M. Khayet, *Pervaporation, Vapour Permeation and Membrane Distillation, Principles and Applications*, 1st Edition, Woodhead Publishing, 2015.
- [122] W. Kujawski, Application of Pervaporation and Vapor Permeation in Environmental Protection, *Polish J. Environ. Stud.* 9 (2000) 13–26.
- [123] C. Brazinha, D.S. Barbosa, J.G. Crespo, Sustainable recovery of pure natural vanillin from fermentation media in a single pervaporation step, *Green Chem.* 13 (2011) 2197–2203.
- [124] L. A. Blanchard, Z. Gu, J.F. Brennecke, High-Pressure Phase Behavior of Ionic Liquid/CO₂ Systems, *J. Phys. Chem. B.* 105 (2001) 2437–2444.
- [125] R. Bogel-Łukasik, N.M.T. Lourenço, P. Vidinha, M.D.R.G. da Silva, C. A. M. Afonso, M.N. da Ponte, S. Barreiros, Lipase catalysed mono and di-acylation of secondary alcohols with succinic anhydride in organic media and ionic liquids, *Green Chem.* 10 (2008) 243–248.
- [126] R. Bogel-Łukasik, V. Najdanovic-visak, S. Barreiros, M.N. Ponte, Distribution Ratios of Lipase-Catalyzed Reaction Products in Ionic Liquid Supercritical CO₂ Systems : Resolution of 2-Octanol Enantiomers, *Ind. Eng. Chem. Res.* 47 (2008) 4473–4480.

- [127] N.M.T. Lourenço, C.A.M. Afonso, One-pot enzymatic resolution and separation of sec-alcohols based on ionic acylating agents, *Angew. Chemie - Int. Ed.* 46 (2007) 8178–8181.
- [128] R. Teixeira, N.M.T. Lourenço, Enzymatic kinetic resolution of sec-alcohols using an ionic liquid anhydride as acylating agent, *Tetrahedron Asymmetry*. 25 (2014) 944–948.
- [129] R. Dohrn, J.M.S. Fonseca, S. Peper, Experimental methods for phase equilibria at high pressures., *Annu. Rev. Chem. Biomol. Eng.* 3 (2012) 343–67.
- [130] R. Dohrn, S. Peper, J.M.S. Fonseca, Fluid Phase Equilibria High-pressure fluid-phase equilibria: Experimental methods and systems investigated (2000–2004), *Fluid Phase Equilib.* 288 (2010) 1–54.
- [131] S. Rebocho, A.V.M. Nunes, V. Najdanovic-Visak, S. Barreiros, P. Simões, A. Paiva, High pressure vapor–liquid equilibrium for the ternary system ethanol/(±)-menthol/carbon dioxide, *J. Supercrit. Fluids*. 92 (2014) 282–287.
- [132] A.B. Paninho, A.V.M. Nunes, A. Paiva, V. Najdanovic-Visak, High pressure phase behavior of the binary system (ethyl lactate+carbon dioxide), *Fluid Phase Equilib.* 360 (2013) 129–133.
- [133] V. Najdanovic-Visak, J.M.S.S. Esperança, L.P.N. Rebelo, M. Nunes da Ponte, H.J.R. Guedes, K.R. Seddon, H.C. de Sousa, J. Szydlowski, Pressure, Isotope, and Water Co-solvent Effects in Liquid–Liquid Equilibria of (Ionic Liquid + Alcohol) Systems, *J. Phys. Chem. B*. 107 (2003) 12797–12807.
- [134] E.G. Azevedo, A.M. Alves, *Engenharia de Processos de Separação*, IST Press, Lisboa, 2009.
- [135] D.-Y. Peng, D.B. Robinson, A New Two-Constant Equation of State, *Ind. Eng. Chem. Fundam.* 15 (1976) 59–64.
- [136] P.M. Mathias, H.C. Klotz, J.M. Prausnitz, Equation-of-State mixing rules for multicomponent mixtures: the problem of invariance, *Fluid Phase Equilib.* 67 (1991) 31–44.
- [137] H. Monhemi, M.R. Housaindokht, M.R. Bozorgmehr, M.S.S. Googheri, Enzyme is stabilized by a protection layer of ionic liquids in supercritical CO₂: Insights from molecular dynamic simulation, *J. Supercrit. Fluids*. 69 (2012) 1–7.
- [138] Y. Fan, J. Qian, Lipase catalysis in ionic liquids/supercritical carbon dioxide and its applications, *J. Mol. Catal. B Enzym.* 66 (2010) 1–7.

- [139] O. Pfohl, S. Petkov, G. Brunner, Usage of PE - A Program to Calculate Phase Equilibria, Herbert Utz Verlag, München, 1998.
- [140] P.J. Pereira, M. Gonçalves, B. Coto, E.G. Azevedo, M.N. Ponte, Phase equilibria of CO₂ + dl- α -tocopherol at temperatures from 292 K to 333 K and pressures up to 26 MPa, Fluid Phase Equilib. 91 (1993) 133–143.
- [141] A. Ruiz-Rodriguez, V. Najdanovic-Visak, Z.P. Visak, M. do R. Bronze, C. Antunes, M. Nunes da Ponte, High-pressure phase behaviour of binary (CO₂ + nicotine) and ternary (CO₂ + nicotine + solanesol) mixtures, Fluid Phase Equilib. 282 (2009) 58–64.
- [142] H. Sovová, R.P. Stateva, A. A. Galushko, High-pressure equilibrium of menthol + CO₂, J. Supercrit. Fluids. 41 (2007) 1–9.
- [143] D.W. Jennings, R.J. Lee, A.S. Teja, Vapor-liquid equilibria in the carbon dioxide + ethanol and carbon dioxide + 1-butanol systems, Chem. Eng. Data. 36 (1991) 303–307.
- [144] C. Secuianu, V. Feroiu, D. Geană, Phase behavior for carbon dioxide + ethanol system: Experimental measurements and modeling with a cubic equation of state, J. Supercrit. Fluids. 47 (2008) 109–116.
- [145] A.A. Galushko, H. Sovová, R.P. Stateva, Solubility of Menthol in Pressurised Carbon Dioxide – Experimental Data and Thermodynamic Modelling, Chem. Ind. Chem. Eng. Q. 12 (2006) 152–158.
- [146] R.C. Reid, J.M. Prausnitz, B.E. Poling, The properties of gases and liquids, 4th Edition, McGraw-Hill, New York, 1987.
- [147] J.-H. Xu, T. Kawamoto, A. Tanaka, High-performance continuous operation for enantioselective esterification of menthol by use of acid anhydride and free lipase in organic solvent, Appl. Microbiol. Biotechnol. 43 (1995) 639–643.
- [148] S. Podila, L. Plasseraud, H. Cattey, D. Ballivet-Tkatchenko, G.V.S.M. Carrera, M. Nunes Da Ponte, Synthesis of 1,2-glycerol carbonate from carbon dioxide: The role of methanol in fluid phase equilibrium, Indian J. Chem. - Sect. A Inorganic, Phys. Theor. Anal. Chem. 51 (2012) 1330–1338.
- [149] C.L. Yaws, Thermophysical Properties of Chemicals and Hydrocarbons, 1st Edition, William Andrew Inc., New York, 2008.
- [150] M. Wang, J. Zhao, Facile synthesis of Au supported on ionic liquid functionalized reduced graphene oxide for simultaneous determination of sunset yellow and tartrazine in drinks, Sensors and Actuators B-Chemical 216 (2015) 578–585.

- [151] G. Kamal, A. Chouhan, A task-specific ionic liquid [bmim] SCN for the conversion of alkyl halides to alkyl thiocyanates at room temperature, *Tetrahedron Lett.* 46 (2005) 1489–1491.
- [152] P.U. Naik, S.J. Nara, J.R. Harjani, M.M. Salunkhe, Ionic liquid anchored substrate for enzyme catalysed kinetic resolution, *J. Mol. Catal. B Enzym.* 44 (2007) 93–98.
- [153] C.M. Monteiro, N.M.T. Lourenço, C.A.M. Afonso, Separation of secondary alcohols via enzymatic kinetic resolution using fatty esters as reusable acylating agents, *Tetrahedron Asymmetry.* 21 (2010) 952–956.
- [154] N.M.T. Lourenço, C.M. Monteiro, C.A.M. Afonso, Ionic acylating agents for the enzymatic resolution of *sec*-alcohols in ionic liquids, *European J. Org. Chem.* (2010) 6938–6943.
- [155] F. Van Rantwijk, R.A. Sheldon, *Biocatalysis in Ionic Liquids*, Society. (2007).
- [156] P. Lozano, T. de Diego, D. Carrié, M. Vaultier, J.L. Iborra, Continuous green biocatalytic processes using ionic liquids and supercritical carbon dioxide., *Chem. Commun. (Camb).* (2002) 692–693.
- [157] R. Bogel-Lukasik, V. Najdanovic-Visak, S. Barreiros, M. Nunes da Ponte, Distribution Ratios of Lipase-Catalyzed Reaction Products in Ionic Liquid Supercritical CO₂ Systems: Resolution of 2-Octanol Enantiomers, *Ind. Eng. Chem. Res.* 47 (2008) 4473–4480.
- [158] J. Gordo, J. Avó, A.J. Parola, J.C. Lima, A. Pereira, P.S. Branco, Convenient synthesis of 3-vinyl and 3-styryl coumarins., *Org. Lett.* 13 (2011) 5112–5.
- [159] C. Reichardt, Polarity of ionic liquids determined empirically by means of solvatochromic pyridinium N-phenolate betaine dyes, *Green Chem.* 7 (2005) 339.
- [160] F. van Rantwijk, F. Secundo, R.A. Sheldon, Structure and activity of *Candida antarctica* lipase B in ionic liquids, *Green Chem.* 8 (2006) 282.
- [161] S.N.V.K. Aki, B.R. Mellein, E.M. Saurer, J.F. Brennecke, High-Pressure Phase Behaviour of Carbon Dioxide with Imidazolium-Based Ionic Liquids, *J. Phys. Chem. B.* 108 (2004) 20355–20365.
- [162] F. Lipnizki, J. Olsson, P. Wu, A. Weis, G. Trägårdh, R.W. Field, Hydrophobic pervaporation: influence of the support layer of composite membranes on the mass transfer, *Sep. Sci. Technol.* 37 (2002) 1747–1770.
- [163] O. Trifunović, G. Trägårdh, The influence of support layer on mass transport of homologous series of alcohols and esters through composite pervaporation membranes, *J. Memb. Sci.* 259 (2005) 122–134.

- [164] W. Kujawski, A. Warszawski, W. Ratajczak, T. Porębski, W. Capała, I. Ostrowska, Application of pervaporation and adsorption to the phenol removal from wastewater, *Sep. Purif. Technol.* 40 (2004) 123–132.
- [165] A.E. Ivanov, M.P. Schneider, Methods for the immobilization of lipases and their use for ester synthesis, *J. Mol. Catal. B Enzym.* 3 (1997) 303–309.
- [166] K. Suginaka, Y. Hayashi, Y. Yamamoto, Highly selective resolution of secondary alcohols and acetoacetates with lipases and diketene in organic media, *Tetrahedron: Asymmetry.* 7 (1996) 1153–1158.

